Intertwined detection and recognition roles of tetrazine in synergistic anion-π and H-bond based anion receptor

Romain Plais, Guy Gouarin, Anne Gaucher, Violette Haldys, Arnaud Brosseau, Gilles Clavier, Jean-Yves Salpin, Damien Prim

RESEARCH ARTICLE

Intertwined detection and recognition roles of tetrazine in synergistic anion-π and H-bond based anion receptor

Romain Plais,[a] Guy Gouarin,[a] Anne Gaucher,[a] Violette Haldys,[b], [c] Arnaud Brosseau,[d] Gilles Clavier,[d] Jean-Yves Salpin,[b], [c] and Damien Prim*[a]

Dedication ((optional))

[a] Mr. R. Plais, Mr. G. Gouarin, Dr. A. Gaucher, Prof. Dr. D. Prim
ILV
Université Paris-Saclay, UVSQ, CNRS
78035 Versailles (France)
E-mail: damien.prim@uvsq.fr
[b] Mme. V. Haldys, Dr. J.-Y. Salpin
LAMBE
Université Paris-Saclay, CNRS, Univ. Evry
91025 Evry (France)
[c] Mme. V. Haldys, Dr. J.-Y. Salpin
LAMBE
Université Paris-Seine, CNRS, U-Cergy
91025 Evry (France)
[d] Mr. A. Brosseau, Dr. G. Clavier
PPSM
Université Paris-Saclay, CNRS, ENS Paris-Saclay,
94235 Cachan (France)

Supporting information for this article is given via a link at the end of the document.

Abstract: The intrinsic properties of tetrazine as a π-anion receptor and as an on/off recognition probe merged with H-bond ability of an urea motif into a single architecture designs a new generation of well-defined anion receptors. Complexation properties directly benefit from the dual and synergistic contribution of tetrazine and urea. In this study, we report on the synthesis and assessment of binding properties to anions of diverse geometries. Association constants have been predicted by theoretical calculations and evaluated by multiple and complementary experimental techniques including electrospray-mass tandem spectroscopy, NMR, UV-Visible, steady state fluorescence spectroscopies and time resolved fluorescence. These results provide the basis for a better understanding of both the complexation and the anion-dependent quenching mechanism.

Introduction

Anions play crucial roles in many biological processes,[1,2] environmental detection[3–5] and catalysis. [6–8].Their wide potential applications but also the deep understanding of biological events and the exploration of noncovalent interactions motivated an increasing interest of the scientific community which rivalled in creativity for selective anion recognition and/or sensing. Historically and predominantly, the design of anionic receptors has incorporated one or more hydrogen bonding donors (HBs).[9] More recently, several distinct weak interactions such as anion-π[10], electrostatic interactions, hydrophobic effects or halogen bonds[11] emerged to complement the panel of noncovalent interactions, thus devising new families of receptors. If such noncovalent interactions have been widely but independently used in current receptors, the cooperation between distinct noncovalent interactions embedded into a unique receptor frame is an emerging area of research, [12–14] almost restricted to theoretical [13] or crystallographic [12] studies. The development of such receptors is in its infancy but is likely to bring new avenues in anion recognition provided that this new generation of receptors (i) exhibits an adaptive behaviour to various anion geometries, (ii) features a user-friendly and straightforward synthesis and (iii) allows accurate detection/characterization of binding properties. Alongside highly pre-organized rigid receptors widely spread in supramolecular chemistry, [15] we focused our attention on single molecules comprising a hydrogen bonding donor linked to a π-deficient heterocycle able to generate anion-π interactions. Based on our recent publications [16–21] and publications from Melguizo and Bianchi, [22,23] we envisioned that the combination of urea and tetrazine moieties would be beneficial to anion binding and allow cross-characterisation of binding properties. On one hand, the urea motif would enable gaining information from ^{1}H NMR techniques and on the second we take benefits from the dual role of the tetrazine fragment acting as anion-π acceptor and as fluorescent probe (*Scheme 1*).

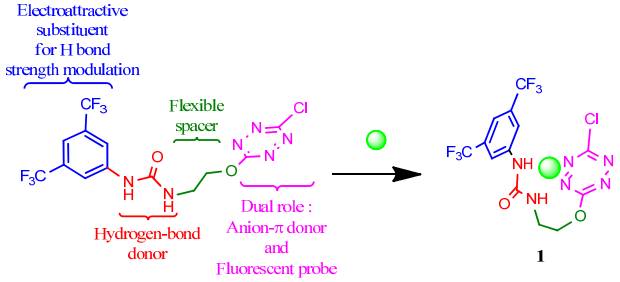

Scheme 1. Structure of ligand **1**

Herein, we report the synthesis and exploration of anion binding properties of an unprecedented urea-tetrazine receptor. Intertwined characterization of the receptor-anion architectures and determination of association constants as well as synergistic contribution of distinct non-covalent interactions, rely on theoretical methods and a broad scope of experimental methods such as electrospray-tandem mass spectrometry, NMR, UV-Visible and steady state fluorescence spectroscopies as well as time resolved fluorescence.

Results and Discussion

Theoretical calculations and structural parameters

To evaluate the potential of this new ligand in anion binding, we have performed DFT calculations using Gaussian 09 software [24] of **1** in combination with a selection of five anions.

Table 1. Optimized geometries, ESP and NCIplot of receptor **1** and complexes with anions at APFD/6-31+G(d,p) level

Entry		Optimized Geometry	ESP	NCIplot	$\Delta G_{int,ACN}$ [a]
1	**1**		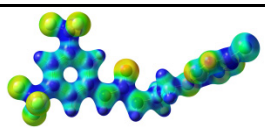	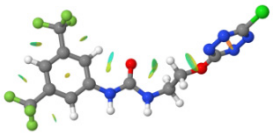	-
2	**1**-Cl	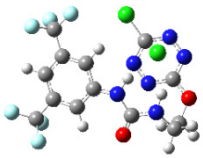	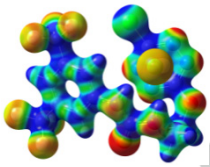	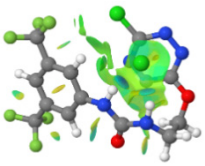	-29.7
3	**1**-Br	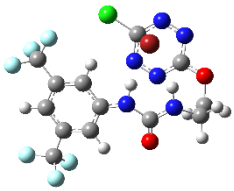	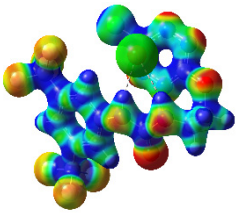	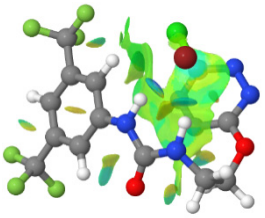	-29.9
4	**1**-I	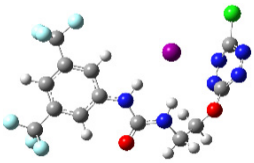	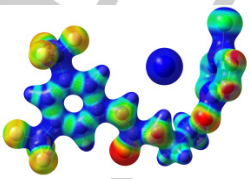	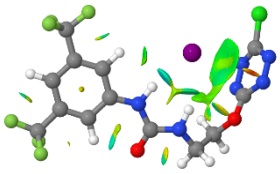	-17.0
5	**1**-SCN	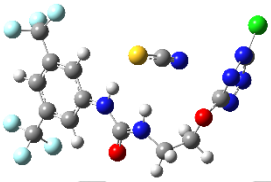	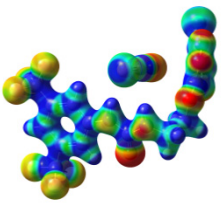	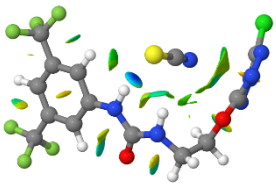	-11.5
6	**1**-PF_6	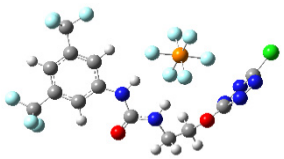	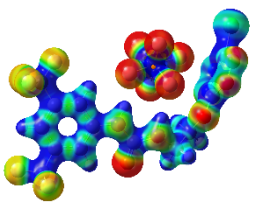	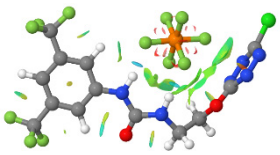	+6.7

[a] Interaction energy in kJ/mol, with Polarizable Continuum Model for Acetonitrile, calculated from Gibbs Free Energies

Optimization and frequency calculations were performed using the APFD/6-31G+(d,p) level without any solvent correction. APFD functional was chosen due to its accuracy in computing long-range interactions and modelling of hydrogen bond complexes. [25] The effect of solvent was evaluated by optimizing the geometries using an IEFPCM model for acetonitrile (ESI §2.1). No significant changes in geometries were observed on applying solvent correction. For complexes including bromide and iodide ions, two basis set were used: APFD/LANL2DZ for bromide and iodide, respectively and APFD/6-31G+(d,p) and others atoms. Optimized geometries are detailed in *Supporting Information (p.7-20).* Electrostatic Potentials Surfaces (ESP) were calculated using Gaussview software from optimized structures using a fine grid for Total Density and a medium grid of ESP. To visualize non-covalent interactions in real space, we have used a tool called Non-Covalent Interactions plot (NCIplot). These 3D plots were calculated using the script developed by Rzepa available on the website application of the Imperial College London. [26,27] Interaction energies with and without solvent effect were calculated by generating frequencies calculations from optimized geometries using triple zeta basis set APFD/aug-ccpvtz level of calculation. [28] All the results of these calculations are showed in *Table 1 and in Supporting Information (ESI §2.2).*

As shown in *Table 1*, the receptor **1** adopts a conformation in which the tetrazine core is almost perpendicular to the hydrogen bond donor, thus minimizing repulsive interactions between the tetrazine and the urea fragments (table 1, entry 1, NCIplot). As evidenced by the NCIplot, this conformation and the overall 3D shape of receptor **1** are set by several weak interactions involving (i) ortho protons of the aromatic fragment and the urea carbonyl motif, (ii) a combination of two hydrogen bonds between protons of the aliphatic spacer and the urea carbonyl on one hand and the tetrazine nitrogen atoms on the other hand. Interactions between receptor **1** and anions of different geometries were then characterized. Optimized geometries show that the presence of an anion close to the receptor deeply impact the overall geometry enabling the folding around the anion thus maximizing attractive interactions between X^- and both the urea and the tetrazine motifs. Noteworthy, the folding depends on the size and the geometry of the guest anion. All NCIplots evidence defined dish-shaped surfaces allowing visualization of anion-π interactions. Large NCIplot surfaces can be observed for **1**-Cl and **1**-Br complexes suggesting strong interactions, whereas **1**-I, **1**-SCN and **1**-PF_6 display less pronounced surfaces and interactions. As anticipated by NCIplot surface intensities, calculated interaction energies in acetonitrile follow similar trend: high interaction energies of a close order of magnitude for **1**-Cl (-29.7 kJ/mol) and **1**-Br complexes (-29.9 kJ/mol) and decreasing interaction energies obtained for **1**-**I** (-17.0 kJ/mol) and **1**-SCN (-11.5 kJ/mol). A positive value was obtained for **1**-PF_6, indicative of a non-spontaneous complexation in acetonitrile. As illustrated in *Table 1*, both the anion size and geometry impact the topology of complexes **1**-X. Even in a same anion geometry series, variations of the relative orientation of the urea, the anion and the tetrazine fragments clearly modify the overall topology of the corresponding complexes. For all spherical anions, the general trend of the 3D topology (*Figure 1*) is set by two main elements: (i) the strong interaction between urea protons H_a and H_b and the anion contributes to the formation of straight plane composed by C, N and H atoms of the urea motif and the anion. (ii) due to the anion-π interaction, the latter plane almost parallels the planar tetrazine ring. The strength of both H-bonds and anion-π interactions is clearly depending on the size and properties of the anion which might thus impact the relative spatial orientation of the triptych urea/anion/tetrazine within the complex series. Key parameters allowing complete characterization of their structures are compiled in *Table 2* and compared within the spherical anion series. Indeed, N-H_a/H_b bond lengths and through space H_a/H_b-X^- distances are privileged features of the complexation to the urea motif. In addition, distances between X and the centroïd of the tetrazine but also to all tetrazine nitrogen atoms N_a/N_b/N_c/N_d are indicative of the precise location of the anion and the directionality of the anion-π interaction (*Table 2)*.

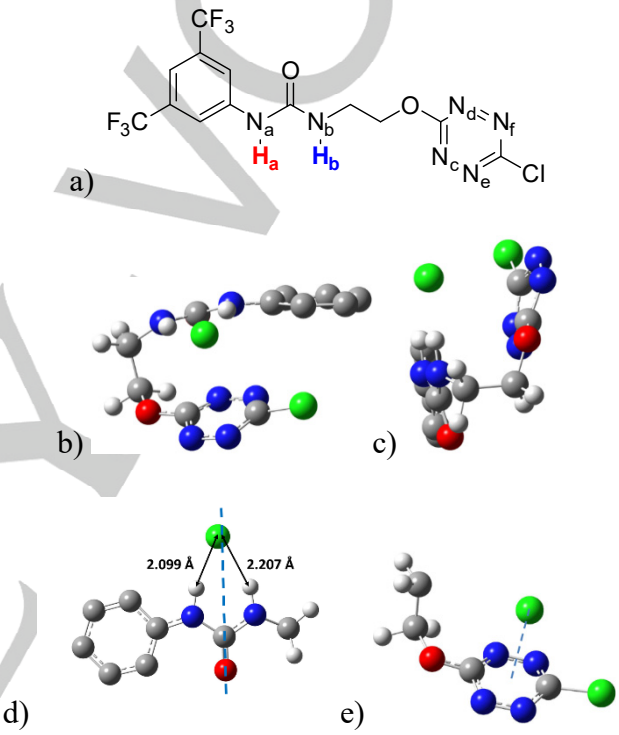

Figure 1. a) Labelling system and selected views of **1**-Cl (CF_3 groups are omitted for clarity). b) and c) front and side views of cofacial arrangement between the urea/Cl and the tetrazine planes. d) position of Cl^- with respect to median axis of the urea. e) distance between Cl^- and the tetrazine centroïd.

If receptor **1** displays identical N_a-H_a and N_b-H_b bond distances, the latter increased consistently in **1**-Cl, **1**-Br and **1**-I with the formation of H-bond interaction. Interestingly, the H-bond interaction allowed discriminating N_a-H_a and N_b-H_b bond distances. Indeed, in all cases the electron withdrawing effect of the aromatic fragment proximal to H_a strengthen the H-bond inducing the increase of the N_a-H_a bond distances in a larger extent by comparison with the corresponding N_b-H_b. In addition, depending on the nature of the anion the through space distance between the anion and H_a and H_b are also impacted. Strong interaction led to shortest distances as evidenced by the H_a- or H_b-X which increase from Cl^- to I^- (compare entries 3 and 4 for each anion). Again H_a-X or H_b-X distances are different, H_a-X being the shortest reflecting a strongest interaction. The anion-π interaction with the tetrazine fragment also induces modifications on the overall shape depending on the anion. As expected, the X^--

centroid distances are close for Cl^- (3.12Å) and Br^- (3.15Å) but markedly increased for I^- (3.49Å). The fact that N_a-H_a and N_b-H_b but also H_a-X or H_b-X distances are discriminated in complexes **1**-Cl, **1**-Br and **1**-I also impacted the relative orientation of the tetrazine planar ring. Indeed, in **1**-Cl, N_c-X and N_d-X on one hand and N_e-X and N_f-X on the other hand display very close through space distances indicating an almost cofacial arrangement between the tetrazine and the urea/Cl plane. In contrast, in both **1**-Br and **1**-I, N_c-X and N_d-X as well as N_e-X and N_f-X differ markedly from each other, inducing a twist of the tetrazine ring with respect to the **1**-Cl case. This deformation might originate from the joint increase of anion size and concomitant decrease of H-bonding order and increase of anion-π interaction.

Table 2. Key structural parameters of **1**-X topologies calculated on the APFD/6-31+G(d,p) level

Entry	Bond[a]	**1**	**1**-Cl	**1**-Br	**1**-I
1	N_a-H_a	1.011	1.037	1.034	1.029
2	N_b-H_b	1.011	1.030	1.027	1.023
3	N_a-X	--	2.099	2.217	2.545
4	N_b-X	--	2.207	2.399	2.751
5	X-centroïd	--	3.12	3.15	3.49
6	N_c-X	--	3.491	3.515	3.774
7	N_d-X	--	3.500	3.579	3.722
8	N_e-X	--	3.411	3.393	3.874
9	N_f-X	--	3.403	3.436	3.822

[a] distance in Å

The linear thioisocyanate anion adopts a conformation almost orthogonal to the urea moiety. As a result, the overall topology of **1**-SCN appears more flared shaped than the corresponding spherical anion geometry. The polarisable sulphur atom generates a strong interaction with the urea as shown in *Table 1*. Interestingly, carbon and nitrogen atoms are interacting with the tetrazine as evidenced by the dish-shaped surface characteristic of an anion-π interaction. The large hexahedral PF_6^- behaves similarly to other anions interacting with the urea fragment. As expected, distances between PF_6^- and both urea and tetrazine motifs increases leading to a loose anion-π interaction by comparison with previous geometries.

Synthesis

Synthesis of receptor **1** was achieved using a two steps short sequence *(Scheme 2)* involving the condensation of ethanolamine on the commercially available 3,5-bis(trifluoromethyl)phenyl isocyanate to form the urea moiety **S1** in the first step in 89% yield. [29] In a second step, a nucleophilic aromatic substitution of dichlorotetrazine enables the formation of receptor **1** in 58% yields. [30] In order to evaluate the impact of the presence of the tetrazine unit in the receptor on the complexing properties, receptor **2** was synthesized by a reaction sequence similar to **S1** using 2-methoxyethylamine in 66% yield.

All the compounds were fully characterized by spectroscopic methods (*Supporting Information p. 22-31)*.

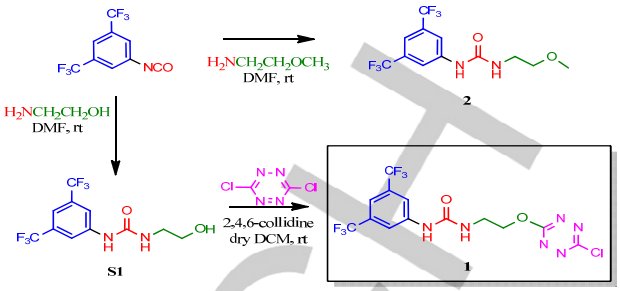

Scheme 2. Synthesis of receptors **1** and **2**

Tandem mass spectrometry

In order to get some insights about the nature of the complex(es) generated by the association of the receptor **1** with the different anions, we first performed a series of tandem mass spectrometry experiments, by using a 3D ion trap instrument (Bruker Amazon Speed ETD). This allows to access to the intrinsic reactivity of **1** towards the series of anions. Complexes were generated in the gas phase by electrospraying equimolar mixtures of **1**/TBAX. Starting from 10^{-1} M stock solutions of **1** and TBAX prepared in acetonitrile (ACN) and purified water, respectively, 10^{-4} M mixtures of **1**/TBAX (90/10 ACN/H_2O) were introduced in the electrospray source by a syringe pump (3 µL/min). Detailed experimental conditions can be found in the *Supporting Information*. For the sake of simplicity, the *m/z* values given in this section correspond to the monoisotopic peak. A Typical ESI spectrum for such mixtures is given in *Figure 2a* for the **1**/TBACl system.

Whatever the anion studied, electrospray spectra of these mixtures result in the formation of two very intense complexes of general formula $[(\mathbf{1})_n\text{-}X]^-$ (n=1,2). Depending on the experimental conditions, $[(\mathbf{1})_3\text{-}X]^-$ can be observed but generally in very weak abundance (presently *m/z* 1325.0). We do not observe complexes with remaining solvent molecules. The chemical composition of the complexes can be confirmed by examining the experimental isotopic distributions (see insert of *Figure 2a* for the $[(\mathbf{1})\text{-}Cl]^-$ complex). Consequently, formation of these singly charged ions turned to be a very facile process. On the other hand, we did not detect any doubly charged anion that would correspond to the interaction of **1** with two X^- anions.

We then tried to obtain structural information about these complexes by recording their MS/MS spectra. Whatever the anion considered, MS/MS spectra of the dimeric species $[(\mathbf{1})_2\text{-}X]^-$ systematically correspond to the elimination of an intact molecule of receptor **1**, leading to $[(\mathbf{1})\text{-}X]^-$. On the other hand, different behaviors are observed upon collision for the 1:1 complex. Elimination of **1** and formation of X^- from $[\mathbf{1}\text{-}X]^-$ is not the only process, except for PF_6^- (see *Figure S19*), which indicates that for this anion the interaction is particularly weak in the gas phase. This finding is in agreement with the very small computed interaction energy (*Table 1 and ESI §2.2*). This is also consistent with data obtained in solution by NMR, UV of fluorescence experiments, which indicate that PF_6^- does not interact with the receptor in solution (*Table 1 and vide infra*).

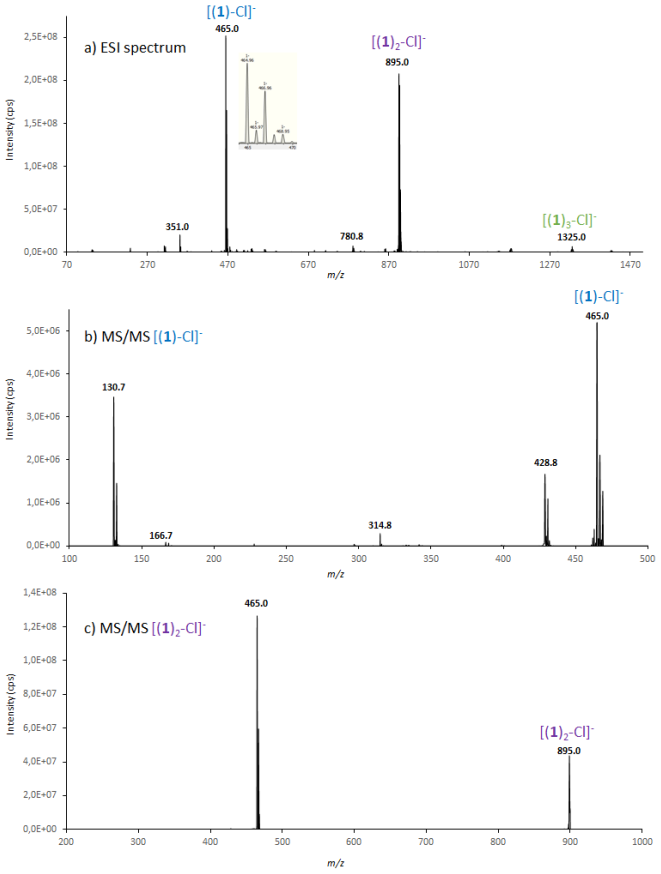

Figure 2. a) Electrospray mass spectrum of an equimolar (10^{-4} M) mixture of **1**/TBACl (90/10 acetonitrile/water) - b) MS/MS spectrum of the [1-Cl]⁻ ion (m/z 465) – c) MS/MS spectrum of the [(**1**)$_2$-Cl]⁻ ion (m/z 895)

For the other [(**1**)-X]⁻ anions, dissociation channels involving the cleavage of covalent bonds are observed, therefore suggesting a strong interaction of the anion with the receptor. Note that in some cases (SCN, Cl), the formation of the X⁻ ions corresponds to *m/z* values which were well below the low-mass cutoff of our ion trap. We tried to lower as much as possible the low mass cut-off, in order to try to detect X⁻, but it can result in the complete loss of the signal. This was the case for X=Cl or SCN, and therefore we could not be able to detect SCN⁻ or Cl⁻, although their formation cannot be rigorously discarded. Br⁻ could be detected in weak amounts. Note however that formation of X⁻ should be associated to a small interaction energy, and therefore the abundance of X⁻ should decrease as the interaction energy increases. Consistently, I⁻ and PF_6- are observed in significant abundances (*Figures S17 and S19*).

Our series of MS/MS experiments allowed to demonstrate that the various adducts share several fragmentation processes. This dissociation pattern is summarized in *Scheme 3*, and the MS/MS spectrum obtained for the [(**1**)-Cl]⁻ ion is reported in *Figure 2b*.

Elimination of HX associated to deprotonation of **1** (*m/z* 429), is observed for three anions, namely Cl⁻, SCN⁻ and Br⁻. This process is not observed with iodide or PF6⁻. The extent of this fragmentation is correlated to the gas-phase acidity of HX.[31] The m/z 429 ion is indeed intense for Cl⁻ and SCN⁻ ($\Delta H°_{acid}$(HCl)= 1395 kJ/mol) ; $\Delta H°_{acid}$(HSCN)= 1361 kJ/mol), weaker for Br⁻ ($\Delta H°_{acid}$(HBr)= 1353 kJ/mol) and is absent for I⁻ ($\Delta H°_{acid}$(HI)= 1315 kJ/mol).

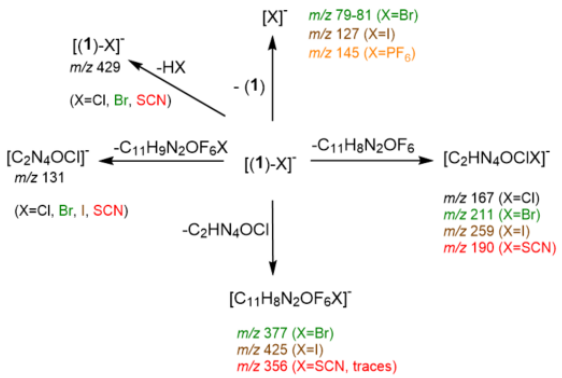

Scheme 3. General dissociation scheme for the [(**1**)-X]⁻ complex under CID conditions

Formation of *m/z* 429 probably implies removal of one of the urea proton (See section 4.5 of the *Supporting Information*). Reasonably, removal of H_a should be more favorable since the resulting anion would be stabilized by a mesomeric effect involving the benzenic ring. This process therefore suggests interaction of the anion with the urea moiety, in agreement with the calculations.

Another characteristic fragment ion is the [C_2N_4OCl]⁻ ion (*m/z* 131). This fragmentation, together with the elimination of the 132 u [C_2HN_4OCl] neutral undoubtedly involves the tetrazine moiety. These processes may correspond in a first step a S_N2-like mechanism leading to the cleavage of the C(H_2)-O bond and formation of an intermediate ion/neutral complex, evolving subsequently either directly towards the *m/z* 131 ion, or leading, after internal proton transfer, to the elimination of 132 u. The initial interaction of X⁻ with the urea moiety through hydrogen bonding may result to the favorable positioning of X⁻ for the S_N2 process.

The last characteristic fragment observed for all anions but PF_6⁻ (*Figure 2* and *Figures S16-S19*) is the formation of a [C_2HN_4OClX]⁻ anion. This fragment ion can be formed through the direct attack of the tetrazine moiety by X⁻ MS/MS spectra (see section 4.5 of the *SI*). To summarize, the various fragmentation processes seem to suggest that the anion interacts with both the urea and the tetrazine moieties, as already underlined by the calculations.

NMR Titrations: fundamental state binding studies

The affinity of **1** towards Cl⁻, Br⁻, I⁻, SCN⁻ and PF_6⁻ anions was assessed by ^{1}H NMR titrations in CD_3CN *(ESI Figures S20 to S29)*. The case of spherical Cl⁻, Br⁻, I⁻ anions has been considered first. Linear and hexahedral SCN⁻ and PF_6⁻ will be discussed afterwards.

^{1}H NMR titration spectra of **1** with TBACl is reported in *Figure 3*. In CD_3CN, the iterative addition of Cl⁻ anion to the receptor resulted in significant modifications in the ^{1}H NMR spectrum. Noteworthy large downfield shifts of urea protons are observed. If both protons are downshifted, they behave somewhat differently. H_a undergoes a shift from 7.81 to 11.04 ppm ($\Delta\delta_{ClHa}$ = 3.23 ppm) and H_b from 5.82 to 7.57 ppm ($\Delta\delta_{ClHb}$ = 1.75 ppm).

a)

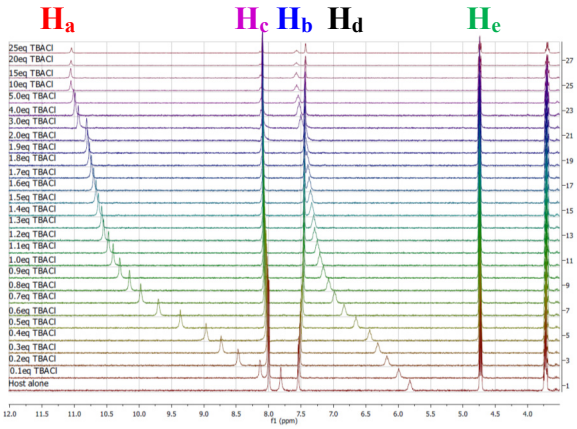

b)

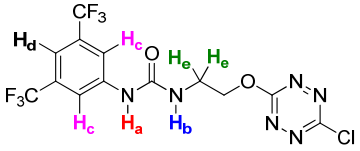

Figure 3. a) NMR titration of anion receptor **1** by chloride anion (0 to 25 equivalents) – b) Proton attribution

This difference plausibly arises from the electron withdrawing effect of the aromatic fragment proximal to H_a. The large $\Delta\delta_{Cl}$ observed strongly suggest tight interactions between Cl^- and the receptor. As evidenced by the spectrum aromatic protons H_d and aliphatic proton H_e were only poorly affected by progressive addition of TBACl. Evolution of chemical environment of aromatic proton H_c through complexation allow identifying modification of the chemical shifts albeit with a lesser extent. Indeed, $\Delta\delta_{XHc}$ ranges from 0.05 to 0.16 ppm for all anion studied. Titration of receptor **1** with TBABr and TBAI were next realized. The corresponding ^{1}H NMR spectra display similar general shape (SI, *Figures S24 and S26)*. Again $\Delta\delta_{BrHa}$ (2.69 ppm) and $\Delta\delta_{IHa}$ (1.64 ppm) were increased by comparison with the corresponding $\Delta\delta_{Hb}$ shifts. Comparison of $\Delta\delta_{Ha}$ in titrations with spherical anions plotted in *Figure 4* and the number of equivalents of anion required to reach the endpoint, suggests a stronger interaction between Cl^- and **1** than between Br^- or I^- and **1** in decreasing order.

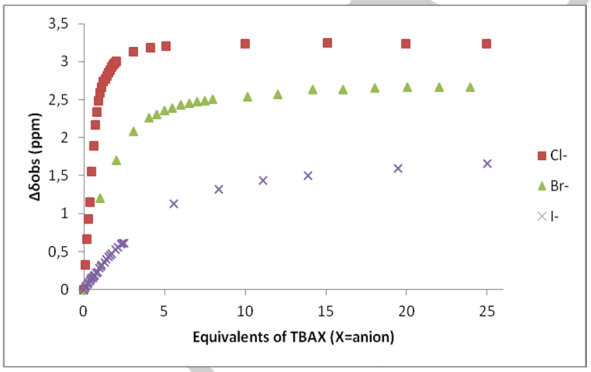

Figure 4. $\Delta\delta_{Ha}$ calculated as a function of the number of equivalents of TBAX (X = Cl, Br and I) added for proton H_a

Titration was next extended to linear anion SCN^-. The same approach led to ^{1}H NMR spectrum which showed similar features *(ESI, Figure S28)*. Signals of H_a and H_b are downfield shifted upon progressive addition of SCN^-. Complexation to receptor **1** was characterized by $\Delta\delta_{SCNHa}$ = 1.69 ppm for H_a and $\Delta\delta_{SCNHb}$ = 0.76 ppm for H_b suggesting a moderate interaction between **1** and SCN^-. Finally, in the case of PF_6^-, no significant shift was observed after addition of 20 equivalents of the anion. Although less pronounced complexation process cannot be fully ruled out, interaction between **1** and PF_6^- could not be evidenced.

^{1}H NMR spectra obtained after titration with various anions exhibit similar shapes. However, the marked decrease of $\Delta\delta_{XHa}$ and $\Delta\delta_{XHb}$ moving from Cl^- to SCN^- is indicative of the general affinity trend between receptor **1** and the anions. To clarify and confirm this tendency, binding constants of the corresponding complexes were determined using two different methods : a single proton method developed by Gonzàlez-Gaitano *et al.* [32] and a global analysis of the three protons using SPECFIT software. The first method is based on the differences in chemical shifts observed (Δδ) plotted as a function of number of equivalents of TBAX added (Table 3, *Figure 4 and S31)*.

Table 3. Binding constants calculated from mathematical equations and with SPECFIT® software

	Entry	$K_{A,\ Ha}$[a]	$K_{A,\ Hb}$[a]	$K_{A,\ Hc}$[a]	$K_{A,\ SPECFIT}$[a]
1	**1**-Cl	5893	5700	5000	4892 ± 1 (0.6%)
2	**2**-Cl	1804	1811	1764	1757 ± 1 (0.1%)
2	**1**-Br	375	371	452	375 ± 1 (0.1%)
3	**1**-I	64	67	77	70 ± 1 (0.2%)
4	**1**-SCN	37	37	59	37 ± 1 (0.4%)
5	**1**-PF_6	--[b]	--[b]	--[b]	--[b]

[a] Binding constants in L/mol [b] No binding was observed

As anticipated after analysis of ^{1}H NMR spectra, **1**-Cl exhibit the strongest binding constant of the series of anions (4892 L/mol). As expected, in a similar system bearing only a urea (**2**-Cl), a significant drop in association constant is observed (1757 L/mol), evidencing the clear cooperative and beneficial effect of the presence of both fragments *(Figure S30)*. Moreover, a strong decrease is observed from **1**-Br (375 L/mol) to **1**-I (70 L/mol) and **1**-SCN (37 L/mol) and no binding constant could be calculated for **1**-PF_6.

Photophysical analysis: excited state binding studies

Taking advantage of the photophysical properties of the ligand, the affinity of **1** towards Cl^-, Br^-, I^-, and SCN^- (as Bu_4N^+ salts) was also assessed by UV-Visible and steady state fluorescence spectroscopies as well as time-resolved fluorescence decay in acetonitrile.

Absorption spectrum of **1** was first recorded in acetonitrile and displays 4 absorption maxima at 511, 324, 295 and 246 nm (*Figure S37*). A TDDFT calculation (PBE0/6-311+g(d,p) level) has been done to attribute those bands. The calculated and experimental spectra match quite well (mean deviation between calculated and experimental maxima is 7%, *Figure S34*). The 511,

324 nm bands could then be attributed to the n-π* and π-π* transitions of the tetrazine and the 295 and 246 nm bands to two π-π* transitions centered on the phenyl urea moiety (*Figures S23 and S24*). Fluorescence spectra of compound **1** was also recorded in the same solvent and display the typical emission band of a tetrazine [18] with a maximum at 561nm *(Figure S38)*.

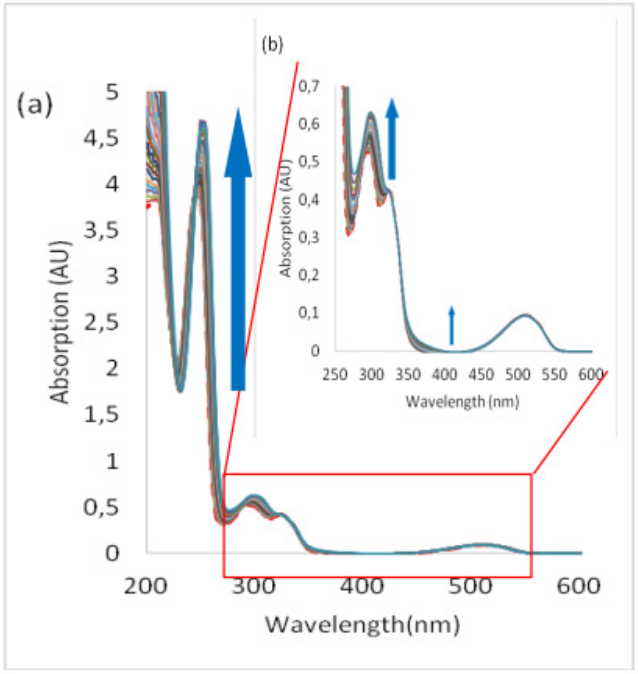

Figure 5. Absorption spectra measured during the titration of **1** with tetrabutylammonium chloride (from 0 to 70 equivalents of TBACl): a) total spectrum b) zoom

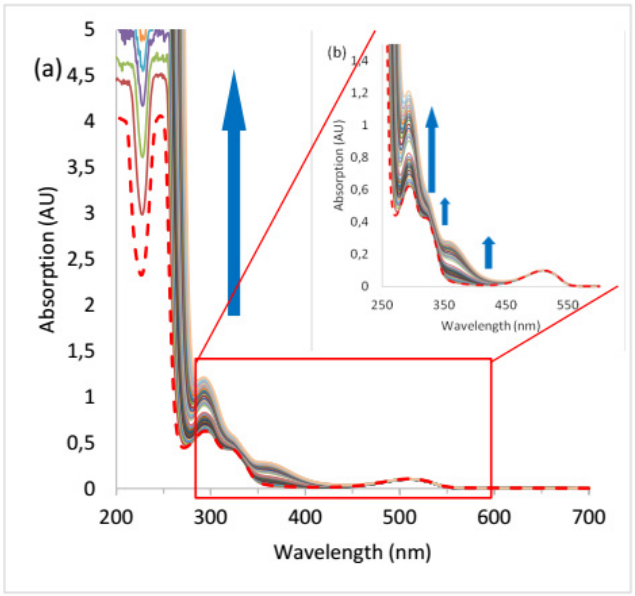

Figure 6. Absorption spectra measured during the titration of **1** with tetrabutylammonium iodide (from 0 to 200 equivalents of TBAI): a) total spectrum b) zoom

The fluorescence quantum yield was determined to 39% using Rhodamine-6G as reference.[33] This value is quite high and in agreement with literature reported values.[18] This will facilitate the characterization of the formation of complex since it has previously been demonstrated that interaction of the tetrazine with electron rich species leads to quenching of fluorescence.[30] UV-Visible spectra measured during the titration of **1** with chloride anion are reported in *Figure 5.* We can observe both hyperchromic and bathochromic shifts of the absorption bands associated with the phenylurea moiety. A smaller variation is also observed for the tetrazine π-π* bands but its n-π* one is almost not affected by the addition of chloride anion. Similar observations can be made from the other anions UV-vis. titrations (*Figures S47* [Br^-], *6* [I^-], and *S63* [SCN^-]). From these results, we can conclude that the major interaction involved in the complexation of anions by **1** in the ground state is hydrogen bonding with urea.

Association constants for 1 to 1 complex were determined using the SPECFIT software (*Table 4*). Values obtained for all halides are of the same order of magnitude and lower for the thioisocyanate ion. Nevertheless, due to the relatively small variations of the spectra during the titration, the values are obtained with a large margin of error and we cannot safely interpret them.

Iodide and thiocyanate anions seem to have a particular behavior towards complexation with **1**. As can be seen in the absorption spectra, a new band appears as a shoulder at approximately 360 nm. The origin of this new band is not clear.

The tetrazine is a strong electron acceptor that becomes a very strong oxidizer in its first excited state.[34] Two consequences can be expected from this property: the interaction between the tetrazine and anions should be stronger in the excited state and fluorescence quenching. We took advantage of this property to evidence the complexation of anions by **1** by fluorescence titrations.

Emission quenching is very clear from the fluorescence spectra recorded during the titration of **1** with tetrabutylammonium chloride (*Figure 7).* Nevertheless, it can be observed that despite the large excess of salts added, complete quenching is not reached. This behavior indicates that the complex formed by **1** and chloride anion exhibits a residual fluorescence. Fluorescence decays will help further analysis of this residual fluorescence.

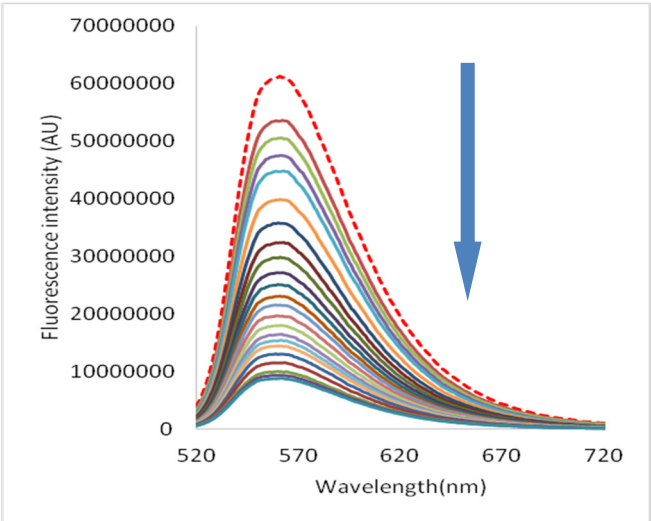

Figure 7. Fluorescence spectra measured during the titration of **1** with tetrabutylammonium chloride (from 0 to 70 equivalents of TBACl)

Similar quenching was observed with bromide, iodide and thioisocyanate anions (*Figures S49* [Br], *S57* [I] and *S65* [SCN]*).* From these data, new values of association constants have been extracted (*Table 4*) by two methods: a global spectral analysis with the SPECFIT software ($K_{A,\ fluo}$ SPECFIT) and a single wavelength nonlinear least squares fitting for a 1 to 1 model[35] ($K_{A,fluo}$, see Supporting Information for details and *Table 4 and Figures S40, S43, S48, S51, S56, S59, S64, S67).* Both approaches give similar values and trend between the different anions. A slightly higher value is observed for chloride anion.

Table 4. Binding constants determined from photophysical essays from mathematical equations and using SPECFIT® software

	Entry	$K_{A,\ abs,\ SPECFIT}$[a]	$K_{A,\ fluo}$[a]	$K_{A,\ fluo\ SPECFIT}$ [a]	$K_{A,\ decay,\ 65ns}$[a]
1	**1**-Cl	108 ± 1 (10%)	1763	1875 ± 1 (1%)	1461
2	**1**-Br	810 ± 1 (11%)	1176	1217 ± 1 (3%)	478
3	**1**-I	980 ± 1 (14%)	1479	1390 ± 1 (1%)	532
4	**1**-SCN	26 ± 1 (1%)	1386	1341 ± 1 (1%)	163
5	**1**-PF_6	--[b]	--[b]	--[b]	--[b]

[a] Binding constants in L/mol [b] No binding was observed

Further insight in the excited state behaviour was gained when recording fluorescence decays during the titrations of the various anions. Time resolved fluorescence gives information on the quenching mechanism: if the quenching is purely dynamic, then the fluorescence lifetime decreases while the initial fluorescence intensity of the decay remains unchanged. Inversely, if the quenching is static, the fluorescence lifetime remains constant while the initial fluorescence intensity of the decay decreases. Intermediate cases are also possible where both phenomena are observed.

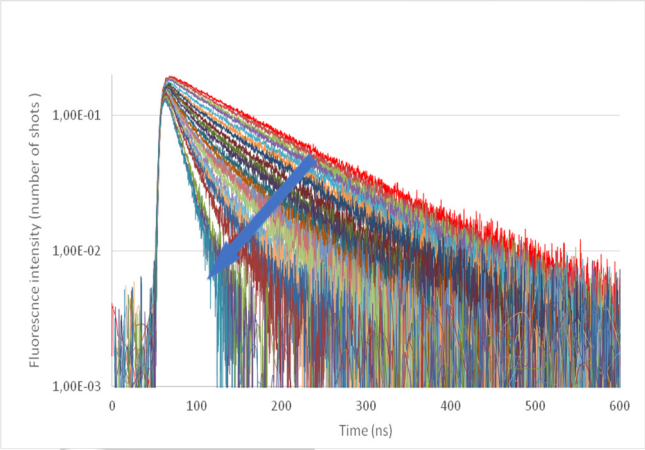

Figure 8. Fluorescence decay titration of **1** with TBACl (0 to 70 equivalents), logarithmic scale.

Fluorescence decays of **1** recorded for the titration with TBACl are presented in *Figure 8 and S46*. The decays become clearly shorter upon addition of the anion while the initial intensity undergo a small decrease. Mathematical fitting show 3 regimes: first a single exponential is needed with an initial lifetime of 133 ns corresponding to the unquenched tetrazine. Upon addition of chloride this lifetime decreases gradually. At 4 equivalents a second exponential with a short lifetime (20 ns) is needed to fit the decays. Finally at 50 equivalents the decay are mono-exponential again and the longer lifetime does not contribute anymore. It can thus be concluded that the complex **1-Cl** is slightly fluorescent and that the tetrazine–anion interaction is mainly dynamic in this case. A similar situation was found for the complex **1-Br** (*Figures S52-S54*) except that the complex fluorescence is weaker with a shorter lifetime of approximately 7 ns.

In the case of the iodide (*Figures S60-S62*) and thiocyanate anions (*Figure S68-S70*) the behaviour is different since there is a much larger drop in initial intensity accompanying the shortening of the decay. The quenching is thus much more pronounced.
In all cases it appears that there is both static and dynamic quenching but to a different extent depending on the nature of the anion. For the smaller ones (Cl^- and Br^-), the dynamic quenching is more pronounced than the static one and the final complexes are weakly fluorescent. However, for the larger ones (I^- and SCN^-) the static quenching plays an important role. This could indicate that in the ground state the tetrazine–anion interaction is stronger with the larger more polarizable anions as expected for anion-π interactions leading to a more pronounced static quenching. When in the excited state, the tetrazine is strongly electron attractor and interact with all anions leading to dynamic quenching.

Conclusion

In summary, we have designed a new approach towards anion recognition. Our approach takes not only benefit on the joint presence of an urea and a tetrazine moieties as a H-bond donor and anion-π acceptor respectively. In addition, the design of the molecular architecture of the anion receptor is focused on the tetrazine unit which is expected to play the dual role of anion-π acceptor and on/off fluorescence probe. Theoretical calculations enabled to foresee the complexation of anions of various geometries including chloride, bromide, iodide, thiocyanate and hexafluorophosphate and predict the interaction strength. The new receptor architecture is readily prepared in good yield through a short two-step-synthetic sequence. A complementary set of experimental techniques have been further used to accurately determine anion-receptor interactions. First, tandem mass spectroscopy studies underlined the synergistic roles of hydrogen bonding and anion-π interaction during the complexation process. Complexation was next evaluated by NMR titrations, enabling the assessment of binding constants and confirming the tendency observed by theoretical calculations. Exciting photophysical properties of this new receptor have next been exploited and UV-Visible and steady state fluorescence spectroscopies were performed. In complete agreement with NMR, photophysics confirmed the tendency in the association constants already observed. Further, time resolved fluorescence studies were realized and allowed gaining insights on the quenching mechanism. The latter appeared anion-dependent

combining both static and dynamic quenching. A preponderant dynamic quenching mode seems to act for smaller spherical anions (Cl- and Br-) while the static mode accounts for larger anions consistently with ground- and excited-states properties of the tetrazine unit. Further studies combining modified receptors and other anions are under way and will be reported in due time.

Acknowledgements

We are grateful to the CNRS and the University of Versailles Saint Quentin-en-Yvelines. We thank the French Ministère de l'Enseignement Supérieur et de la Recherche for funding (R. P.). This work was also supported by the French National Research Agency under the program CHARMMMAT ANR-11-LABX-0039-grant. This work was granted access to the HPC resources of CINES under the allocation 2019-A0060810812 made by GENCI.

Keywords: anion recognition • tetrazine • anion-π • fluorescence • mass spectroscopy

[1] L. M. Eytel, H. A. Fargher, M. M. Haley, D. W. Johnson, *Chem. Commun.* **2019**, *55*, 5195–5206.
[2] J.-B. Kim, *Korean J. Pediatr.* **2014**, *57*, 1–18.
[3] X. Xia, S. Zhang, S. Li, L. Zhang, G. Wang, L. Zhang, J. Wang, Z. Li, *Environ. Sci. Process. Impacts* **2018**, *20*, 863–891.
[4] H. Nakamura, *Anal. Methods* **2010**, *2*, 430–444.
[5] Z. Zhang, P. R. Schreiner, *Chem. Soc. Rev.* **2009**, *38*, 1187–1198.
[6] N. Mittal, D. X. Sun, D. Seidel, *Org. Lett.* **2014**, *16*, 1012–1015.
[7] T. Le, T. Courant, J. Merad, C. Allain, P. Audebert, G. Masson, *J. Org. Chem.* **2019**, *84*, 16139–16146.
[8] S. Beckendorf, S. Asmus, O. G. Mancheño, *ChemCatChem* **2012**, *4*, 926–936.
[9] T. L. Mako, J. M. Racicot, M. Levine, *Chem. Rev.* **2019**, *119*, 322–477.
[10] P. Gamez, *Inorg. Chem. Front.* **2014**, *1*, 35–43.
[11] G. Cavallo, P. Metrangolo, R. Milani, T. Pilati, A. Priimagi, G. Resnati, G. Terraneo, *Chem. Rev.* **2016**, *116*, 2478–2601.
[12] M. Mascal, I. Yakovlev, E. B. Nikitin, J. C. Fettinger, *Angew. Chemie - Int. Ed.* **2007**, *46*, 8782–8784.
[13] Y. Z. Liu, K. Yuan, L. L. Lv, Y. C. Zhu, Z. Yuan, *J. Phys. Chem. A* **2015**, *119*, 5842–5852.
[14] W. L. Huang, X. D. Wang, S. Li, R. Zhang, Y. F. Ao, J. Tang, Q. Q. Wang, D. X. Wang, *J. Org. Chem.* **2019**, *84*, 8859–8869.
[15] A. S. Mahadevi, G. N. Sastry, *Chem. Rev.* **2016**, *116*, 2775–2825.
[16] P. Audebert, F. Miomandre, G. Clavier, M. C. Verniéres, S. Badré, R. Méallet-Renault, *Chem. - A Eur. J.* **2005**, *11*, 5667–5673.
[17] G. Clavier, P. Audebert, *Chem. Rev.* **2010**, *110*, 3299–3314.
[18] Y. H. Gong, F. Miomandre, R. Méallet-Renault, S. Badré, L. Galmiche, J. Tang, P. Audebert, G. Clavier, *European J. Org. Chem.* **2009**, *2009*, 6121–6128.
[19] I. Janowska, F. Miomandre, G. Clavier, P. Audebert, J. Zakrzewski, H. T. Khuyen, I. Ledoux-Rak, *J. Phys. Chem. A* **2006**, *110*, 12971–12975.
[20] H. Boufroura, S. Poyer, A. Gaucher, C. Huin, J. Y. Salpin, G. Clavier, D. Prim, *Chem. - A Eur. J.* **2018**, *24*, 8656–8663.
[21] O. Colin, H. Boufroura, C. Thomassigny, S. Perato, A. Gaucher, J. Marrot, D. Prim, *European J. Org. Chem.* **2017**, *2017*, 746–752.
[22] M. Savastano, C. Bazzicalupi, C. Giorgi, C. García-Gallarín, M. D. López De La Torre, F. Pichierri, A. Bianchi, M. Melguizo, *Inorg. Chem.* **2016**, *55*, 8013–8024.
[23] M. Savastano, C. García-Gallarín, M. D. López de la Torre, C. Bazzicalupi, A. Bianchi, M. Melguizo, *Coord. Chem. Rev.* **2019**, *397*, 112–137.
[24] M. J. Frisch, G. W. Trucks, H. B. Schlegel, G. E. Scuseria, M. A. Robb, J. R. Cheeseman, G. Scalmani, V. Barone, B. Mennucci, G. A. Petersson, et al., *Gaussian 09, Revis. B.01, Gaussian, Inc., Wallingford CT* **2009**.
[25] A. Austin, G. A. Petersson, M. J. Frisch, F. J. Dobek, G. Scalmani, K. Throssell, in *J. Chem. Theory Comput.*, American Chemical Society, **2012**, pp. 4989–5007.
[26] J. Contreras-García, E. R. Johnson, S. Keinan, R. Chaudret, J. P. Piquemal, D. N. Beratan, W. Yang, *J. Chem. Theory Comput.* **2011**, *7*, 625–632.
[27] Henry S. Rzepa, "Script for creating an NCI surface as a JVXL compressed file from a (Gaussian) cube of total electron density," can be found under https://www.ch.ic.ac.uk/rzepa/cub2nci/, **2013**.
[28] B. P. Pritchard, D. Altarawy, B. Didier, T. D. Gibson, T. L. Windus, *J. Chem. Inf. Model.* **2019**, *59*, 4814–4820.
[29] R. D. J. Gless, S. K. Anandan, *Soluble Epoxide Hydrolase Inhibitors*, **2008**, WO 2008/116145 A2.
[30] Y. H. Gong, P. Audebert, G. Clavier, F. Miomandre, J. Tang, S. Badré, R. Méallet-Renault, E. Naidus, *New J. Chem.* **2008**, *32*, 1235–1242.
[31] P. J. Linstrom, W. G. Mallard, *NIST Chemistry WebBook, NIST Standard Reference Database Number 69*, National Institute of Standards and Technology, Gaithersburg MD, 20899, **1997**.
[32] G. González-Gaitano, G. Tardajos, *J. Chem. Educ.* **2004**, *81*, 270–274.
[33] C. Würth, M. Grabolle, J. Pauli, M. Spieles, U. Resch-Genger, *Nat. Protoc.* **2013**, *8*, 1535–1550.
[34] A. P. De Silva, H. Q. N. Gunaratne, T. Gunnlaugsson, A. J. M. Huxley, C. P. McCoy, J. T. Rademacher, T. E. Rice, *Chem. Rev.* **1997**, *97*, 1515–1566.
[35] B. Valeur, M. N. Berberan-Santos, *Molecular Fluorescence: Principles and Applications, Second Edition*, Wiley-VCH, **2012**.

Entry for the Table of Contents

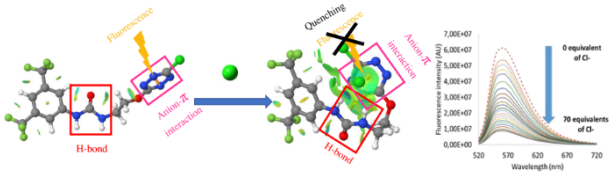

Detection AND recognition: on the prominent dual role of tetrazine in anion-π / H-bond based anion receptors. The rational design and complexation properties of a new molecular platform combining tetrazine and urea patterns are reported. Binding constants have been predicted by DFT calculations and cross-determined by a complementary set of experimental techniques taking benefits from the joint presence of tetrazine and urea units.

SUPPORTING INFORMATION

Supporting Information

69451 Weinheim, Germany

Intertwined detection and recognition roles of tetrazine in synergistic anion-π and H-bond based anion receptor

Romain Plais, [a] Guy Gouarin, [a] Anne Gaucher, [a] Violette Haldys, [b],[c] Arnaud Brosseau, [d] Gilles Clavier, [d] Jean-Yves Salpin, [b],[c] Damien Prim*[a]

Abstract: The intrinsic properties of tetrazine as a p-anion receptor and as an on/off recognition probe merged with H-bond ability of an urea motif into a single architecture designs a new generation of well-defined anion receptors. Complexation properties directly benefit from the dual and synergistic contribution of tetrazine and urea. In this study, we report on the synthesis and assessment of binding properties to anions of diverse geometries. Association constants have been predicted by theoretical calculations and evaluated by multiple and complementary experimental techniques including electrospray-mass tandem spectroscopy, NMR, UV-Visible, steady state fluorescence spectroscopies and time resolved fluorescence. These results provide the basis for a better understanding of both the complexation and the anion-dependent quenching mechanism.

[a] Mr. R. Plais, Mr. G. Gouarin, Dr. A. Gaucher, Prof. Dr. D. Prim
Université Paris-Saclay, UVSQ, CNRS, ILV, 78035 Versailles, France
E-mail: damien.prim@uvsq.fr
[b] Mme. V. Haldys, Dr. J.-Y. Salpin
Université Paris-Saclay, Univ Evry CNRS, LAMBE, 91025 Evry-Courcouronnes, France
[c] Mme. V. Haldys, Dr. J.-Y. Salpin
CYU Paris Cergy Université, CNRS, LAMBE, 95000, Cergy, France
[d] Mr. A Brosseau, Dr. G. Clavier
Université Paris-Saclay, ENS Paris-Saclay, CNRS, PPSM, 94235 Cachan, France

SUPPORTING INFORMATION

Table of contents

Table of illustrations

SUPPORTING INFORMATION

1. General procedures, Material and Instrumentation

1.1 General experimental procedures and Materials

Unless otherwise noted, all starting materials were obtained from commercial suppliers and used without purification. N,N-Dimethylformamide (100mL, Anhydrous, 99.8%) was purchased at Sigma-Aldrich. Dichloromethane was distilled over Sodium and under argon. For NMR titrations, deuterated acetonitrile (99.80% D) was purchased in 0.75mL precoated bulbs from Eurisotop®. For photophysical analysis, acetonitrile RS –SPECTROSOL – For optical spectroscopy was purchased from Carlo Erba®.

Reaction progress was carried out using pre-coated TLC sheets ALUGRAM® Xtra SIL G/UV_{254} (0.20mm) from Macherey-Nagel® and visualized under 254 and 365 nm UV lamp from Fisher Bioblock Scientific®. Flash chromatography were proceeded using Silica 60M (0.04-0.063mm) for column chromatography silica gel from Macherey-Nagel®.

1.2 Instrumentation

^{1}H NMR spectra were recorded with Bruker AV-I 300MHz spectrometer at 298K, referenced to TMS signal and were calibrated using residual proton in MeOD (δ=3.31ppm), according to the literature. [1] ^{19}F NMR spectra were recorded with Bruker AV-I 300MHz spectrometer at 282MHz and 298K and were calibrated using $CFCl_3$ (δ=0.00ppm). [2] ^{13}C NMR spectra were recorded with a Bruker AV-I 300MHz spectrometer at 75MHz and 298 K and were calibrated using MeOD (δ = 49.00 ppm). [1] ^{1}H NMR spectroscopic data are reported as follow: chemical shift δ [parts per million] (multiplicity, coupling constants in Hertz, integration). Multiplicities are reported as follow: s = singlet, d = doublet, t = triplet, q = quadruplet, quint = quintuplet, sext = sextuplet, hept = heptuplet, dd = doublet of doublet, td = triplet of doublet, tt = triplet of triplet, ddd = doublet of doublet of doublet, m = multiplet. ^{13}C NMR spectroscopic data are reported in terms of chemical shifts δ [ppm] and when it is necessary multiplicity and coupling constant in Hertz.

To check the structure of the product obtained during the synthesis, high resolution mass spectra (HRMS) were obtained with a Waters Xevo QTOF instrument fitted with an electrospray ionization source (ESI+), using Leucine Enkephaline solution as internal calibrant. In order to study the interaction of **1** with the various anions, a 3D ion trap instrument (Bruker Amazon Speed ETD) has been used. Complexes were generated in the gas phase by electrospraying equimolar mixtures of **1**/TBAX. Starting from 10^{-1}M stock solutions of **1** and TBAX prepared in acetonitrile (ACN) and purified water, respectively, 10^{-4} M mixtures of **1**/TBAX (90/10 ACN/H_2O) were introduced in the electrospray source by a syringe pump (3 µL/min). Typical experimental conditions were as followed: Capillary voltage: 4000 V; End plate offset : -550 V; Dry gas: 5 L/min / Dry gas temperature: 200 °C, Nebuliser gas : 7.3 PSI ; Cap exit: -140 ; Trap Drive 49.5 ; MS analysis : ICC mode : “on” and acquisition time : auto.

MS/MS analysis : ICC mode off / accumulation time 1 ms / Isolation window 6 or 8 Da / Fragmentation delay 40 ms / amplitude 0.20-0.50.

UV-Visible spectra were recorded at 25°C on a Cary 400 (Agilent) double-beam spectrometer using a 10 mm path quartz cell.

Emission spectra were measured on a Fluoromax-3 (Horiba) or a Fluorolog-3 (Horiba) spectrofluorometer. An angle configuration of 90° was used. Optical density of the samples was checked to be less than 0.1 to avoid reabsorption artifacts.

Fluorescence decay curves in the ns regime were obtained by the time-correlated single-photon counting (TCSPC) method with a femtosecond laser excitation composed of a Titanium Sapphire laser (Tsunami, Spectra-Physics) pumped by a double Nd:YV04 laser (Millennia Xs, Spectra Physics). Light pulses at 990 nm from the oscillator were selected by an acousto-optic crystal at a repetition rate of 4 MHz, and then tripled at 330 nm by non-linear crystals. Fluorescence photons were detected at 90° through a monochromator and a polarizer at magic angle by means of a Hamamatsu MCP R3809U photomultiplier, connected to a SPC-630 TCSPC module from Becker & Hickl. The instrumental response function was recorded before each decay measurement with a fwhm (full width at half-maximum) of ~25 ps.

1.3 Molecular modelling and software

All calculations were carried out using Gaussian 09® program:
Gaussian 09, Revision D.01, M. J. Frisch, G. W. Trucks, H. B. Schlegel, G. E. Scuseria, M. A. Robb, J. R. Cheeseman, G. Scalmani, V. Barone, B. Mennucci, G. A. Petersson, H. Nakatsuji, M. Caricato, X. Li, H. P. Hratchian, A. F. Izmaylov, J. Bloino, G. Zheng, J. L. Sonnenberg, M. Hada, M. Ehara, K. Toyota, R. Fukuda, J. Hasegawa, M. Ishida, T. Nakajima, Y. Honda, O. Kitao, H. Nakai, T. Vreven, J. A. Montgomery, Jr., J. E. Peralta, F. Ogliaro, M. Bearpark, J. J. Heyd, E. Brothers, K. N. Kudin, V. N. Staroverov, T. Keith, R. Kobayashi, J. Normand, K. Raghavachari, A. Rendell, J. C. Burant, S. S. Iyengar, J. Tomasi, M. Cossi, N. Rega, J. M. Millam, M. Klene, J. E. Knox, J. B. Cross, V. Bakken, C. Adamo, J. Jaramillo, R. Gomperts, R. E. Stratmann, O. Yazyev, A. J. Austin, R. Cammi, C. Pomelli, J. W. Ochterski, R. L. Martin, K. Morokuma, V. G. Zakrzewski, G. A. Voth, P. Salvador, J. J. Dannenberg, S. Dapprich, A. D. Daniels, O. Farkas, J. B. Foresman, J. V. Ortiz, J. Cioslowski, and D. J. Fox, Gaussian, Inc., Wallingford CT, 2013.

Computed structures were preoptimized with a MM2 forcefield using Chem3D®. Then, optimizations were calculated at APFD/6-31G+(d,p) calculation level using Gaussian® software without any solvent correction. For the complex including bromide and iodide ions, a double basis set composed of APFD/6-31G+(d,p) for carbon, nitrogen, hydrogen, fluoride, oxygen, chloride and LANL2DZ for bromide or iodine, respectively, was used. Stationary points were verified by a harmonic vibrational frequencies calculation. None of the predicated geometry has any imaginary frequency implying that the optimized geometry of each of the molecules under study lay at a minimum local point on the potential energy surface.

Effect of solvent (acetonitrile) on geometries was evaluated by proceeding optimizations calculations at APFD/6-31G+(d,p) by adding the Polarizable Continuum Model (PCM) using the integral equation formalism variant (IEFPCM). Once again, stationary points were verified by a harmonic vibrational frequencies calculation. None of the predicated geometry has any imaginary frequency implying that the optimized geometry of each of the molecules under study lay at a minimum local point on the potential energy surface.

Gibbs free energies without solvent effect were calculated by generating frequencies calculations from optimized geometries of anions, receptor and complexes with and without anions using the triple zeta basis set APFD/aug-cc-pvtz level of calculation. Basis sets of bromide and iodide atoms at aug-cc-pvtz level of calculation were downloaded on basissetexchange.org.

Effect of solvent (acetonitrile) on Gibbs Free Energies was evaluated by generating frequencies calculations from optimized structures of anions, receptor and complexes with and without anions using the triple zeta basis set APFD/aug-cc-pvtz level of calculation. Basis sets of bromide and iodide atoms at aug-cc-pvtz level of calculation were downloaded on basissetexchange.org.

Theoretical UV-Visible spectra were calculated on optimized geometries structures in vacuum by an energy calculation using time dependant DFT calculation at TDpbe0/6-311+g(d,p)//b3lyp/6-31+g(d) level and solving on 12 first singlet states. When specified, a standard solvation model for acetonitrile was used.

Electrostatic Potentials Surfaces (ESP) were thus calculated using Gaussview® software from optimized structures in vacuum using a fine grid for Total Density and a medium grid for ESP. NCIplots were generated from total densities calculations using the script developed by Rzepa available on the website application of the Imperial College London. [3,4]

2. Computational Data of 1, anions and 1-anion complexes

2.1 Coordinates and thermodynamic data

Electronic energies reported afterwards are defined as the sum of electronic and zero-point energies calculated from Gaussian software. All energies, unless precised, are expressed in Hartrees.

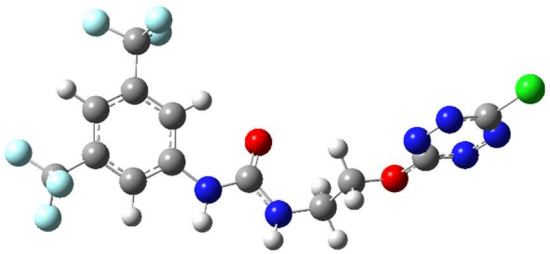

1

APFD/6-31+G(d,p)
Charge: 0
Spin Multiplicity: Singlet
Imaginary frequencies: 0
Electronic Energy (ZPE correction): -2037.491528 Hartree

Symbol	X	Y	Z
C	-3.56056400	1.34585500	-0.29396900
C	-4.72867300	0.78309600	0.21034900
C	-4.73227200	-0.58346100	0.47221200
C	-3.60433600	-1.36255300	0.24635200
C	-2.43290700	-0.78264000	-0.25691400
C	-2.41553300	0.59073300	-0.53217100
N	-1.33542800	-1.62493300	-0.45076800
C	-0.10047400	-1.29624200	-0.98853500
N	0.78991500	-2.34718800	-0.99041100
O	0.17982800	-0.19559100	-1.44238000
C	2.13363100	-2.13909100	-1.48648300
C	2.99423000	-1.38971600	-0.47904700
O	4.29347700	-1.28321600	-1.07897700
C	5.23612000	-0.64688300	-0.40573600
N	6.42006900	-0.57932400	-1.04667600
N	7.38307700	0.04694500	-0.43416700
C	7.11156000	0.56432100	0.77453200
N	5.95398900	0.48266000	1.41962000
N	4.97501800	-0.14861800	0.80687900
Cl	8.39097600	1.39902400	1.55817200
C	-3.49490900	2.82932400	-0.55939300
F	-2.83158300	3.47454500	0.42768800
F	-4.71969700	3.38690600	-0.64112700
F	-2.84830600	3.10599100	-1.70947900
C	-5.95306800	-1.24429000	1.05666200
F	-6.17644100	-2.45875400	0.50527800
F	-7.06736100	-0.51118900	0.88128100
F	-5.81482300	-1.44632700	2.38832500
H	-5.61230000	1.38653000	0.38300000
H	-3.64233000	-2.42884800	0.45949900

H	-1.52269800	1.04907400	-0.93779000
H	-1.50647000	-2.60068700	-0.24990300
H	0.63586800	-3.13328500	-0.37421300
H	2.57501600	-3.11391500	-1.71613600
H	2.07467400	-1.56803200	-2.41674100
H	2.59060200	-0.39192600	-0.28366600
H	3.07522600	-1.92991600	0.47169900

Cl^-
APFD/6-31+G(d,p)
Charge: -1
Spin Multiplicity: Singlet
Imaginary frequencies: 0
Electronic Energy (ZPE correction): -460.149600 Hartree

Frequencies calculation (vacuum)	***Frequencies calculation (IEFPCM, Acetonitrile)***
APFD/aug-cc-pvtz	APFD/aug-cc-pvtz scrf=(iefpcm,solvent=acetonitrile)
Zero-point correction= 0.000000 (Hartree/Particle)	Zero-point correction= 0.000000 (Hartree/Particle)
Thermal correction to Energy= 0.001416	Thermal correction to Energy= 0.001416
Thermal correction to Enthalpy= 0.002360	Thermal correction to Enthalpy= 0.002360
Thermal correction to Gibbs Free Energy= -0.015023	Thermal correction to Gibbs Free Energy= -0.015023
Sum of electronic and zero-point Energies= -460.184512	Sum of electronic and zero-point Energies= -460.293942
Sum of electronic and thermal Energies= -460.183096	Sum of electronic and thermal Energies= -460.292526
Sum of electronic and thermal Enthalpies= -460.182151	Sum of electronic and thermal Enthalpies= -460.291582
Sum of electronic and thermal Free Energies= -460.199535	Sum of electronic and thermal Free Energies= -460.308965

Br^-
APFD/6-31+G(d,p)
Charge: -1
Spin Multiplicity: Singlet
Imaginary frequencies: 0
Electronic Energy (ZPE correction): -2571.803183 Hartree

Frequencies calculation (vacuum)	***Frequencies calculation (IEFPCM, Acetonitrile)***
APFD/aug-cc-pvtz	APFD/aug-cc-pvtz scrf=(iefpcm,solvent=acetonitrile)
Zero-point correction= 0.000000 (Hartree/Particle)	Zero-point correction= 0.000000 (Hartree/Particle)
Thermal correction to Energy= 0.001416	Thermal correction to Energy= 0.001416
Thermal correction to Enthalpy= 0.002360	Thermal correction to Enthalpy= 0.002360
Thermal correction to Gibbs Free Energy= -0.016176	Thermal correction to Gibbs Free Energy= -0.016176
Sum of electronic and zero-point Energies= -416.970349	Sum of electronic and zero-point Energies= -417.072485
Sum of electronic and thermal Energies= -416.968933	Sum of electronic and thermal Energies= -417.071068
Sum of electronic and thermal Enthalpies= -416.967989	Sum of electronic and thermal Enthalpies= -417.070124
Sum of electronic and thermal Free Energies= -416.986525	Sum of electronic and thermal Free Energies= -417.088660

I^-
APFD/LANL2DZ
Charge: -1
Spin Multiplicity: Singlet
Imaginary frequencies: 0
Electronic Energy (ZPE correction): -11.483295 Hartree

Frequencies calculation (vacuum)	***Frequencies calculation (IEFPCM, Acetonitrile)***
APFD/aug-cc-pvtz	APFD/aug-cc-pvtz scrf=(iefpcm,solvent=acetonitrile)
Zero-point correction= 0.000000 (Hartree/Particle)	Zero-point correction= 0.000000 (Hartree/Particle)
Thermal correction to Energy= 0.001416	Thermal correction to Energy= 0.001416
Thermal correction to Enthalpy= 0.002360	Thermal correction to Enthalpy= 0.002360

Thermal correction to Gibbs Free Energy= -0.016848 Sum of electronic and zero-point Energies= -295.867896 Sum of electronic and thermal Energies= -295.866479 Sum of electronic and thermal Enthalpies= -295.865535 Sum of electronic and thermal Free Energies= -295.884744	Thermal correction to Gibbs Free Energy= -0.016848 Sum of electronic and zero-point Energies= -295.961510 Sum of electronic and thermal Energies= -295.960094 Sum of electronic and thermal Enthalpies= -295.959150 Sum of electronic and thermal Free Energies= -295.978358

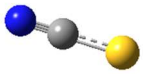

SCN^- *(in vacuum)*
APFD/6-31+G(d,p)
Charge: -1
Spin Multiplicity: Singlet
Imaginary frequencies: 0
Electronic Energy (ZPE correction): -490.914975 Hartree

	Symbol	X	Y	Z
S		0.00000000	0.00000000	1.03127300
C		0.00000000	0.00000000	-0.63279000
N		0.00000000	0.00000000	-1.81480500

Frequencies calculation (vacuum)
APFD/aug-cc-pvtz

Zero-point correction= 0.008766 (Hartree/Particle)
Thermal correction to Energy= 0.011658
Thermal correction to Enthalpy= 0.012602
Thermal correction to Gibbs Free Energy= -0.013732
Sum of electronic and zero-point Energies= -490.977609
Sum of electronic and thermal Energies= -490.974717
Sum of electronic and thermal Enthalpies= -490.973773
Sum of electronic and thermal Free Energies= -491.000107

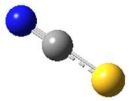

SCN^- (*in acetonitrile*)
APFD/6-31+G(d,p) scrf=(iefpcm,solvent=acetonitrile)
Charge: -1
Spin Multiplicity: Singlet
Imaginary frequencies: 0
Electronic Energy (ZPE correction): -491.005654 Hartree

	Symbol	X	Y	Z
N		0.00143600	1.81136600	0.00000000
C		0.00000000	0.62966800	0.00000000
S		-0.00062800	-1.02859800	0.00000000

Frequencies calculation (in acetonitrile)
Zero-point correction= 0.008743 (Hartree/Particle)
Thermal correction to Energy= 0.011634
Thermal correction to Enthalpy= 0.012578
Thermal correction to Gibbs Free Energy= -0.013749
Sum of electronic and zero-point Energies= -491.067360
Sum of electronic and thermal Energies= -491.064469
Sum of electronic and thermal Enthalpies= -491.063525
Sum of electronic and thermal Free Energies= -491.089853

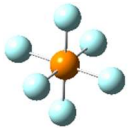

PF_6^- *(in vacuum)*
APFD/6-31+G(d,p)
Charge: -1
Spin Multiplicity: Singlet
Imaginary frequencies: 0
Electronic Energy (ZPE correction): -940.181307 Hartree

	Symbol	X	Y	Z
P		0.00000000	0.00000000	0.00000000
F		0.00000000	0.00000000	1.63960500
F		0.00000000	1.63960500	0.00000000
F		1.63960500	0.00000000	0.00000000
F		0.00000000	0.00000000	-1.63960500
F		-1.63960500	0.00000000	0.00000000
F		0.00000000	-1.63960500	0.00000000

Frequencies calculation (in vacuum)
APFD/aug-cc-pvtz

Zero-point correction= 0.018592 (Hartree/Particle)
Thermal correction to Energy= 0.024763
Thermal correction to Enthalpy= 0.025707
Thermal correction to Gibbs Free Energy= -0.008607
Sum of electronic and zero-point Energies= -940.449084
Sum of electronic and thermal Energies= -940.442914
Sum of electronic and thermal Enthalpies= -940.441969
Sum of electronic and thermal Free Energies= -940.476283

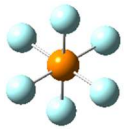

PF_6^- *(in acetonitrile)*
APFD/6-31+G(d,p) scrf=(iefpcm,solvent=acetonitrile)
Charge: -1
Spin Multiplicity: Singlet
Imaginary frequencies: 0
Electronic energy (ZPE correction): -940.265191 Hartree

	Symbol	X	Y	Z
P		0.00002200	0.00000100	0.00003400
F		1.27676500	0.90597500	0.48117400
F		-0.55510200	-0.03606200	1.54014000
F		-0.86282100	1.36402500	-0.27901800
F		-1.27679500	-0.90605200	-0.48114100
F		0.55519600	0.03600600	-1.54003700
F		0.86272100	-1.36389400	0.27882700

Frequencies calculation (in acetonitrile)
APFD/aug-cc-pvtz

Zero-point correction= 0.018328 (Hartree/Particle)
Thermal correction to Energy= 0.024532
Thermal correction to Enthalpy= 0.025476
Thermal correction to Gibbs Free Energy= -0.011879
Sum of electronic and zero-point Energies= -940.532848
Sum of electronic and thermal Energies= -940.526643
Sum of electronic and thermal Enthalpies= -940.525699
Sum of electronic and thermal Free Energies= -940.563054

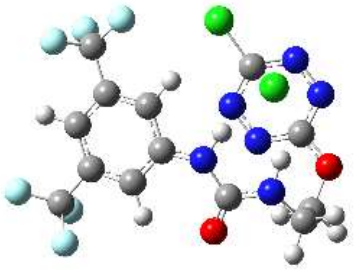

1+Cl^- *(in vacuum)*
APFD/6-31+G(d,p)
Charge: -1
Spin Multiplicity: Singlet
Imaginary frequencies: 0
Electronic Energy (ZPE correction): -2497.728308 Hartree

Symbol	X	Y	Z
C	-2.86035500	-1.21693200	-0.08209500
C	-3.27345800	0.10931900	-0.03818700
C	-2.38449700	1.05148800	0.48341500
C	-1.12944700	0.68778700	0.94205200
C	-0.72181800	-0.65985600	0.88963600
C	-1.60396700	-1.61794100	0.36995800
N	0.53972600	-0.94594400	1.36627000
C	1.29385900	-2.06917900	1.07643800
N	2.60560400	-1.90788500	1.44717300
O	0.85834600	-3.10023300	0.56146900
C	3.59699600	-2.76827500	0.85803600
C	3.82072600	-2.48640700	-0.62513500
O	4.34011600	-1.15671100	-0.82451100
C	3.50125600	-0.15509800	-1.05451100
N	2.18978900	-0.36861200	-1.17933300
N	1.41446800	0.68730100	-1.23839600
C	2.01903900	1.86627300	-1.16783000
N	3.32738800	2.06940000	-1.35712700
N	4.10029200	1.02284900	-1.31316200
Cl	1.01513300	3.25445700	-1.02733200
C	-3.76949300	-2.25006200	-0.68431400
F	-3.50804600	-2.45726600	-2.00047500
F	-5.07639600	-1.89512400	-0.61178000
F	-3.65993100	-3.45479900	-0.08163600
C	-2.82342800	2.48722800	0.51823400
F	-1.93275700	3.30372900	1.10792200
F	-3.99866000	2.63570900	1.18863600
F	-3.04725700	2.97815200	-0.72753300
H	-4.25552200	0.40509100	-0.39150600
H	-0.44082900	1.43582300	1.32666900
H	-1.29139200	-2.65328800	0.31818300
H	1.10104600	-0.12205300	1.65124600
H	2.89571800	-0.94947800	1.68809100
H	4.53438900	-2.63356300	1.40859900
H	3.28098700	-3.81282500	0.96226000
H	2.89184600	-2.61704900	-1.18568900
H	4.59651000	-3.14268700	-1.03237500
Cl	2.68331600	1.23861000	1.87971500

Frequencies calculation (vacuum, with Cl-)	***Frequencies calculation (vacuum, without Cl-)***
APFD/aug-cc-pvtz	APFD/aug-cc-pvtz

Zero-point correction= 0.238903 (Hartree/Particle) Thermal correction to Energy= 0.264486 Thermal correction to Enthalpy= 0.265430 Thermal correction to Gibbs Free Energy= 0.181399 Sum of electronic and zero-point Energies= -2498.327756 Sum of electronic and thermal Energies= -2498.302173 Sum of electronic and thermal Enthalpies= -2498.301229 Sum of electronic and thermal Free Energies= -2498.385260	Zero-point correction= 0.238338 (Hartree/Particle) Thermal correction to Energy= 0.262005 Thermal correction to Enthalpy= 0.262950 Thermal correction to Gibbs Free Energy= 0.182895 Sum of electronic and zero-point Energies= -2038.055403 Sum of electronic and thermal Energies= -2038.031735 Sum of electronic and thermal Enthalpies= -2038.030791 Sum of electronic and thermal Free Energies= -2038.110845

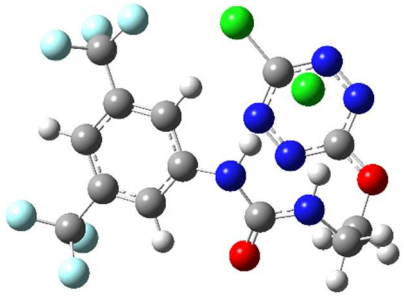

1+Cl^-+ACN *(in acetonitrile)*
APFD/6-31+G(d,p), scrf=(iefpcm,solvent=acetonitrile)
Charge: -1
Spin Multiplicity: Singlet
Imaginary Frequencies: 0
Electronic Energy (ZPE correction): -2497.817538 Hartree

Symbol	X	Y	Z
C	-2.80939000	-1.26655300	-0.05961700
C	-3.25539500	0.04817100	-0.01108500
C	-2.39126700	1.00626600	0.52216200
C	-1.12903100	0.66857600	0.98146600
C	-0.68671500	-0.66537700	0.91632800
C	-1.54477800	-1.64066900	0.39390500
N	0.59068900	-0.92213000	1.38430600
C	1.37884300	-2.01520300	1.07284300
N	2.68662700	-1.82689800	1.42811700
O	0.96107200	-3.05228700	0.55055800
C	3.71267500	-2.67156000	0.86190900
C	3.95522200	-2.39478400	-0.61758500
O	4.37648700	-1.02133500	-0.81261800
C	3.48043200	-0.08772300	-1.06808300
N	2.18453700	-0.38456200	-1.21398900
N	1.34506000	0.61640100	-1.31886300
C	1.86145000	1.83761000	-1.27172900
N	3.16285600	2.12922100	-1.35539500
N	4.00346600	1.13907600	-1.26567500
Cl	0.75994900	3.15559500	-1.22194200
C	-3.68670200	-2.32569800	-0.66798100
F	-3.35436000	-2.56997600	-1.96185900
F	-4.99245700	-1.98202800	-0.66551500
F	-3.58764700	-3.50879100	-0.02140500
C	-2.85026100	2.43714700	0.55706900
F	-2.00936600	3.24408700	1.23326100
F	-4.06918800	2.56054700	1.13580400
F	-2.97177400	2.95465000	-0.69142800
H	-4.24215000	0.32019600	-0.36836400
H	-0.46812900	1.43219800	1.38023900
H	-1.21524000	-2.66965700	0.34115700
H	1.11789300	-0.08919000	1.68044500
H	2.95673600	-0.87846700	1.69786400
H	4.63293300	-2.51190100	1.42993100
H	3.42763700	-3.72240600	0.96947000
H	3.06218500	-2.59375700	-1.21228300
H	4.78963200	-2.99058200	-0.99175600

Cl	2.65640500	1.38365000	1.96564500

Frequencies calculation (Acetonitrile, with Cl-)	***Frequencies calculation (Acetonitrile, without Cl-)***
APFD/aug-cc-pvtz scrf=(iefpcm,solvent=acetonitrile)	APFD/aug-cc-pvtz scrf=(iefpcm,solvent=acetonitrile)
Zero-point correction= 0.238577 (Hartree/Particle)	Zero-point correction= 0.238446 (Hartree/Particle)
Thermal correction to Energy= 0.264373	Thermal correction to Energy= 0.262098
Thermal correction to Enthalpy= 0.265318	Thermal correction to Enthalpy= 0.263042
Thermal correction to Gibbs Free Energy= 0.180552	Thermal correction to Gibbs Free Energy= 0.182963
Sum of electronic and zero-point Energies= -2498.397789	Sum of electronic and zero-point Energies= -2038.079950
Sum of electronic and thermal Energies= -2498.371992	Sum of electronic and thermal Energies= -2038.056298
Sum of electronic and thermal Enthalpies= -2498.371048	Sum of electronic and thermal Enthalpies= -2038.055354
Sum of electronic and thermal Free Energies= -2498.455813	Sum of electronic and thermal Free Energies= -2038.135433

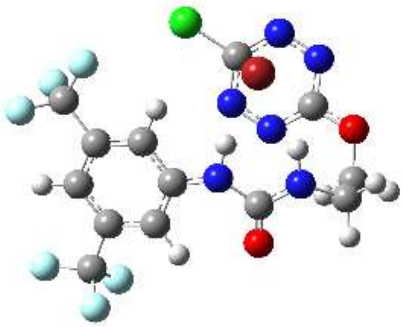

1+Br^- (in vacuum)
APFD/6-31+G(d,p) for H,C,N,O,F,Cl and APFD/LANL2DZ for Br
Charge: -1
Spin Multiplicity: Singlet
Imaginary frequencies: 0
Electronic Energy (ZPE correction): -4609.816138 Hartree

Symbol	X	Y	Z
C	3.15540200	-1.07081100	0.01690100
C	3.44585300	0.28671700	0.02627400
C	2.45645000	1.16756200	-0.41968000
C	1.22342200	0.71310200	-0.85490100
C	0.94205800	-0.66802300	-0.85692500
C	1.92401800	-1.56393500	-0.41706000
N	-0.30896000	-1.04675900	-1.30288300
C	-0.95996500	-2.23105400	-1.00668000
N	-2.29959900	-2.16960300	-1.30323600
O	-0.41816700	-3.23681500	-0.54704800
C	-3.18361200	-3.12610600	-0.68978200
C	-3.33275800	-2.91999000	0.81494700
O	-3.94052400	-1.64734200	1.10822300
C	-3.17070100	-0.59467700	1.35421200
N	-3.84066400	0.50088600	1.76095600
N	-3.15654600	1.60524200	1.83690200
C	-1.85626700	1.53716200	1.52602700
N	-1.15254700	0.41417000	1.44829800
N	-1.84009800	-0.69885400	1.35845000
Cl	-0.98496600	3.01483300	1.43988800
C	4.17455800	-2.06747000	0.49060400
F	5.36017600	-1.49657700	0.80868900
F	4.43938400	-3.01159600	-0.44620000
F	3.76118600	-2.73810200	1.59282600
C	2.75953200	2.63822800	-0.38884700
F	3.89791800	2.92903500	-1.07649300
F	2.97114600	3.08396600	0.87576800
F	1.78195400	3.39530100	-0.91489600
H	4.40728100	0.65503700	0.36674100
H	0.45371400	1.41280100	-1.17213300
H	1.70908100	-2.62553800	-0.40459300
H	-0.93589400	-0.26199100	-1.54002700
H	-2.68796200	-1.23938400	-1.49599300
H	-4.16134700	-3.04418200	-1.17694100

H	-2.79679500	-4.13802500	-0.85756500
H	-2.36213200	-2.99868400	1.31088500
H	-4.02639200	-3.65421500	1.23749900
Br	-2.71915900	1.18334900	-1.62721700

Frequencies calculation (in vacuum, with Br-)	***Frequencies calculation (in vacuum, without Br-)***
APFD/aug-cc-pvtz	APFD/aug-cc-pvtz
Zero-point correction= 0.238229 (Hartree/Particle)	Zero-point correction= 0.237896 (Hartree/Particle)
Thermal correction to Energy= 0.264034	Thermal correction to Energy= 0.261651
Thermal correction to Enthalpy= 0.264978	Thermal correction to Enthalpy= 0.262595
Thermal correction to Gibbs Free Energy= 0.179968	Thermal correction to Gibbs Free Energy= 0.182475
Sum of electronic and zero-point Energies= -2455.106768	Sum of electronic and zero-point Energies= -2038.055450
Sum of electronic and thermal Energies= -2455.080963	Sum of electronic and thermal Energies= -2038.031694
Sum of electronic and thermal Enthalpies= -2455.080019	Sum of electronic and thermal Enthalpies= -2038.030750
Sum of electronic and thermal Free Energies= -2455.165029	Sum of electronic and thermal Free Energies= -2038.110870

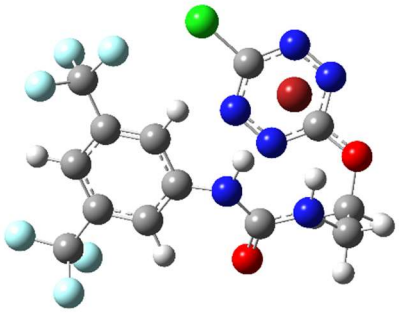

1+Br⁻-ACN (*in acetonitrile*)
APFD/6-31+G(d,p) for H,C,N,O,F,Cl and APFD/aug-cc-pvtz for Br, scrf=(iefpcm,solvent=acetonitrile)
Charge: -1
Spin Multiplicity: Singlet
Imaginary frequencies: 0
Electronic Energy (ZPE correction): -2454.612489 Hartree

C	-3.09536100	1.12628300	-0.02015000
C	-3.41656600	-0.22403700	-0.00532500
C	-2.44733000	-1.12532500	-0.45327000
C	-1.20565500	-0.69706000	-0.89108800
C	-0.89201300	0.67512000	-0.89206100
C	-1.85466800	1.59251000	-0.45812000
N	0.37590900	1.02461900	-1.32872300
C	1.05983500	2.18559200	-1.01455000
N	2.39777400	2.09040400	-1.28538700
O	0.53269300	3.20328700	-0.55779800
C	3.31789100	3.03747500	-0.69842100
C	3.47693900	2.85326200	0.80667700
O	3.98764500	1.53016500	1.10617700
C	3.15174400	0.54664800	1.37794800
N	3.75405800	-0.61028600	1.71995000
N	2.99000200	-1.65714000	1.84486300
C	1.67891300	-1.48657300	1.64850600
N	1.06563300	-0.31411000	1.54495600
N	1.82865600	0.74201200	1.40474100
Cl	0.69131500	-2.89211500	1.65466500
C	-4.08994300	2.14952000	0.45425000
F	-5.28134100	1.61090000	0.78353800
F	-4.33104900	3.09400100	-0.48730400
F	-3.64406000	2.81445800	1.54887600
C	-2.77276300	-2.59239800	-0.42039400
F	-3.91780400	-2.86875900	-1.09153400
F	-2.96411600	-3.03497700	0.84751300
F	-1.80547400	-3.35869000	-0.96037000
H	-4.38525600	-0.56763600	0.33909600
H	-0.45895500	-1.41640400	-1.21497300
H	-1.62364800	2.64987100	-0.45516600
H	0.97702100	0.22615100	-1.56943600
H	2.76183800	1.16074600	-1.49952800
H	4.28420100	2.92184000	-1.19643600

H	2.96459000	4.05697000	-0.88048400
H	2.53088600	3.00816300	1.32784700
H	4.23389100	3.53331500	1.20176700
Br	2.68413200	-1.30747700	-1.66406600

Frequencies calculation (in acetonitrile, with Br-)	***Frequencies calculation (in acetonitrile, without Br-)***
APFD/aug-cc-pvtz scrf=(iefpcm,solvent=acetonitrile)	APFD/aug-cc-pvtz scrf=(iefpcm, solvent=acetonitrile)
Zero-point correction= 0.237884 (Hartree/Particle)	Zero-point correction= 0.237519 (Hartree/Particle)
Thermal correction to Energy= 0.263197	Thermal correction to Energy= 0.259806
Thermal correction to Enthalpy= 0.264142	Thermal correction to Enthalpy= 0.260751
Thermal correction to Gibbs Free Energy= 0.179976	Thermal correction to Gibbs Free Energy= 0.184888
Sum of electronic and zero-point Energies= -2455.176092	Sum of electronic and zero-point Energies= -2038.081206
Sum of electronic and thermal Energies= -2455.150779	Sum of electronic and thermal Energies= -2038.058919
Sum of electronic and thermal Enthalpies= -2455.149835	Sum of electronic and thermal Enthalpies= -2038.057975
Sum of electronic and thermal Free Energies= -2455.234001	Sum of electronic and thermal Free Energies= -2038.133837

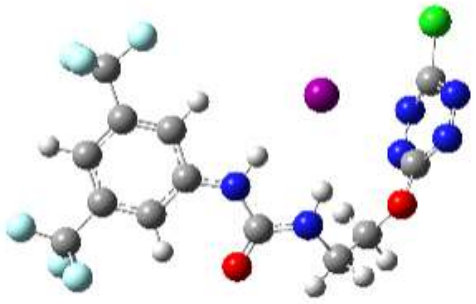

1+I^- *(in vacuum)*
APFD/6-31+G(d,p) for C, N, F, H, O, Cl and LANL2DZ for I
Charge: -1
Spin Multiplicity: Singlet
Imaginary frequencies: 0
Electronic Energy (ZPE correction): - 2049.031705 Hartree

Symbol	X	Y	Z
C	4.56096200	-0.61138100	0.18554800
C	4.70663100	0.76954900	0.18916900
C	3.56882900	1.54435900	-0.04999100
C	2.33126800	0.96629100	-0.28265000
C	2.19803400	-0.43786600	-0.28595800
C	3.33118200	-1.22802500	-0.04417500
N	0.94333300	-0.94584500	-0.55369300
C	0.51830800	-2.25784100	-0.41780200
N	-0.77500400	-2.42417500	-0.83433600
O	1.22146400	-3.17414000	0.01052100
C	-1.54151400	-3.56276800	-0.38999500
C	-2.71648600	-3.11174700	0.45550700
O	-3.62695500	-2.45388900	-0.44212800
C	-4.36036500	-1.45005400	0.00718100
N	-4.41440600	-1.16695800	1.31315100
N	-4.98862900	-0.03465000	1.64713800
C	-5.48158400	0.69308000	0.65295800
N	-5.73544600	0.23036100	-0.57768300
N	-5.16615700	-0.88906000	-0.91480800
Cl	-6.05179000	2.27162900	1.02864000
C	5.74435900	-1.49519800	0.46534900
F	5.64703700	-2.10890100	1.67013400
F	6.91399000	-0.81435900	0.47397000
F	5.87419200	-2.48143800	-0.45234700
C	3.72903800	3.03881500	-0.05095000
F	2.58011900	3.69821100	-0.27296300
F	4.61021600	3.44487000	-1.00279700
F	4.22614400	3.48990500	1.12944600
H	5.66954000	1.23450700	0.36957000
H	1.45424300	1.58555400	-0.45773700
H	3.23526200	-2.30684000	-0.03215100

H	0.19618200	-0.24865500	-0.67756300
H	-1.30723800	-1.58149900	-1.06491100
H	-1.90669800	-4.14623600	-1.24614300
H	-0.87857800	-4.20565000	0.19780300
H	-2.39737600	-2.41525400	1.23630700
H	-3.24348200	-3.95607900	0.91631900
I	-1.99887900	1.03511500	-0.57260500

Frequencies calculation (in vacuum, with I-)	***Frequencies calculation (in vacuum, without I-)***
APFD/aug-cc-pvtz	APFD/aug-cc-pvtz
Zero-point correction= 0.235945 (Hartree/Particle)	Zero-point correction= 0.235975 (Hartree/Particle)
Thermal correction to Energy= 0.262412	Thermal correction to Energy= 0.260006
Thermal correction to Enthalpy= 0.263357	Thermal correction to Enthalpy= 0.260950
Thermal correction to Gibbs Free Energy= 0.175066	Thermal correction to Gibbs Free Energy= 0.180518
Sum of electronic and zero-point Energies= -2333.988539	Sum of electronic and zero-point Energies= -2038.051929
Sum of electronic and thermal Energies= -2333.962072	Sum of electronic and thermal Energies= -2038.027898
Sum of electronic and thermal Enthalpies= -2333.961127	Sum of electronic and thermal Enthalpies= -2038.026954
Sum of electronic and thermal Free Energies= -2334.049418	Sum of electronic and thermal Free Energies= -2038.107386

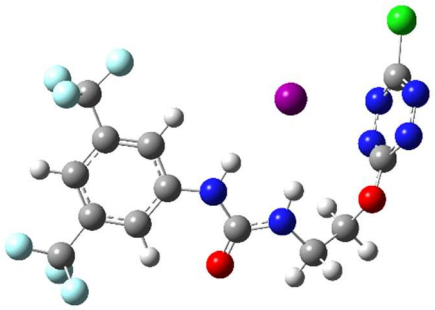

1+I$^-$-ACN *(in acetonitrile)*
APFD/6-31+G(d,p) for C, N, F, H, O, Cl and aug-cc-pvtz for I, scrf=(iefpcm,solvent=acetonitrile)
Charge: -1
Spin Multiplicity: Singlet
Imaginary frequencies: 0
Electronic Energy (ZPE correction): - 2333.491977 Hartree

Symbol	X	Y	Z
C	4.60976100	-0.64873100	0.17688600
C	4.79392000	0.72697700	0.16860700
C	3.66528300	1.52882800	-0.01744000
C	2.40381500	0.98123300	-0.18496400
C	2.23214700	-0.41669200	-0.17204800
C	3.35436300	-1.23453300	0.01194800
N	0.94486200	-0.88994000	-0.36016500
C	0.49981600	-2.19976400	-0.29600800
N	-0.81617100	-2.31755200	-0.61986800
O	1.21796400	-3.15654500	0.01408700
C	-1.55020300	-3.54486600	-0.41967700
C	-2.83550200	-3.27100100	0.32961000
O	-3.66170100	-2.47818200	-0.55754600
C	-4.39437400	-1.49217000	-0.08445800
N	-4.45941400	-1.23455800	1.22685500
N	-5.06621900	-0.12721400	1.58540300
C	-5.58520400	0.61699800	0.61725900
N	-5.73325100	0.23298000	-0.65646100
N	-5.12679200	-0.85722400	-1.02246400
Cl	-6.24391600	2.14223600	1.05400800
C	5.78014200	-1.56854000	0.39344700
F	5.69218200	-2.22248100	1.57857000
F	6.96231400	-0.91998000	0.39353000
F	5.85480100	-2.52620800	-0.56109900
C	3.85395300	3.02063600	-0.03288800
F	2.70352600	3.69651600	-0.21705900
F	4.70148000	3.40726800	-1.01788100
F	4.39439200	3.46898000	1.12663000
H	5.77715700	1.16393400	0.29994100

H	1.54184400	1.62683500	-0.32745900
H	3.23552800	-2.31008500	0.02564600
H	0.22219200	-0.17609700	-0.48380900
H	-1.34326500	-1.47354000	-0.83890300
H	-1.77296900	-4.03297600	-1.37692900
H	-0.92796500	-4.22739800	0.16506600
H	-2.64945100	-2.72255300	1.25509900
H	-3.38260800	-4.19173400	0.54963100
I	-2.01794000	1.17416700	-0.53920200

Frequencies calculation (in acetonitrile, with I-)	***Frequencies calculation (in acetonitrile, without I-)***
APFD/aug-cc-pvtz scrf=(iefpcm,solvent=acetonitrile)	APFD/aug-cc-pvtz scrf=(iefpcm,solvent=acetonitrile)
Zero-point correction= 0.237143 (Hartree/Particle)	Zero-point correction= 0.236933 (Hartree/Particle)
Thermal correction to Energy= 0.263830	Thermal correction to Energy= 0.261284
Thermal correction to Enthalpy= 0.264775	Thermal correction to Enthalpy= 0.262228
Thermal correction to Gibbs Free Energy= 0.174903	Thermal correction to Gibbs Free Energy= 0.179028
Sum of electronic and zero-point Energies= -2334.057016	Sum of electronic and zero-point Energies= -2038.076453
Sum of electronic and thermal Energies= -2334.030329	Sum of electronic and thermal Energies= -2038.052103
Sum of electronic and thermal Enthalpies= -2334.029385	Sum of electronic and thermal Enthalpies= -2038.051158
Sum of electronic and thermal Free Energies= -2334.119257	Sum of electronic and thermal Free Energies= -2038.134358

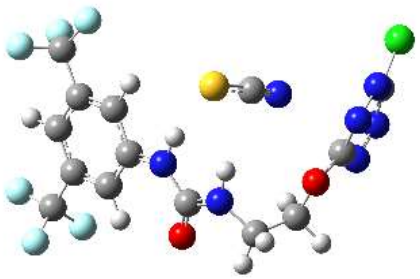

1+SCN^- (*in vacuum)*
APFD/6-31+G(d,p)
Charge: -1
Spin Multiplicity: Singlet
Imaginary frequencies: 0
Electronic Energy (ZPE correction): -2528.475466 Hartree

Symbol	X	Y	Z
C	4.05696400	-0.71253800	0.57261500
C	4.38112800	0.63287900	0.46072700
C	3.46380900	1.47083800	-0.17789500
C	2.26988500	0.98654200	-0.68692600
C	1.95510600	-0.38298100	-0.57168300
C	2.86531500	-1.23480200	0.07038000
N	0.76064000	-0.79685600	-1.12509100
C	0.14225900	-2.02350000	-0.96708400
N	-1.04198500	-2.10615100	-1.65578200
O	0.60652000	-2.95318300	-0.30607600
C	-1.97321100	-3.15672400	-1.32677800
C	-2.97118000	-2.72966700	-0.26691000
O	-3.85438100	-1.78833300	-0.89850100
C	-4.53291800	-0.96246900	-0.12477900
N	-5.30527700	-0.07686300	-0.78094600
N	-5.78742800	0.90017900	-0.06924900
C	-5.49626000	0.89964800	1.23542300
N	-5.04575900	-0.14671400	1.91358100
N	-4.55552900	-1.13401100	1.20195500
Cl	-5.94092800	2.29964300	2.13615500
C	5.00189200	-1.66682000	1.24830600
F	6.12968500	-1.06274700	1.68865200
F	5.39527500	-2.66324600	0.41758200
F	4.43871300	-2.26900500	2.32150300
C	3.81998400	2.92342300	-0.32375600
F	4.86917700	3.09744400	-1.17124400
F	4.20343700	3.46940300	0.85729400
F	2.80898700	3.67292800	-0.79697600
H	5.31126300	1.02393600	0.85776400

H	1.56159200	1.65652700	-1.16847600*
H	2.62580000	-2.28578400	0.17655400
H	0.19578600	-0.06185300	-1.58061800
H	-1.42418000	-1.24490800	-2.04797700
H	-2.50462300	-3.47011800	-2.23332300
H	-1.39445800	-4.00649900	-0.95402900
H	-2.46667900	-2.24901400	0.57679500
H	-3.56550800	-3.57366700	0.10452100
N	-2.60432300	0.96994300	0.19227500
C	-2.09991200	1.12088400	-0.86159400
S	-1.38795800	1.28697600	-2.35487800

Frequencies calculation (in vacuum, with SCN-)	***Frequencies calculation (in vacuum, without SCN-)***
APFD/aug-cc-pvtz	APFD/aug-cc-pvtz
Zero-point correction= 0.247987 (Hartree/Particle)	Zero-point correction= 0.237938 (Hartree/Particle)
Thermal correction to Energy= 0.275956	Thermal correction to Energy= 0.261973
Thermal correction to Enthalpy= 0.276901	Thermal correction to Enthalpy= 0.262917
Thermal correction to Gibbs Free Energy= 0.186246	Thermal correction to Gibbs Free Energy= 0.180814
Sum of electronic and zero-point Energies= -2529.103003	Sum of electronic and zero-point Energies= -2038.054163
Sum of electronic and thermal Energies= -2529.075033	Sum of electronic and thermal Energies= -2038.030128
Sum of electronic and thermal Enthalpies= -2529.074089	Sum of electronic and thermal Enthalpies= -2038.029184
Sum of electronic and thermal Free Energies= -2529.164744	Sum of electronic and thermal Free Energies= -2038.111287

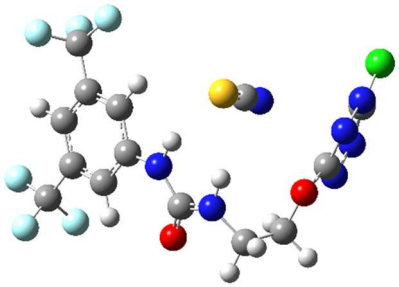

1+SCN^--ACN (*in acetonitrile)*
APFD/6-31+G(d,p), scrf=(iefpcm,solvent=acetonitrile)
Charge: -1
Spin Multiplicity: Singlet
Imaginary frequencies: 0
Electronic Energy (ZPE correction): -2528.559061 Hartree

Symbol	X	Y	Z
C	3.85307200	-0.63729100	0.59878500
C	4.10027100	0.71633600	0.41515000
C	3.17860200	1.44711500	-0.33723200
C	2.05191600	0.85225900	-0.88217100
C	1.81516900	-0.52077400	-0.68757600
C	2.73216100	-1.26879700	0.05974000
N	0.68141100	-1.05495900	-1.28015300
C	0.04282400	-2.23423000	-0.94553300
N	-1.11094500	-2.43017800	-1.65416200
O	0.47510300	-3.04062900	-0.11729100
C	-2.05434500	-3.43870600	-1.22546900
C	-2.96641500	-2.92491900	-0.12918400
O	-3.74243400	-1.86299700	-0.72716800
C	-4.24269400	-0.91961200	0.04064200
N	-4.93417000	0.02539600	-0.62652700
N	-5.28833200	1.07812900	0.05058700
C	-4.95375400	1.11340300	1.34496600
N	-4.49257500	0.08705300	2.04713300
N	-4.13092500	-0.97897900	1.37279600
Cl	-5.27205400	2.57504900	2.19221800
C	4.80722700	-1.48255700	1.39729500
F	5.86138100	-0.78356500	1.86398400
F	5.30734300	-2.50626100	0.66297000
F	4.20287500	-2.04763000	2.47060700
C	3.44578700	2.90900200	-0.56619000
F	4.51137200	3.10026400	-1.38438300
F	3.73542400	3.55434300	0.58818400

F	2.40317100	3.55184400	-1.12778200
H	4.97634700	1.19048100	0.84212100
H	1.34353100	1.44349800	-1.45511400
H	2.55969000	-2.32543200	0.21761000
H	0.13986700	-0.40599300	-1.85817000
H	-1.49047500	-1.63352900	-2.16133200
H	-2.64275200	-3.76100900	-2.08931300
H	-1.50000500	-4.30176900	-0.85050500
H	-2.38945200	-2.52969500	0.71060500
H	-3.65395700	-3.69537200	0.23293700
N	-2.05381900	1.15077100	0.20949600
C	-1.87784800	1.06105400	-0.95280000
S	-1.62872900	0.90479500	-2.58623900

Frequencies calculation (in acetonitrile, with SCN-)	***Frequencies calculation (in acetonitrile, without SCN-)***
APFD/aug-cc-pvtz scrf=(iefpcm,solvent=acetonitrile)	APFD/aug-cc-pvtz scrf=(iefpcm,solvent=acetonitrile)
Zero-point correction= 0.247350 (Hartree/Particle)	Zero-point correction= 0.237527 (Hartree/Particle)
Thermal correction to Energy= 0.275521	Thermal correction to Energy= 0.261637
Thermal correction to Enthalpy= 0.276465	Thermal correction to Enthalpy= 0.262581
Thermal correction to Gibbs Free Energy= 0.185237	Thermal correction to Gibbs Free Energy= 0.180289
Sum of electronic and zero-point Energies= -2529.167805	Sum of electronic and zero-point Energies= -2038.078418
Sum of electronic and thermal Energies= -2529.139634	Sum of electronic and thermal Energies= -2038.054308
Sum of electronic and thermal Enthalpies= -2529.138690	Sum of electronic and thermal Enthalpies= -2038.053364
Sum of electronic and thermal Free Energies= -2529.229918	Sum of electronic and thermal Free Energies= -2038.135656

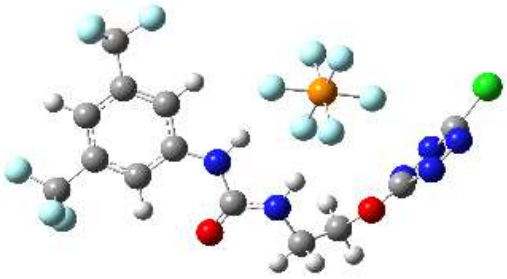

1+PF_6^- *(in vacuum)*
APFD/6-31+G(d,p)
Charge: -1
Spin Multiplicity: Singlet
Imaginary frequencies: 0
Electronic Energy (ZPE correction): -2977.735362 Hartree

Symbol	X	Y	Z
C	4.05696400	-0.71253800	0.57261500
C	4.38112800	0.63287900	0.46072700
C	3.46380900	1.47083800	-0.17789500
C	2.26988500	0.98654200	-0.68692600
C	1.95510600	-0.38298100	-0.57168300
C	2.86531500	-1.23480200	0.07038000
N	0.76064000	-0.79685600	-1.12509100
C	0.14225900	-2.02350000	-0.96708400
N	-1.04198500	-2.10615100	-1.65578200
O	0.60652000	-2.95318300	-0.30607600
C	-1.97321100	-3.15672400	-1.32677800
C	-2.97118000	-2.72966700	-0.26691000
O	-3.85438100	-1.78833300	-0.89850100
C	-4.53291800	-0.96246900	-0.12477900
N	-5.30527700	-0.07686300	-0.78094600
N	-5.78742800	0.90017900	-0.06924900
C	-5.49626000	0.89964800	1.23542300
N	-5.04575900	-0.14671400	1.91358100
N	-4.55552900	-1.13401100	1.20195500
Cl	-5.94092800	2.29964300	2.13615500
C	5.00189200	-1.66682000	1.24830600
F	6.12968500	-1.06274700	1.68865200
F	5.39527500	-2.66324600	0.41758200
F	4.43871300	-2.26900500	2.32150300
C	3.81998400	2.92342300	-0.32375600

F	4.86917700	3.09744400	-1.17124400
F	4.20343700	3.46940300	0.85729400
F	2.80898700	3.67292800	-0.79697600
H	5.31126300	1.02393600	0.85776400
H	1.56159200	1.65652700	-1.16847600
H	2.62580000	-2.28578400	0.17655400
H	0.19578600	-0.06185300	-1.58061800
H	-1.42418000	-1.24490800	-2.04797700
H	-2.50462300	-3.47011800	-2.23332300
H	-1.39445800	-4.00649900	-0.95402900
H	-2.46667900	-2.24901400	0.57679500
H	-3.56550800	-3.57366700	0.10452100
N	-2.60432300	0.96994300	0.19227500
C	-2.09991200	1.12088400	-0.86159400
S	-1.38795800	1.28697600	-2.35487800

Frequencies calculation (in vacuum, with PF6-)	***Frequencies calculation (in vacuum, without PF6-)***
APFD/aug-cc-pvtz	APFD/aug-cc-pvtz
Zero-point correction= 0.258630 (Hartree/Particle)	Zero-point correction= 0.237774 (Hartree/Particle)
Thermal correction to Energy= 0.290404	Thermal correction to Energy= 0.261960
Thermal correction to Enthalpy= 0.291348	Thermal correction to Enthalpy= 0.262904
Thermal correction to Gibbs Free Energy= 0.193317	Thermal correction to Gibbs Free Energy= 0.180568
Sum of electronic and zero-point Energies= -2978.566718	Sum of electronic and zero-point Energies= -2038.054325
Sum of electronic and thermal Energies= -2978.534944	Sum of electronic and thermal Energies= -2038.030139
Sum of electronic and thermal Enthalpies= -2978.534000	Sum of electronic and thermal Enthalpies= -2038.029195
Sum of electronic and thermal Free Energies= -2978.632031	Sum of electronic and thermal Free Energies= -2038.111531

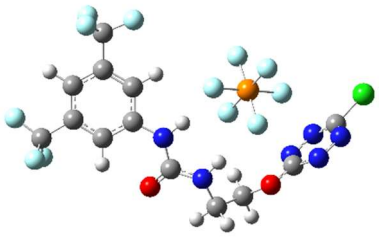

1+PF_6^--ACN *(in acetonitrile)*
APFD/6-31+G(d,p)
Charge: -1
Spin Multiplicity: Singlet
Imaginary frequencies: 0
Electronic Energy (ZPE correction): -2977.817350 Hartree

Symbol	X	Y	Z
C	4.83945900	-0.74926800	0.26759500
C	5.04458500	0.62225400	0.32592600
C	3.95688700	1.45110200	0.04528000
C	2.71212700	0.93389700	-0.27612400
C	2.51974000	-0.45872300	-0.33206200
C	3.60178100	-1.30352000	-0.05869800
N	1.25587200	-0.90995500	-0.68863700
C	0.74659200	-2.18411100	-0.51006800
N	-0.51127600	-2.34124500	-1.01453700
O	1.37817000	-3.09581000	0.03258300
C	-1.31301800	-3.48990900	-0.65416100
C	-2.48061300	-3.09487000	0.22338700
O	-3.38380100	-2.35771000	-0.63148400
C	-4.28671000	-1.56827100	-0.09234200
N	-5.10860300	-0.98582300	-0.98932500
N	-5.95744100	-0.11354400	-0.53265500
C	-5.94506600	0.12233200	0.78499100
N	-5.23864100	-0.54586600	1.68560500
N	-4.38095500	-1.43330700	1.23509500
Cl	-6.99361100	1.35705800	1.36067300
C	5.97638400	-1.69782300	0.53231700
F	7.08914900	-1.07225700	0.96633900
F	6.32389600	-2.38686900	-0.58321500
F	5.65497900	-2.62568900	1.46464600
C	4.16919400	2.93895600	0.09375600
F	5.05823600	3.34727700	-0.84556500
F	4.67288400	3.33505100	1.28746800

F	3.03673800	3.63993300	-0.10850600
H	6.01321100	1.03572100	0.58214400
H	1.88163400	1.60112200	-0.48059800
H	3.46745800	-2.37653900	-0.09327500
H	0.59918600	-0.18018000	-0.94291900
H	-1.00820900	-1.53364400	-1.37075900
H	-1.67879100	-3.99780500	-1.55361300
H	-0.67183700	-4.18764500	-0.11147700
H	-2.15971300	-2.46010800	1.05257200
H	-3.01315000	-3.96829500	0.61216300
P	-1.93225300	1.36585800	-0.51068800
F	-2.40431600	2.53324800	-1.54088300
F	-3.43687600	1.28389700	0.11311900
F	-2.31882300	0.22335400	-1.62283200
F	-1.44123500	0.17678900	0.50189500
F	-0.40788200	1.42698400	-1.15048800
F	-1.51234300	2.48645800	0.59116100

Frequencies calculation (in acetonitrile, with PF6-)	***Frequencies calculation (in acetonitrile, without PF6-)***
APFD/aug-cc-pvtz scrf=(iefpcm,solvent=acetonitrile)	APFD/aug-cc-pvtz scrf=(iefpcm,solvent=acetonitrile)
Zero-point correction= 0.257387 (Hartree/Particle)	Zero-point correction= 0.237178 (Hartree/Particle)
Thermal correction to Energy= 0.289461	Thermal correction to Energy= 0.261511
Thermal correction to Enthalpy= 0.290406	Thermal correction to Enthalpy= 0.262455
Thermal correction to Gibbs Free Energy= 0.191455	Thermal correction to Gibbs Free Energy= 0.179614
Sum of electronic and zero-point Energies= -2978.630481	Sum of electronic and zero-point Energies= -2038.078354
Sum of electronic and thermal Energies= -2978.598407	Sum of electronic and thermal Energies= -2038.054021
Sum of electronic and thermal Enthalpies= -2978.597463	Sum of electronic and thermal Enthalpies= -2038.053077
Sum of electronic and thermal Free Energies= -2978.696413	Sum of electronic and thermal Free Energies= -2038.135919

2.2 Calculation of interaction energies

Interaction energies with and without solvent effect were calculated by generating frequencies calculations from optimized geometries using triple zeta basis set APFD/aug-cc-pvtz level of calculation and the formula:

$$\Delta G_{int,vacuum} = \text{Interaction energy in vacuum} = E_{complex,\ vacuum} - (E_{ion,vacuum} + E_{ligand\ in\ complex,vacuum})$$

Where :

$E_{complex,vacuum}$ is the sum of electronic and thermal Free Energies for the complex in vacuum

$E_{ion,vacuum}$ is the sum of electronic and thermal Free Energies for the ion in vacuum

$E_{ligand\ in\ complex,vacuum}$ is the sum of electronic and thermal Free Energies for the ligand complexed without the anion in vacuum

$$\Delta G_{int,ACN} = \text{Interaction energy in acetonitrile} = E_{complex,\ ACN} - (E_{ion,ACN} + E_{ligand\ in\ complex,ACN})$$

Where :

$E_{complex,ACN}$ is the sum of electronic and thermal Free Energies for the complex in vacuum

$E_{ion,ACN}$ is the sum of electronic and thermal Free Energies for the ion in vacuum

$E_{ligand\ in\ complex,ACN}$ is the sum of electronic and thermal Free Energies for the ligand complexed without the anion in vacuum

Without solvent correction, calculation with thermal Free Energies

	Ecomplex	Eion	Eligand in complex	Einteraction (Hartree)	Einteraction (kJ/mol)
Cl-	-2498.385260	-460.199535	-2038.110845	-0.07488	-194.69
Br-	-2455.165029	-416.986525	-2038.110870	-0.067634	-175.85
I-	-2334.049418	-295.884744	-2038.107386	-0.057288	-148.95
SCN-	-2529.164744	-491.000107	-2038.111287	-0.05335	-138.71
PF6-	-2978.632031	-940.476283	-2038.111531	-0.044217	-114.96

With solvent correction, calculation with thermal Free Energies

	Ecomplex	Eion	Eligand in complex	Einteraction (Hartree)	Einteraction (kJ/mol)
Cl-	-2498.455813	-460.308965	-2038.135433	-0.011415	-29.68
Br-	-2455.234001	-417.088660	-2038.133837	-0.011504	-29.91
I-	-2334.119257	-295.978358	-2038.134358	-0.006541	-17.01
SCN-	-2529.229918	-491.089853	-2038.135656	-0.004409	-11.46
PF6-	-2978.696413	-940.563054	-2038.135919	0.00256	6.65

3. Synthetic Procedures and Characterization Data

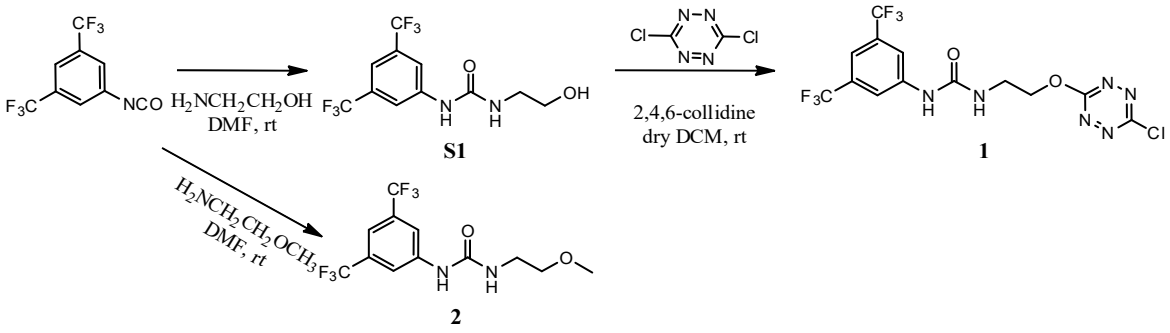

*Figure S1 : General procedure for Synthesis of **1** and **2***

3.1 Preparation of 1-(3,5-bis(trifluoromethyl)phenyl)-3-(2-hydroxyethyl)urea **S1**

Inspired from a published procedure[5].

N,N-Dimethylformamide (3.6mL) was added to a round bottom flask. Ethanolamine (96µL, 1.64mmol, 1.04eq) and then 3,5-bis(trifluoromethyl)phenyl isocyanate (272µL, 1.56mmol, 1eq) were added dropwise to the solution. The mixture was stirred at room temperature for 75 minutes. The mixture was cooled down in an ice bath, diluted into 5mL of water and 5mL of HCl 1M solution. The mixture was then extracted four times with ethyl acetate. Organic phases were gathered and washed with water and brine. The mixture was purified by flash chromatography on silica gel eluting with a mixture of dichloromethane/methanol (95:5) to give 441 mg of 1-(3,5-bis(trifluoromethyl)phenyl)-3-(2-hydroxyethyl)urea **S1** as bright white solid crystals. Yield : 441 mg, 89%

^{1}H NMR (300 MHz, MeOD, 25°C, TMS) δ 7.98 (s, 2H, Ar-*H*), 7.45 (s, 1H, Ar-*H*), 3.63 (t, $^{3}J_{H\text{-}H}$ = 6 Hz, 2H, C*H*$_2$-N), 3.32 (t, $^{3}J_{H\text{-}H}$ = 6 Hz, 2H, C*H*$_2$-O).

^{13}C NMR (75 MHz, MeOD, 25°C, TMS) δ 157.6 (s, 1C, *C*=O), 143.5 (s, 1C, $C_{arom,\ quat}$), 133.2 (q, 2C, $^{2}J_{C\text{-}F}$ = 33 Hz, *C*-CF$_3$), 124.9 (q, 2C, $^{1}J_{C\text{-}F}$ = 270 Hz, C_{arom}), 118.9 (multiplet, 1C, $C_{arom,\ para}$), 115.4 (quint, 2C, $^{3}J_{C\text{-}F}$ = 4 Hz, *C*F$_3$), 62.0 (s, 1C, *C*H$_2$-OH), 43.2 (s, 1C, *C*H$_2$-NH).

^{19}F NMR (282 MHz, MeOD, 25°C) δ (not calibrated) -64.68 (s, 6F, -C*F*$_3$).

HRMS (ESI^{+}-TOF) *m/z [M+H]*$^{+}$ calcd for $C_{11}H_{11}O_2N_2F_6$: 317.0719, found 317.0716.

Rf 0.23 in dichloromethane/methanol (95:5)

Melting Point 146°C

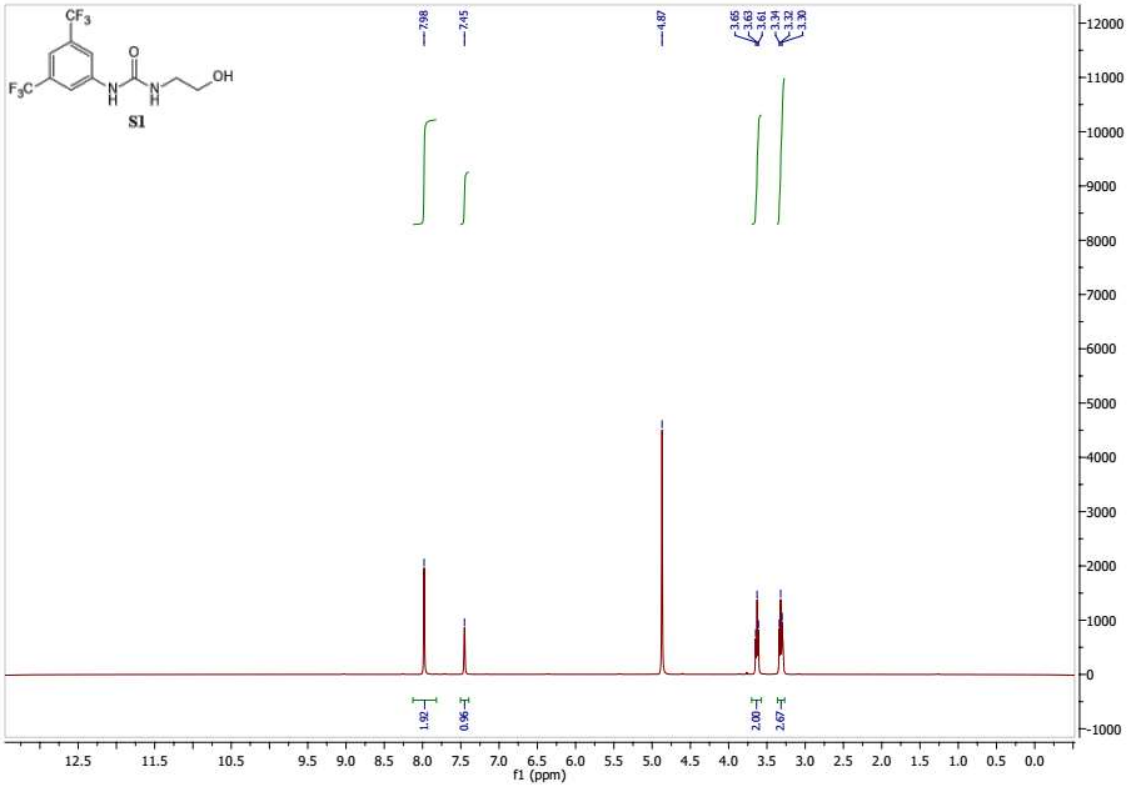

*Figure S2:^{1}H NMR (300 MHz) spectrum of **S1** in MeOD*

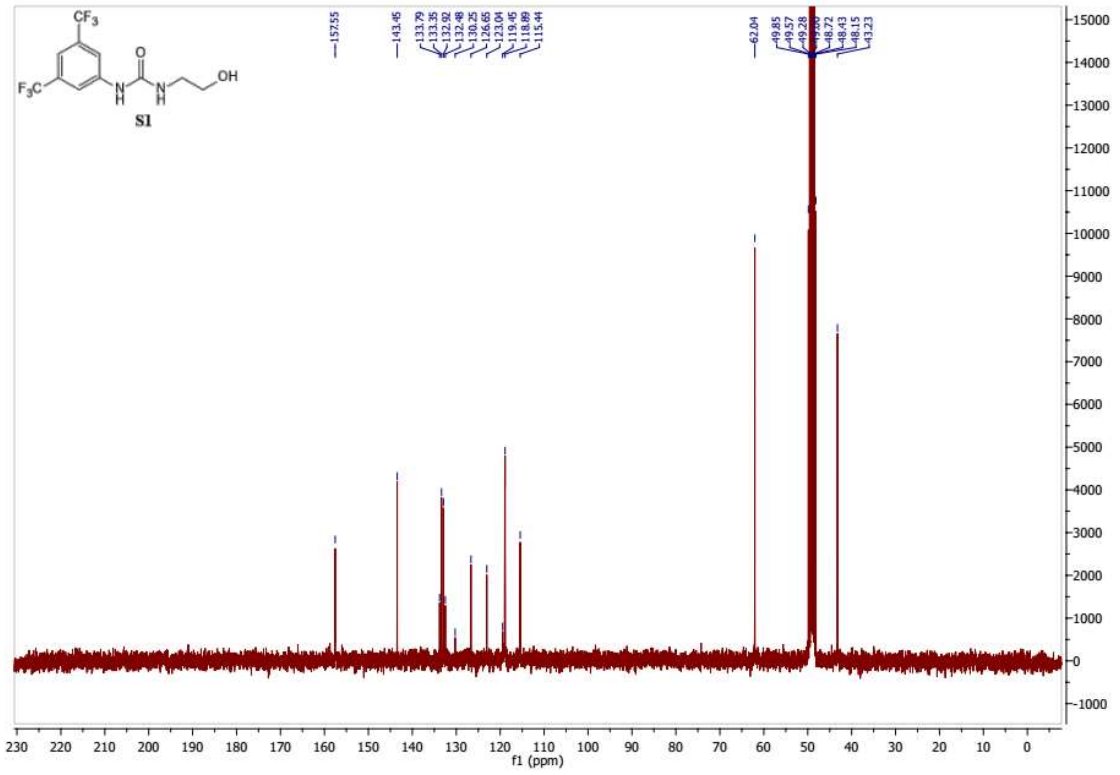

*Figure S3: ^{13}C NMR (75 MHz) spectrum of **S1** in MeOD*

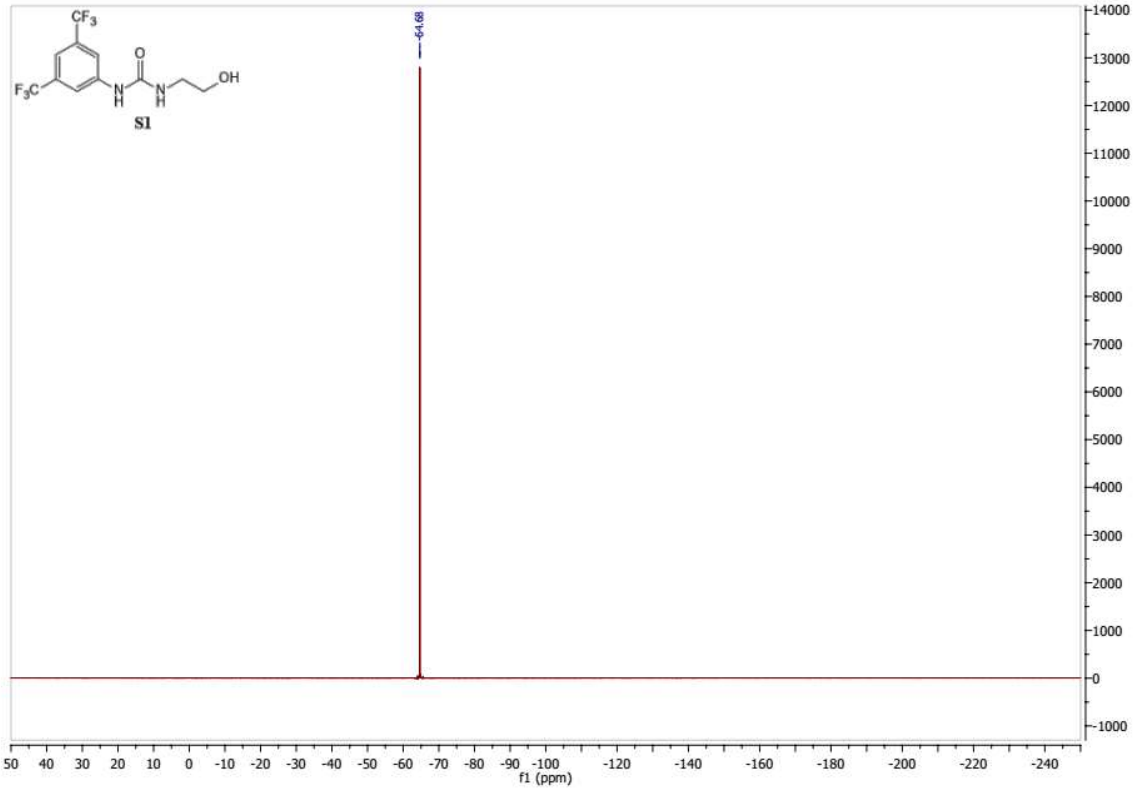

*Figure S4: ^{19}F NMR (282 MHz) spectrum of **1** in MeOD*

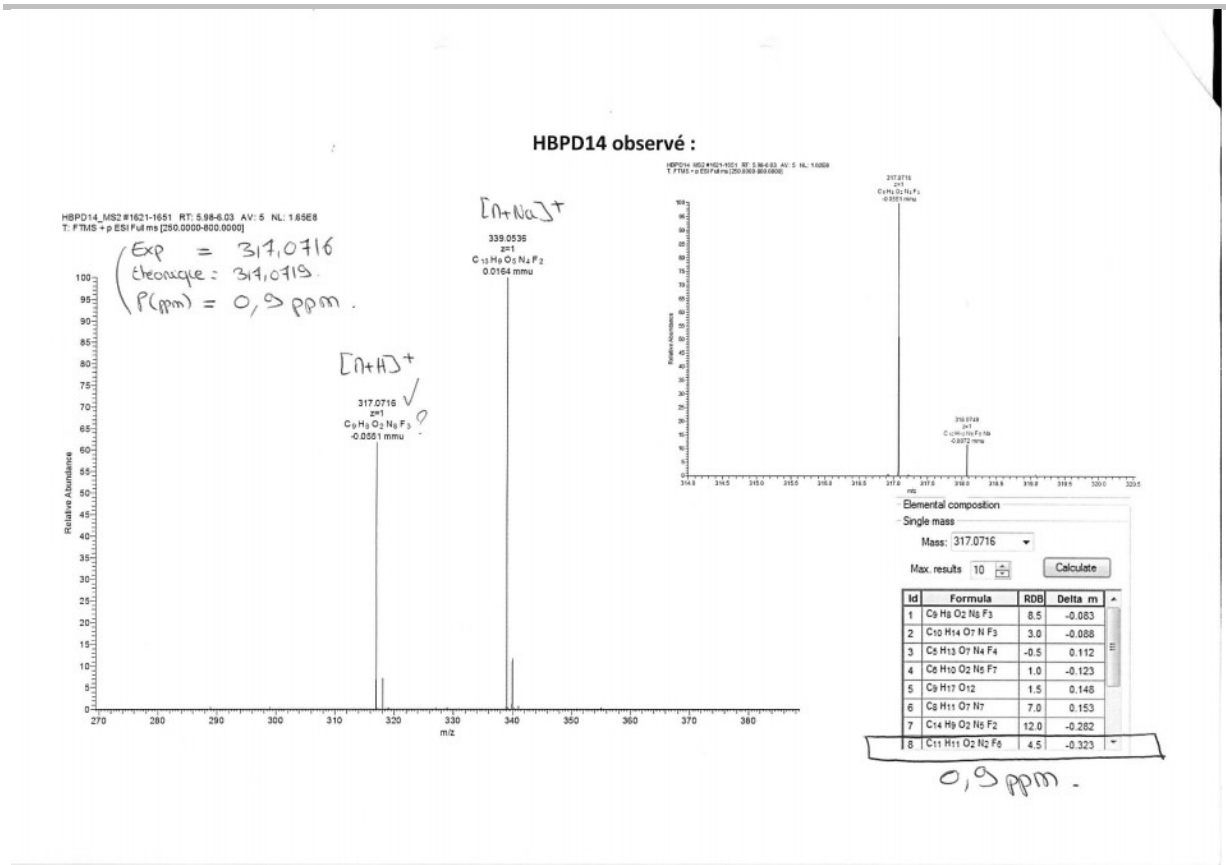

*Figure S5: Mass spectrum of **S1** (TOF ES+)*

3.2 Preparation of 1-(3,5-bis(trifluoromethyl)phenyl)-3-(2-((6-chloro-1,2,4,5-tetrazin-3-yl)oxy)ethyl)urea **1**

Inspired from a published procedure[6].

1-(3,5-bis(trifluoromethyl)phenyl)-3-(2-hydroxyethyl)urea (417mg, 1.32mmol, 1eq) and dichlorotetrazine (200 mg, 1.32mmol, 1eq) were added to a round bottom flask equipped with a magnetic stirrer and dissolved with dry dichloromethane (34mL) under inert atmosphere. A solution of 2,4,6-collidine (183µL, 1.39mmol, 1.05eq) diluted into dry dichloromethane (10mL) was added dropwise to the flask. The mixture was stirred at room temperature for two hours. The solvent was evaporated. The crude product was purified by two iterative flash chromatographies on silica gel eluting with a gradient of petroleum ether/ethyl acetate (90:10 to 60:40) and (80:20 to 60:40), respectively. 355 mg of 1-(3,5-bis(trifluoromethyl)phenyl)-3-(2-((6-chloro-1,2,4,5-tetrazin-3-yl)oxy)ethyl)urea **1** were obtained as a pink fluorescent solid. Yield 355 mg, 63%

^{1}H NMR (300 MHz, MeOD, 25°C, TMS) δ 7.87 (s, 2H, Ar-*H*), 7.38 (s, 1H, Ar-*H*), 4.63 (t, 2H, $^{3}J_{H\text{-}H}$ = 5 Hz, C*H*$_2$-O), 3.64 (t, 2H, $^{3}J_{H\text{-}H}$ = 5 Hz, C*H*$_2$-*N*)

^{13}C NMR (75 MHz, MeOD, 25°C, TMS) δ 168.4 (s, 1C, O-*C*$_{Tz}$), 165.5 (s, 1C, Cl-*C*$_{Tz}$), 157.4 (s, 1C, *C*=O), 143.3 (s, 1C, *C*$_{arom}$-N), 133.8-132.5 (q, 2C, $^{2}J_{C\text{-}F}$ = 31 Hz, *C*-CF$_3$), 130.2-119.5 (q, 2C, $^{3}J_{C\text{-}F}$ = 270 Hz, *C*$_{arom}$), 119.1 (s, 1C, *C*$_{arom}$), 115.7 (quint, 2C, $^{1}J_{C\text{-}F}$ = 4 Hz, *C*F$_3$), 70.6 (s, 1C, *C*H$_2$-O), 39.7 (s, 1C, *C*H$_2$-N)

^{19}F NMR (282 MHz, MeOD, 25°C) δ (not calibrated) -64.6 (6F)

UV/Visible (Acetonitrile) λ_{max} (ε)= 294 nm (0.50 AU), 326 nm (0.41 AU), 511 nm (0.07 AU).

Fluorescence (Acetonitrile) λ_{exc}= 511 nm, λ_{em}= 561 nm.

HRMS (ESI$^+$-TOF) *m/z [M+Na]*$^+$ calculated for $C_{13}H_9ClF_6N_6NaO_2$: 453,03, found 453,0277

Rf 0.28 in petroleum ether/ethyl acetate (7:3)

Melting Point 180-184°C

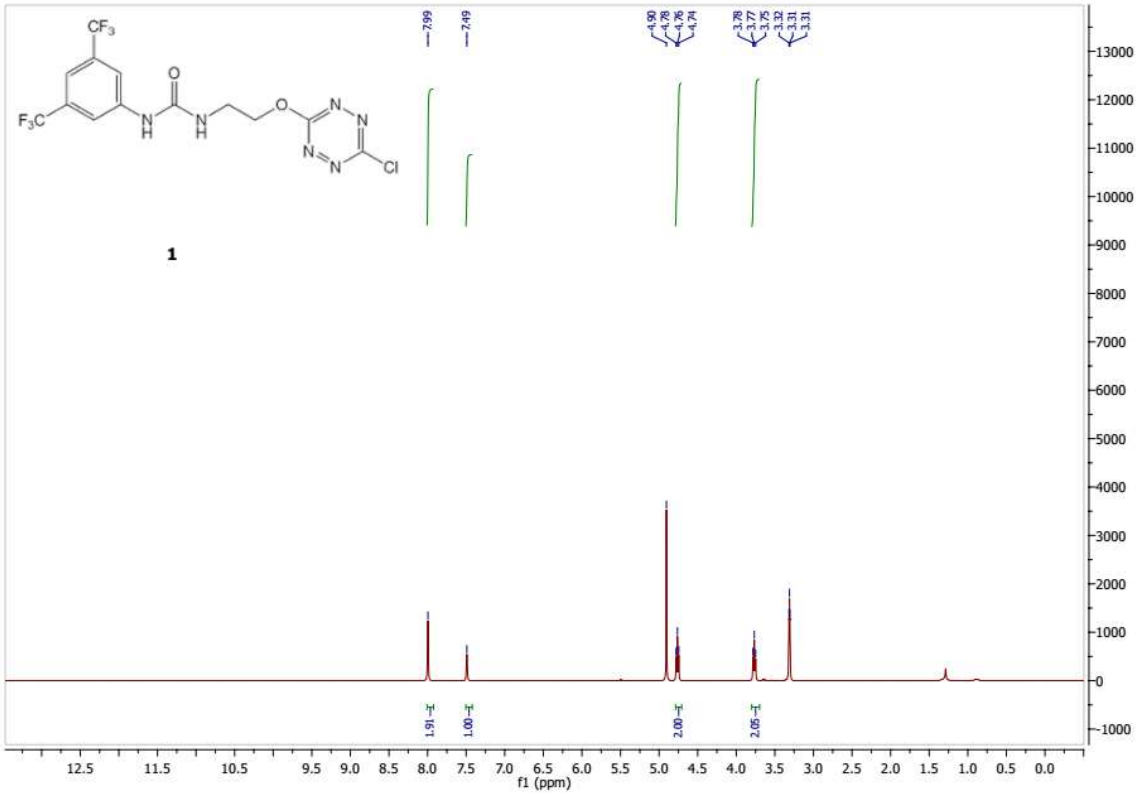

*Figure S6: ^{1}H NMR (300 MHz) spectrum of **1** in MeOD*

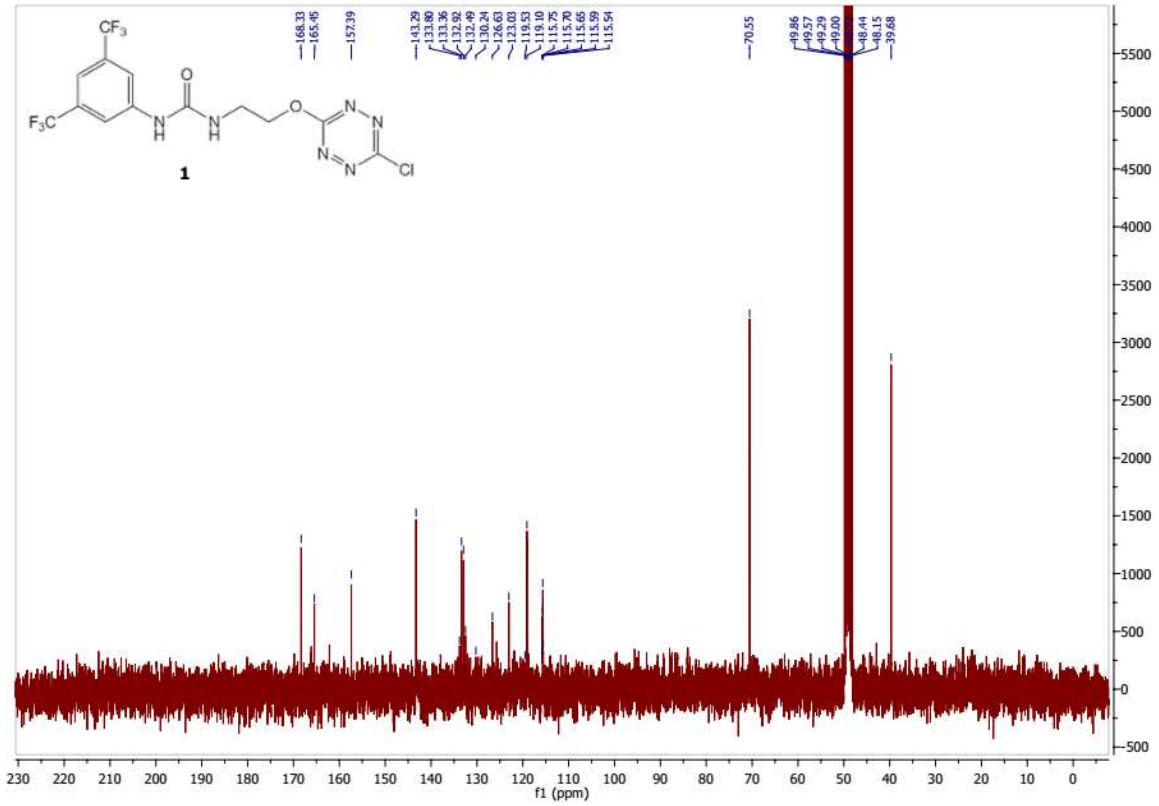

*Figure S7: ^{13}C NMR (75 MHz) spectrum of **1** in MeOD*

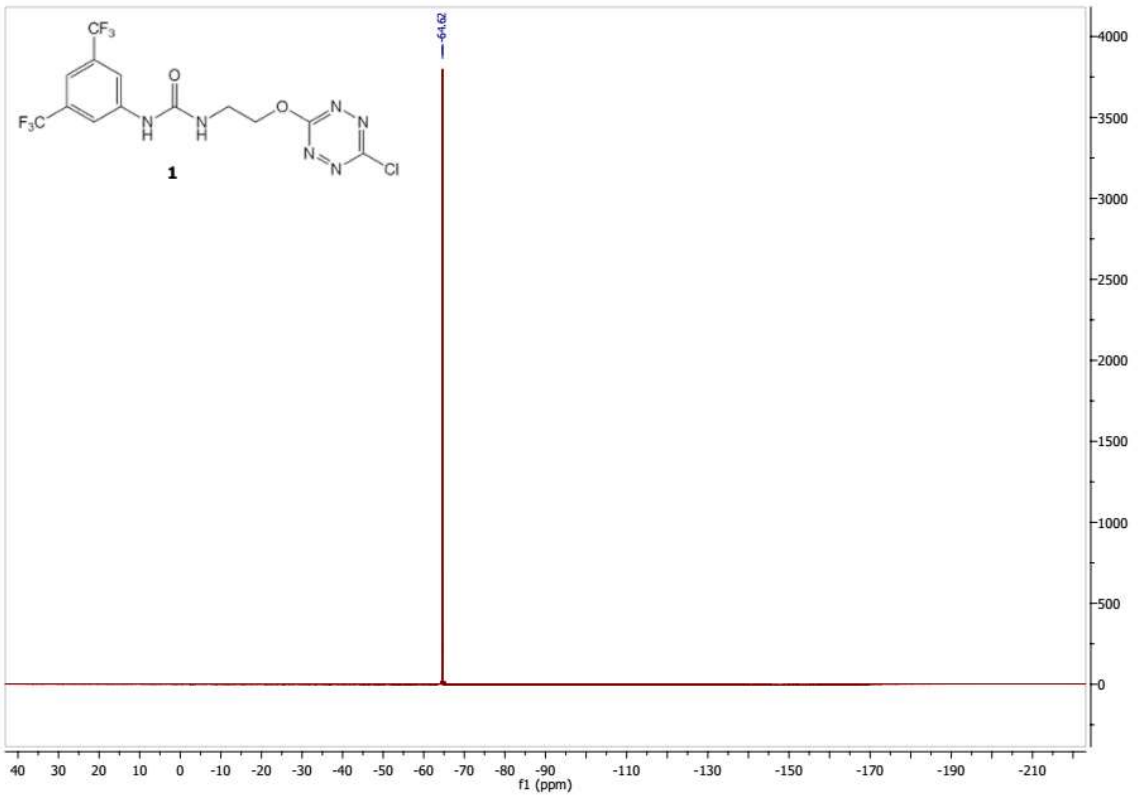

*Figure S8: ^{19}F NMR (300 MHz) spectrum of **1** in MeOD*

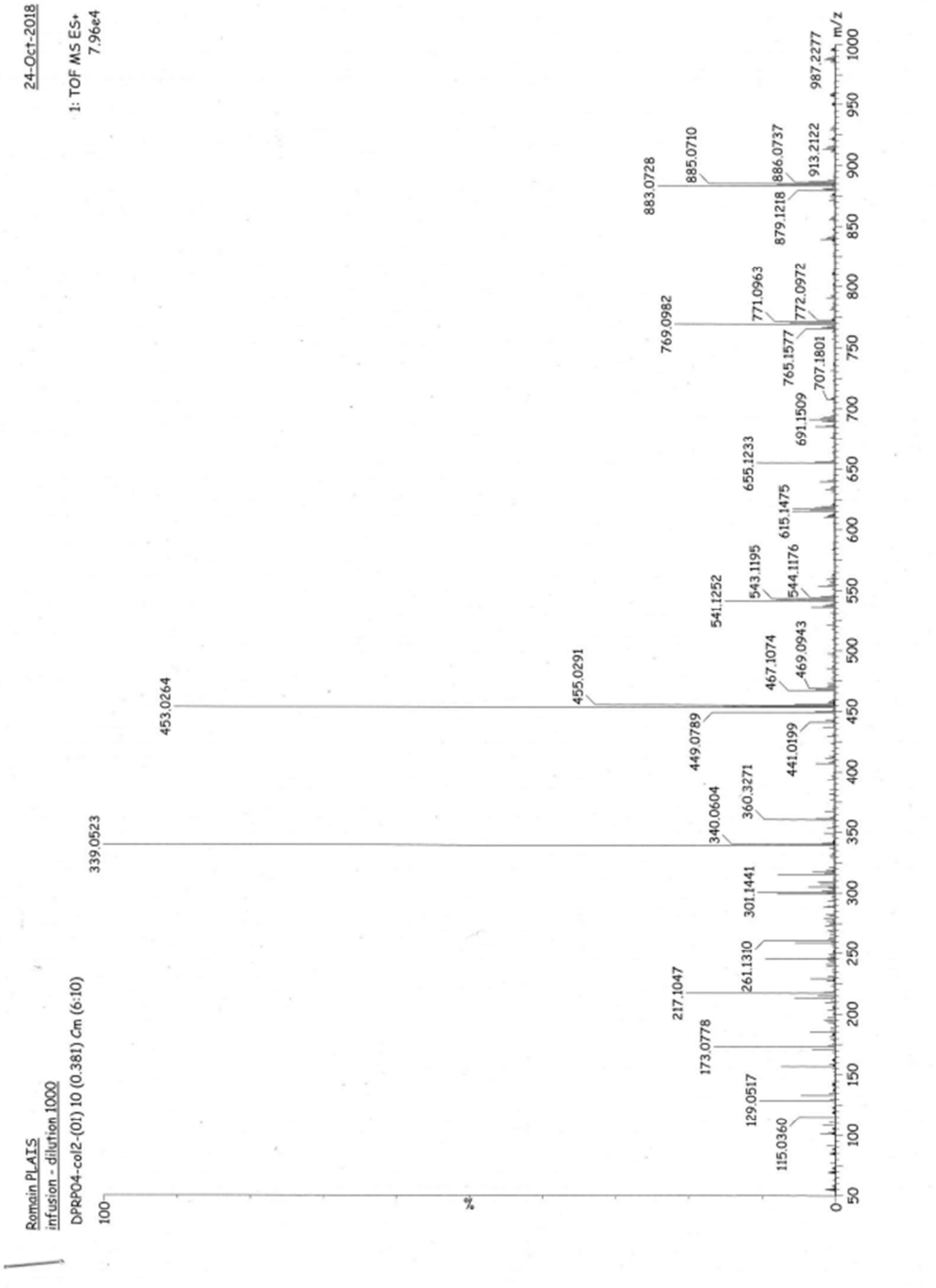
Romain PLAIS
infusion - dilution 1000
DPRP04-col2-(01) 10 (0.381) Cm (6:10)
24-Oct-2018
1: TOF MS ES+
7.96e4
%
m/z
339.0523
453.0264
455.0291
449.0789
340.0604
360.3271
441.0199
467.1074
469.0943
541.1252
543.1195
544.1176
615.1475
655.1233
691.1509
707.1801
765.1577
769.0982
771.0963
772.0972
883.0728
885.0710
879.1218
886.0737
913.2122
987.2277
217.1047
173.0778
261.1310
301.1441
129.0517
115.0360

*Figure S9: Mass spectrum of **1** (TOF ES+)*

Elemental Composition Report **Page 1**

Single Mass Analysis
Tolerance = 5.0 PPM / DBE: min = -1.5, max = 100.0
Element prediction: Off
Number of isotope peaks used for i-FIT = 2

Monoisotopic Mass, Even Electron Ions
20788 formula(e) evaluated with 127 results within limits (all results (up to 1000) for each mass)
Elements Used:
C: 0-150 H: 0-150 N: 0-10 O: 0-10 F: 0-6 Na: 0-1 Cl: 0-1 I: 0-2

Romain PLAIS
infusion - dilution 1000
DPRP04-col2-(01) 10 (0.381) Cm (6:10)

24-Oct-2018
1: TOF MS ES+
7.19e+004

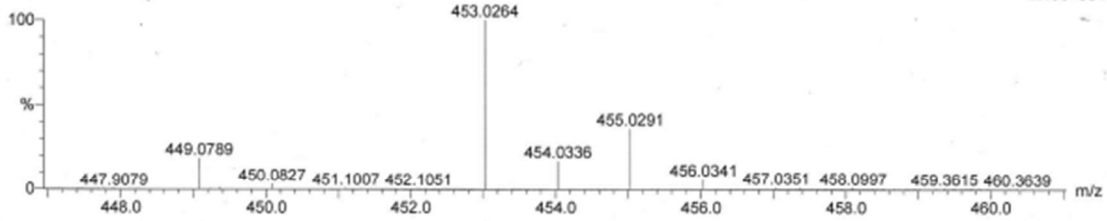

Mass	Calc. Mass	mDa	PPM	DBE	i-FIT	i-FIT (Norm)	Formula
Minimum:				-1.5			
Maximum:		5.0	5.0	100.0			
453.0264	453.0277	-1.3	-2.9	8.5	107.8	1.5	C13 H9 N6 O2 F6 Na Cl
	453.0263	0.1	0.2	4.5	108.1	1.8	C14 H18 N2 O2 F3 Na I
	453.0286	-2.2	-4.9	10.5	108.2	1.8	C12 H11 N8 O8 Na Cl
	453.0286	-2.2	-4.9	10.5	108.5	2.2	C12 H9 N8 O6 F3 Cl
	453.0262	0.2	0.4	4.5	108.7	2.3	C14 H16 N2 F6 I
	453.0260	0.4	0.9	8.5	109.1	2.7	C12 H15 N8 O2 Na I
	453.0271	-0.7	-1.5	6.5	109.4	3.1	C13 H18 N4 O6 I
	453.0260	0.4	0.9	8.5	109.7	3.3	C12 H13 N8 F3 I
	453.0246	1.8	4.0	8.5	110.7	4.4	C13 H8 N4 O6 F6 Na
	453.0261	0.3	0.7	9.5	110.7	4.4	C14 H12 N4 O9 F2 Cl
	453.0256	0.8	1.8	6.5	110.8	4.4	C14 H11 O10 F6
	453.0250	1.4	3.1	11.5	111.5	5.1	C13 H7 N8 O3 F5 Cl
	453.0243	2.1	4.6	12.5	111.6	5.2	C11 H5 N10 O6 F3 Na
	453.0253	1.1	2.4	7.5	111.6	5.2	C15 H12 N2 O5 F5 Na Cl
	453.0254	1.0	2.2	10.5	111.7	5.3	C12 H8 N6 O10 F3
	453.0250	1.4	3.1	11.5	111.9	5.5	C13 H9 N8 O5 F2 Na Cl
	453.0243	2.1	4.6	12.5	112.0	5.7	C11 H3 N10 O4 F6
	453.0270	-0.6	-1.3	3.5	112.1	5.7	C16 H22 O F2 Na Cl I
	453.0254	1.0	2.2	2.5	112.6	6.2	C13 H21 N2 O3 F2 Cl I
	453.0270	-0.6	-1.3	11.5	113.1	6.8	C15 H7 N4 O6 F6
	453.0282	-1.8	-4.0	7.5	113.1	6.8	C12 H10 N4 O9 F4 Na
	453.0270	-0.6	-1.3	11.5	113.3	7.0	C15 H9 N4 O8 F3 Na
	453.0201	-1.7	-3.8	-0.5	113.4	7.0	C13 H23 O2 F3 Na Cl I
	453.0267	-0.3	-0.7	15.5	113.5	7.2	C13 H4 N10 O6 F3
	453.0281	-1.7	-3.8	-0.5	113.6	7.2	C13 H21 F6 Cl I
	453.0268	-0.4	-0.9	15.5	113.7	7.4	C13 H6 N10 O8 Na
	453.0279	-1.5	-3.3	11.5	113.8	7.5	C10 H7 N10 O9 F Na
	453.0284	-2.0	-4.4	11.5	113.9	7.5	C14 H14 N8 O2 I
	453.0259	0.5	1.1	13.5	113.9	7.5	C14 H4 N8 O2 F6 Na
	453.0279	-1.5	-3.3	11.5	114.1	7.7	C10 H5 N10 O7 F4
	453.0279	-1.5	-3.3	3.5	114.2	7.8	C11 H20 N6 O2 Na Cl I
	453.0242	2.2	4.9	6.5	114.2	7.8	C16 H20 N2 O2 F Cl I
	453.0264	0.0	0.0	3.5	114.3	8.0	C12 H13 N2 O6 F6 Na Cl
	453.0278	-1.4	-3.1	3.5	114.3	8.0	C11 H18 N6 F3 Cl I
	453.0264	0.0	0.0	-0.5	114.3	8.0	C12 H27 N2 I2

*Figure S10: Single mass analysis of **1** (TOF ES+)*

3.3 Preparation of 1-(3,5-bis(trifluoromethyl)phenyl)-3-(2-methoxyethyl)urea **2**

Receptor **2** was synthesized from a similar protocol to **S1**. Yield : 66%

^{1}H NMR (300 MHz, Acetone d6, 25°C, TMS) δ 8.62 (s, 1H, Ar-N*H*), 8.15 (s, 2H, Ar-H), 7.52 (s, 1H, Ar-*H*), 6.12 (s, 1H, CH_2-N*H*), 3.47-3.39 (m, 4H, CH_2-CH_2), 3.31 (s, 3H, CH_3-O).
^{13}C NMR (75 MHz, MeOD, 25°C, TMS) δ 155.6 (s, 1C, *C*=O), 143.7 (s, 1C, $C_{arom, quat}$), 133.4 (q, 2C, $^{2}J_{C-F}$ = 33 Hz, *C*-CF_3), 130.0-119.1 (q, 2C, $^{1}J_{C-F}$ = 270 Hz, *C*F_3), 118.3 (m, 1C, C_{arom}-NH), 114.7 (quint, 2C, $^{3}J_{C-F}$ = 4 Hz, *C*F_3), 72.2 (s, 1C, -*C*H_3), 58.9 (s, 1C, *C*H_2-OH), 40.3 (s, 1C, *C*H_2-NH).
^{19}F NMR (282 MHz, MeOD, 25°C) δ (not calibrated) 113.8 (s, 6F, -C*F*$_3$).
HRMS (ESI^{+}-TOF) *m/z [M+H]*$^{+}$ calcd for $C_{12}H_{12}O_2N_2F_6$: 331.0881, found 317.0882.

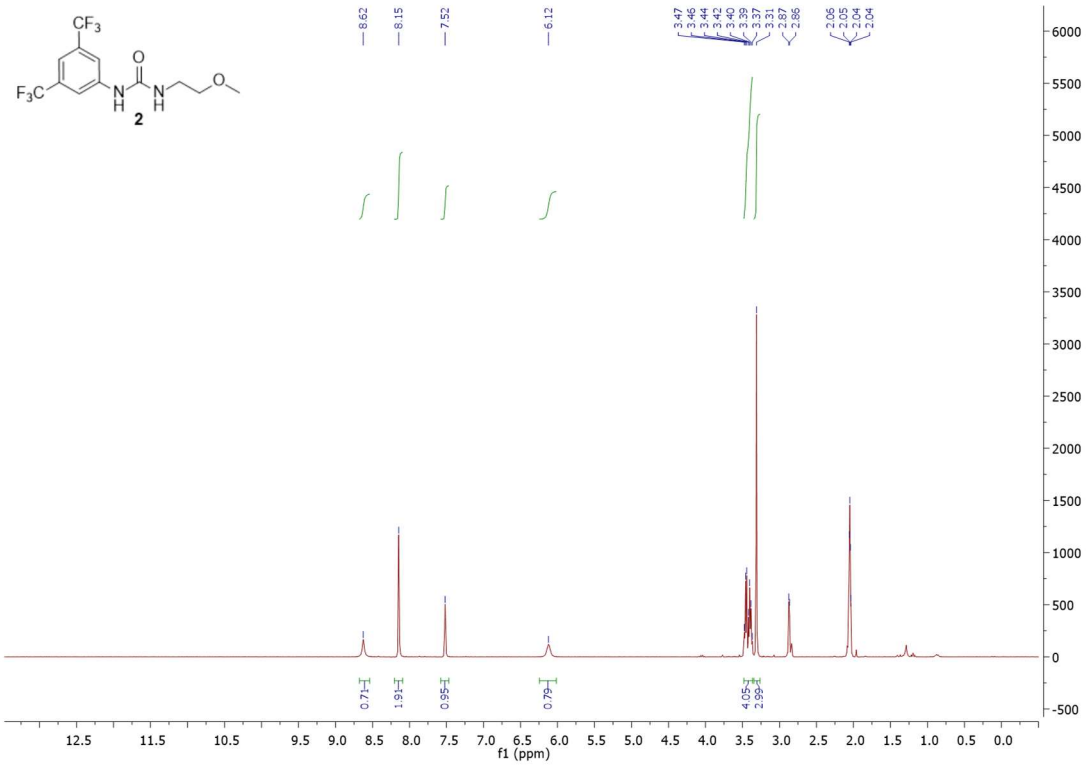

*Figure S11: ^{1}H NMR (300 MHz) spectrum of **2** in Acetone d6*

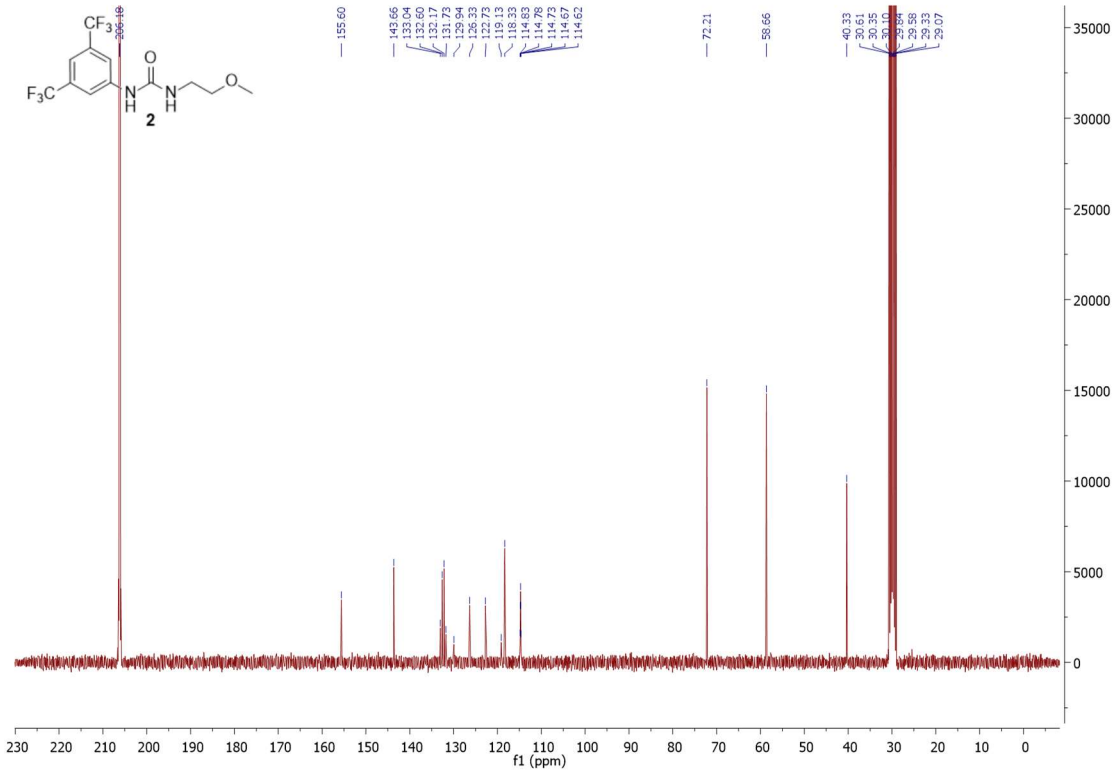

*Figure S12: ^{13}C NMR (75 MHz) spectrum of **2** in Acetone d6*

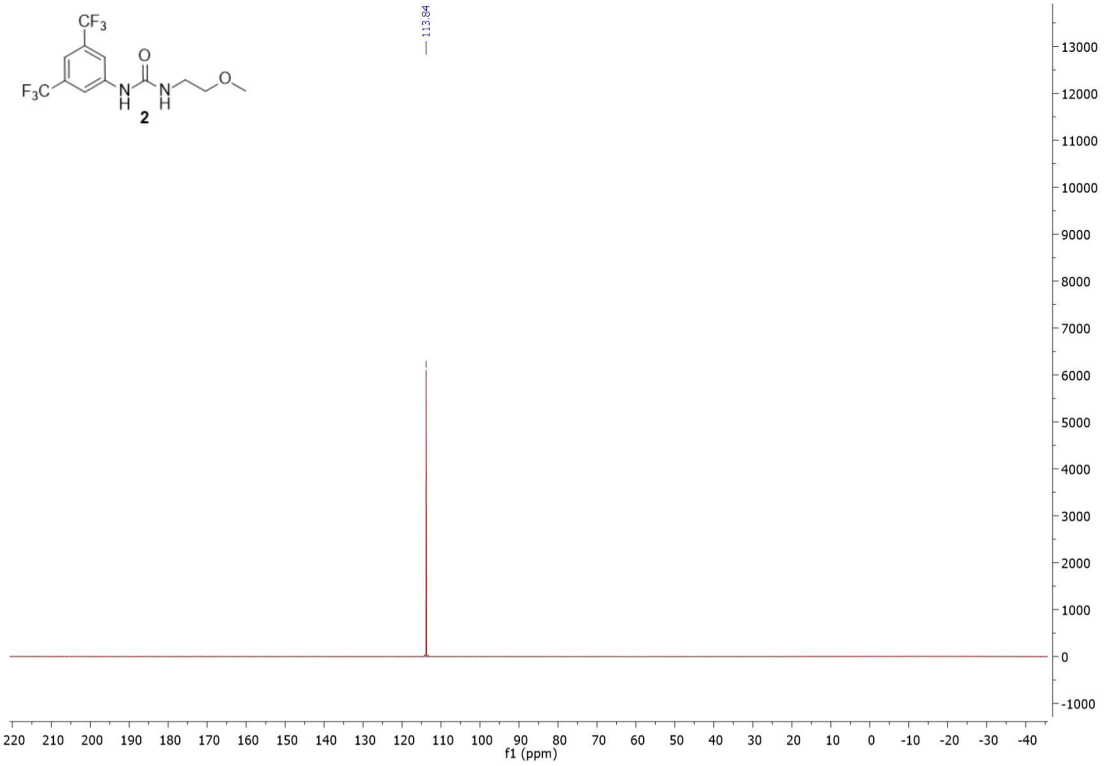

*Figure S13: ^{19}F NMR (300 MHz) spectrum of **2** in Acetone d6*

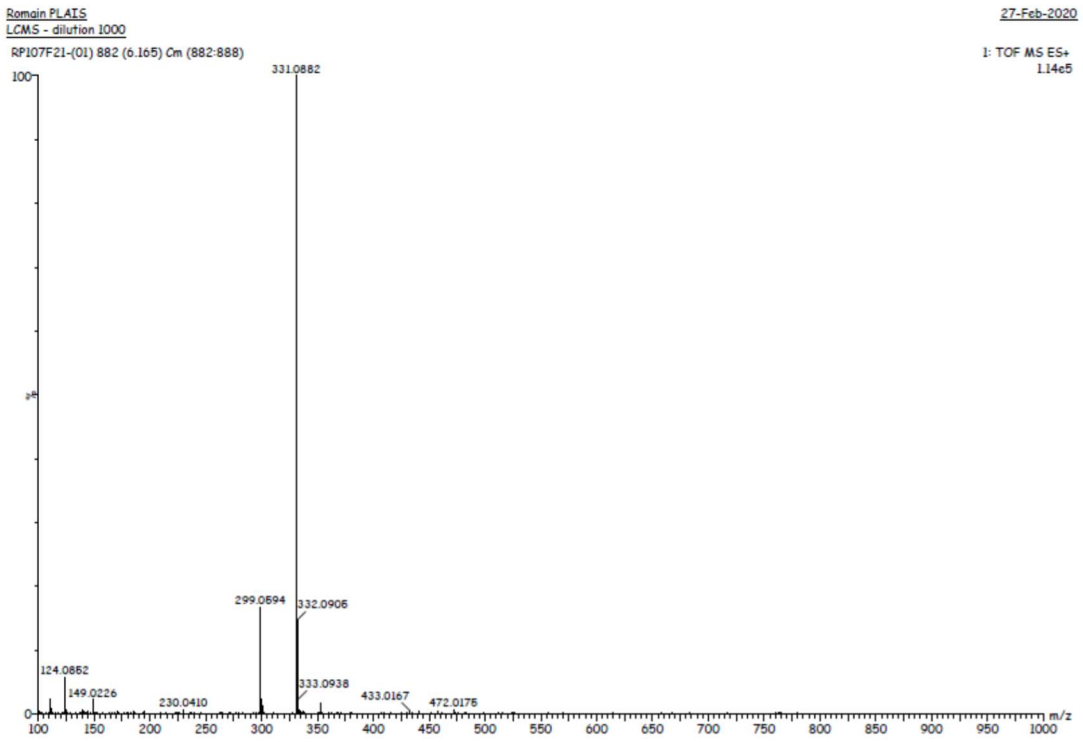

*Figure S14: Mass spectrum of **2** (TOF ES+)*

Elemental Composition Report Page 1

Single Mass Analysis
Tolerance = 5.0 PPM / DBE: min = -1.5, max = 150.0
Element prediction: Off
Number of isotope peaks used for i-FIT = 3

Monoisotopic Mass, Even Electron Ions
2441 formula(e) evaluated with 13 results within limits (all results (up to 1000) for each mass)
Elements Used:
C: 0-100 H: 0-100 N: 0-10 O: 0-10 F: 0-6 Ir: 0-1

Romain PLAIS
LCMS - dilution 1000
RP107F21-(01) 882 (6.165) Cm (882:888)

27-Feb-2020
1: TOF MS ES+
1.14e+005

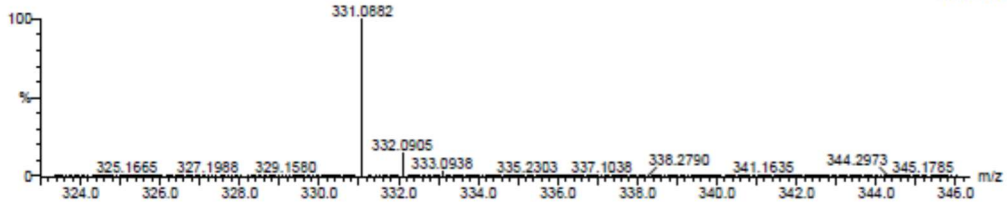

Mass	Calc. Mass	mDa	PPM	DBE	i-FIT	i-FIT (Norm)	Formula
Minimum:				-1.5			
Maximum:		5.0	5.0	150.0			
331.0882	331.0890	-0.8	-2.4	6.5	343.0	0.0	C11 H15 N4 O8
	331.0881	0.1	0.3	4.5	346.7	3.7	C12 H13 N2 O2 F6
	331.0879	0.3	0.9	8.5	348.2	5.2	C10 H10 N8 O2 F3
	331.0870	1.2	3.6	8.5	348.5	5.5	C15 H12 N2 O F5
	331.0867	1.5	4.5	12.5	349.9	7.0	C13 H9 N8 O F2
	331.0890	-0.8	-2.4	4.5	351.2	8.2	C7 H11 N8 O3 F4
	331.0894	-1.2	-3.6	11.5	351.4	8.4	C17 H13 N2 O3 F2
	331.0883	-0.1	-0.3	15.5	351.5	8.5	C20 H12 N2 O2 F
	331.0877	0.5	1.5	-0.5	351.6	8.6	C6 H15 N4 O7 F4
	331.0871	1.1	3.3	19.5	353.1	10.1	C23 H11 N2 O
	331.0874	0.8	2.4	3.5	354.2	11.2	C4 H12 N10 O7 F
	331.0886	-0.4	-1.2	-0.5	357.5	14.5	C H13 N10 O8 F2
	331.0872	1.0	3.0	-0.5	372.5	29.5	C4 H16 N3 O2 Ir

*Figure S15: Single mass analysis of **2** (TOF ES+)*

4. Mass spectrometry experiments

4.1 Typical electrospray spectra obtained for the 1:1 (**1**)/TBABr mixture

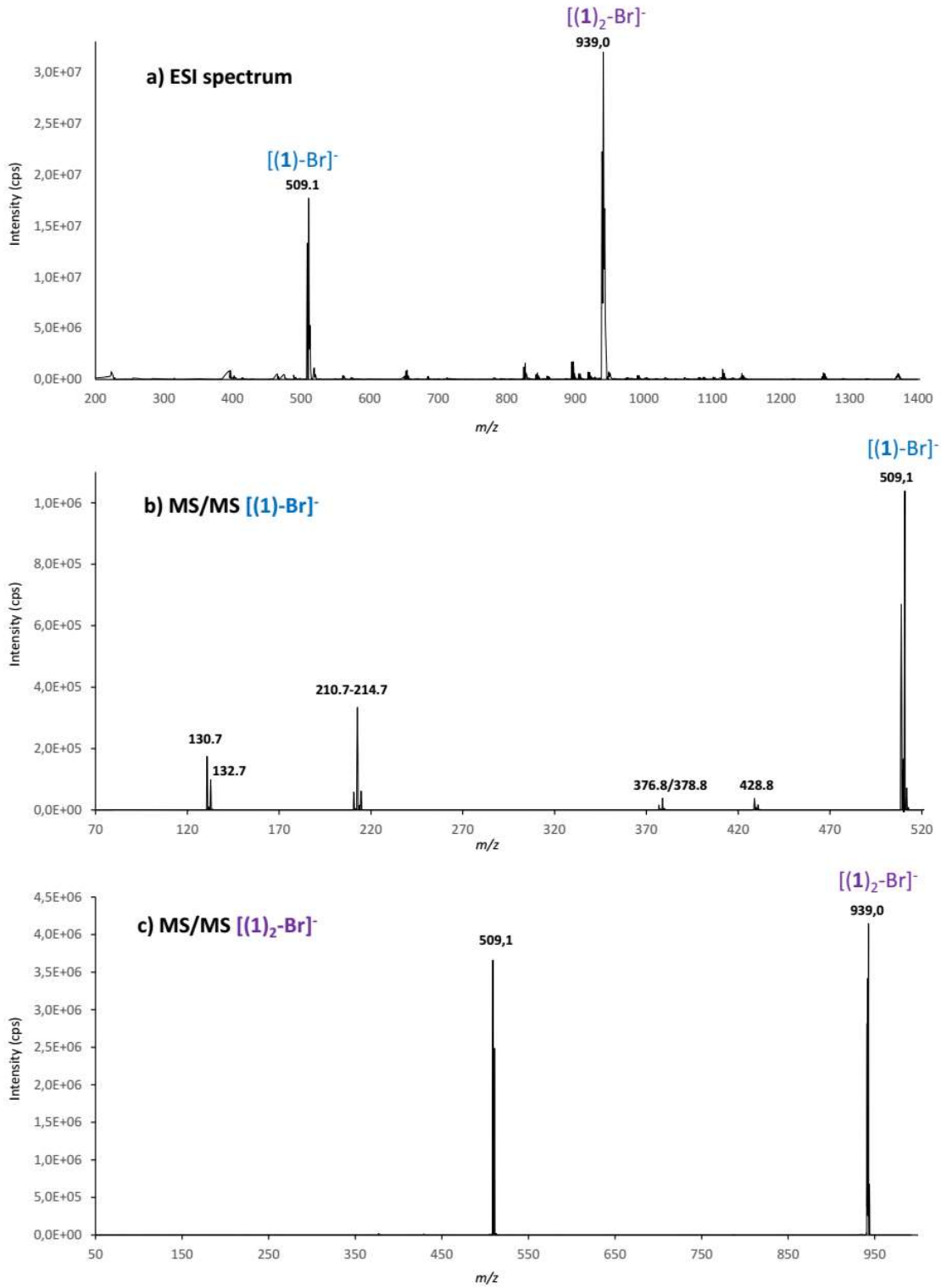

*Figure S16: Typical electrospray spectra obtained for the 1:1 **1**/TBABr mixture*
*a) Electrospray mass spectrum of an equimolar (10^{-4} M) mixture of **1**/TBABr (90/10 acetonitrile/water) b) MS/MS spectrum of the [(**1**)-Br]⁻ ion– c) MS/MS spectrum of the [(**1**)$_2$-Br]⁻ ion*

4.2 Typical electrospray spectra obtained for the 1:1 (**1**)/TBAI mixture

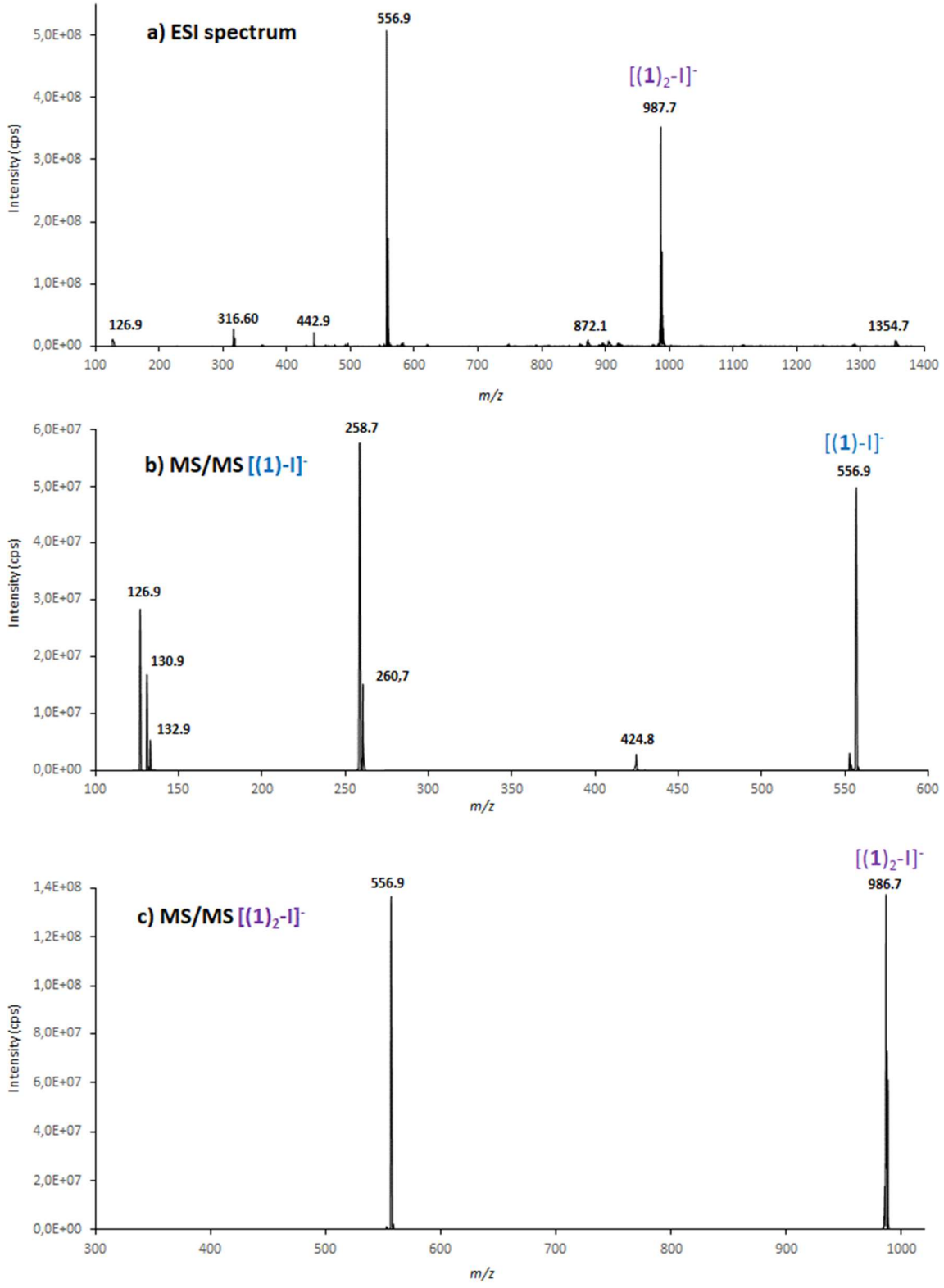

*Figure S17: Typical electrospray spectra obtained for the 1:1 **1**/TBAI mixture*
*a) Electrospray mass spectrum of an equimolar (10^{-4} M) mixture of **1**/TBAI (90/10 acetonitrile/water) b) MS/MS spectrum of the [(**1**)-I]$^-$ ion– c) MS/MS spectrum of the [(**1**)$_2$-I]$^-$ ion*

4.3 Typical electrospray spectra obtained for the 1:1 (**1**)/TBASCN mixture

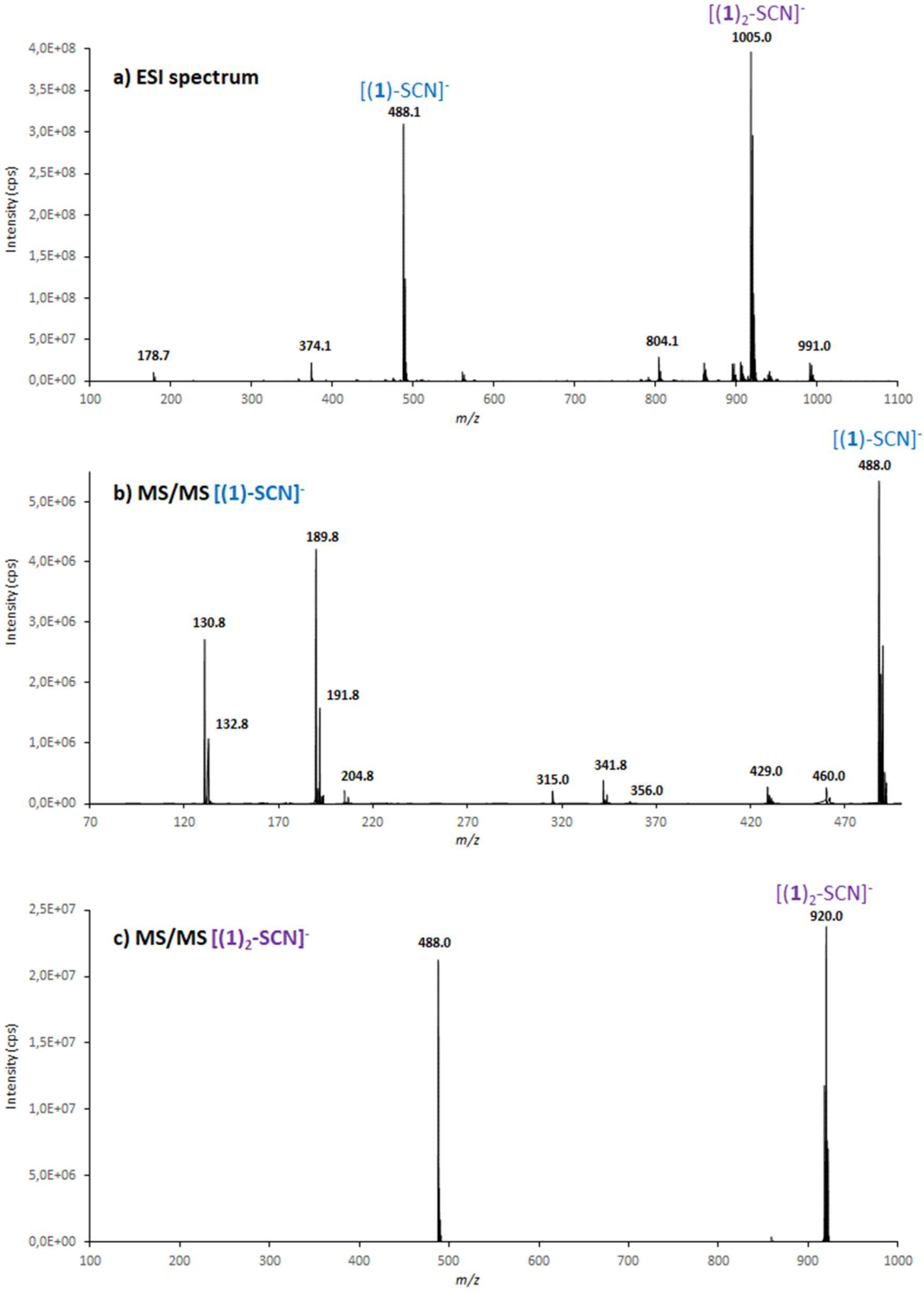

*Figure S18: Typical electrospray spectra obtained for the 1:1 **1**/TBASCN mixture*
*a) Electrospray mass spectrum of an equimolar (10^{-4} M) mixture of **1**/TBASCN (90/10 acetonitrile/water) b) MS/MS spectrum of the [(**1**)-SCN]⁻ ion– c) MS/MS spectrum of the [(**1**)$_2$-SCN]⁻ ion*

4.4 Typical electrospray spectra obtained for the 1:1 (**1**)/$TBAPF_6$ mixture

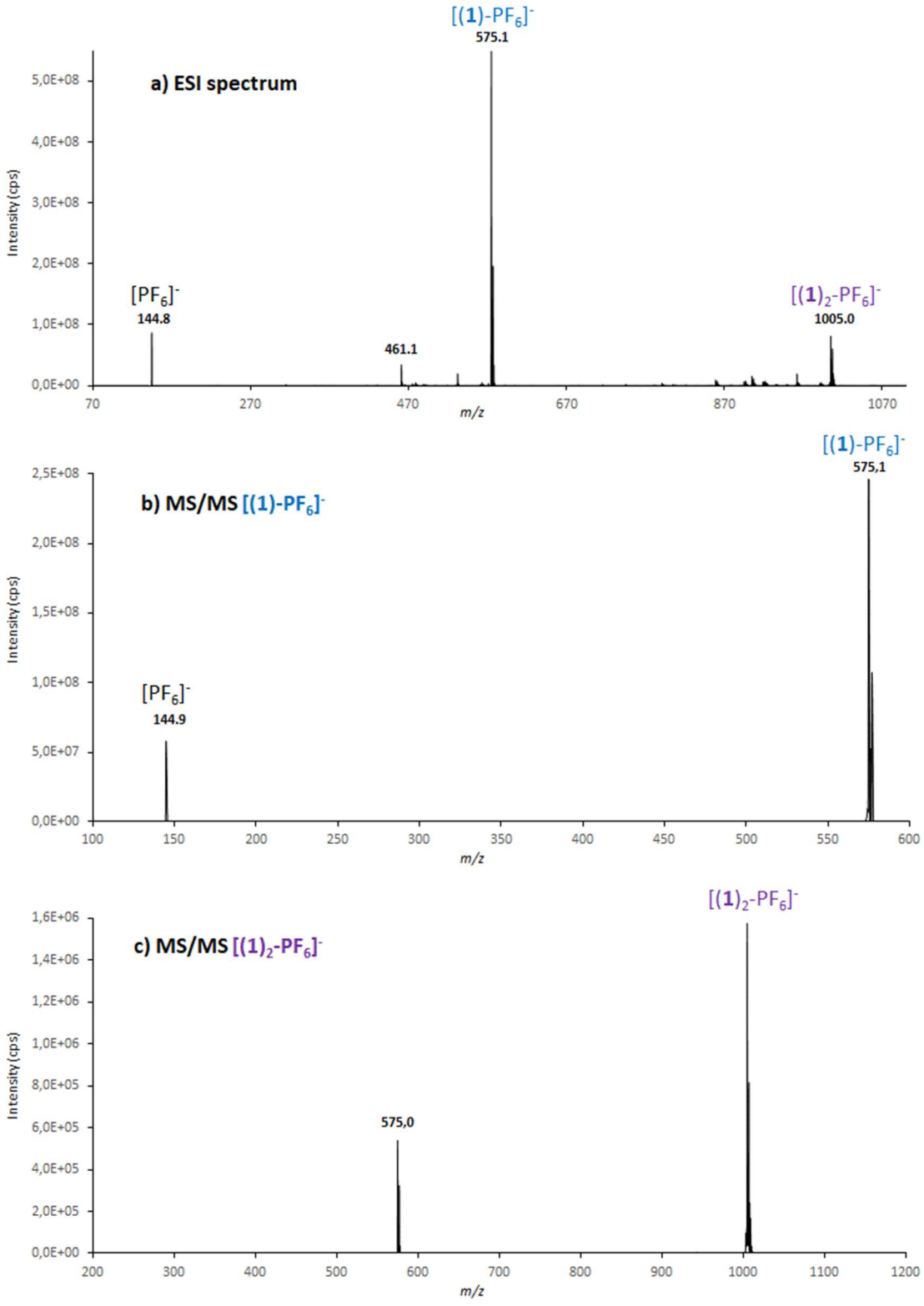

*Figure S19: Typical electrospray spectra obtained for the 1:1 **1**/TBAPF6 mixture*
*a) Electrospray mass spectrum of an equimolar (10^{-4} M) mixture of **1**/$TBAPF_6$ (90/10 acetonitrile/water) b) MS/MS spectrum of the $[(\mathbf{1})\text{-}PF_6]^-$ ion– c) MS/MS spectrum of the $[(\mathbf{1})_2\text{-}PF6]^-$ ion*

4.5 Fragmentation mechanisms associated to *Scheme 3*

Formation of $[M-H]^-$ m/z 429

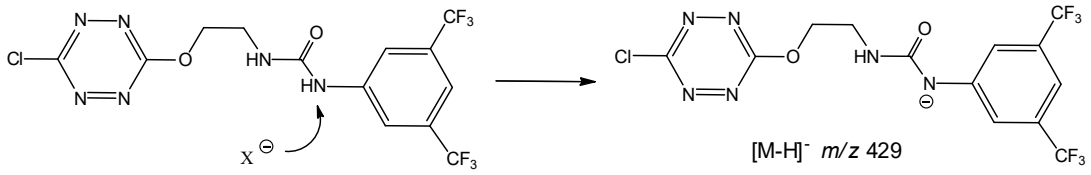

Formation of $[C_2N_4OCl]^-$ m/z 131 and elimination of 132u

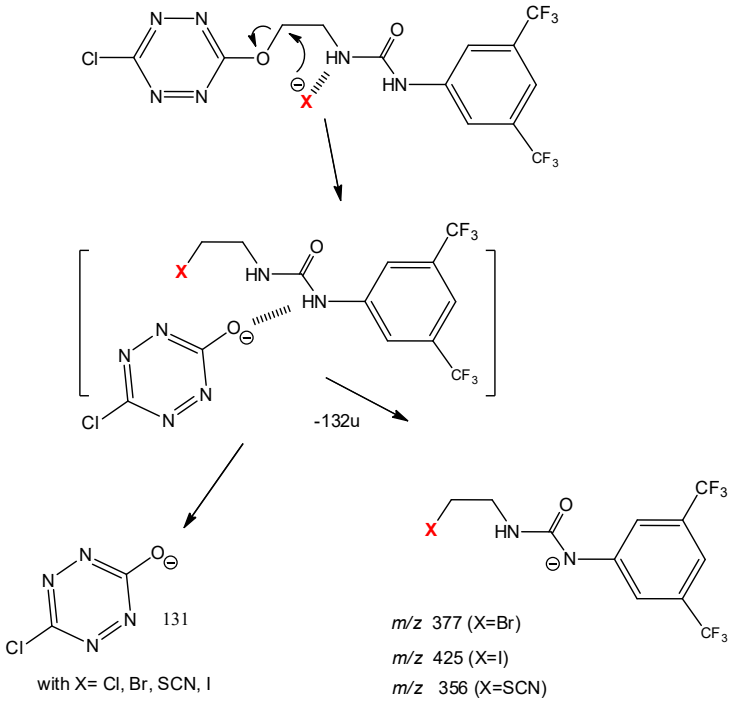

Formation of $[C_2HN_4OClX]^-$

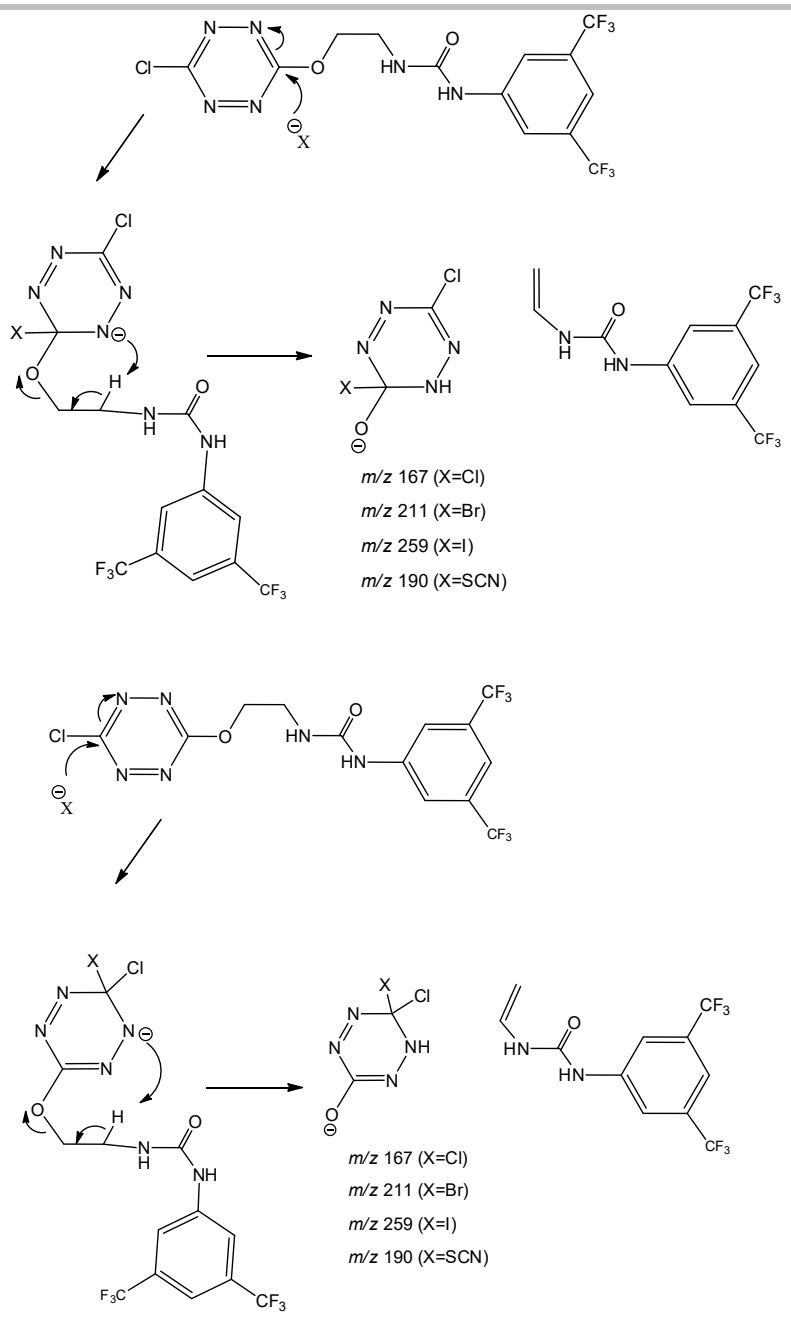
m/z 167 (X=Cl)
m/z 211 (X=Br)
m/z 259 (X=I)
m/z 190 (X=SCN)
m/z 167 (X=Cl)
m/z 211 (X=Br)
m/z 259 (X=I)
m/z 190 (X=SCN)

5. NMR Titrations

5.1 Practical analysis procedure

Previously to each analysis, anion salts were solubilized into acetone and precipitated by addition of diethylether to remove water. Salts were then dried to remove residual solvents and stored in the dessicator until use.

2mL of a solution containing the anion receptor was prepared (3.5mmol/L). 500µL were placed into a new NMR tube. 1mL of stock solution was taken and desired amount of anionic guest as the tetrabutylammonium (TBA) salt was added.

NMR titrations were performed by adding aliquots of a solution containing the anionic guest (0.14M for TBACl, 0.14M for TBABr, 0.55M for TBAI and 1.04M for TBASCN) and the receptor (3.5mM) in MeCN-d_3 to the NMR tube. After each addition, a ^{1}H NMR spectrum was recorded.

^{1}H NMR spectra were calibrated to the residual proton solvent peak in MeCN-d_3 (δ = 1.94ppm) at 300 K. Plot stackings were made using MestReNova Version 6.0. Non-linear least-square curve fitting of the titration data were double checked to be a 1:1 binding model using a reported procedure [7] on Excel software and SPECFIT software.

5.2 Titration of **1** with TBACl

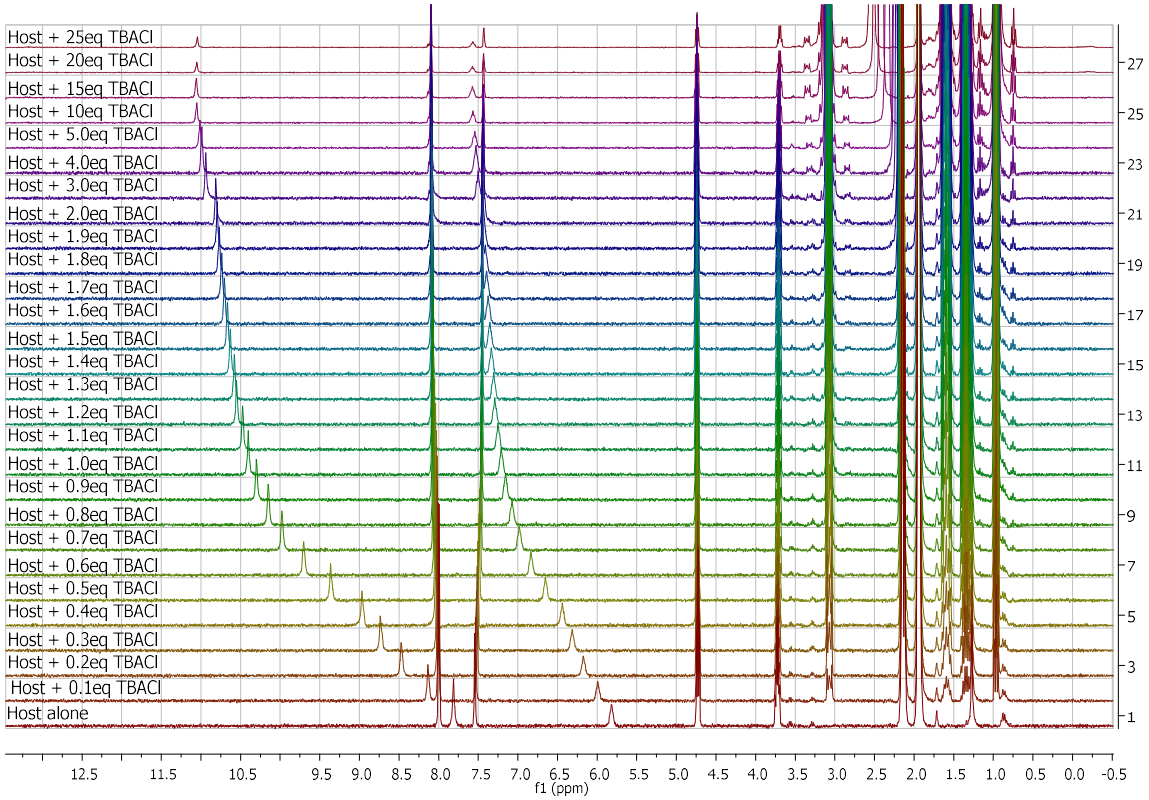

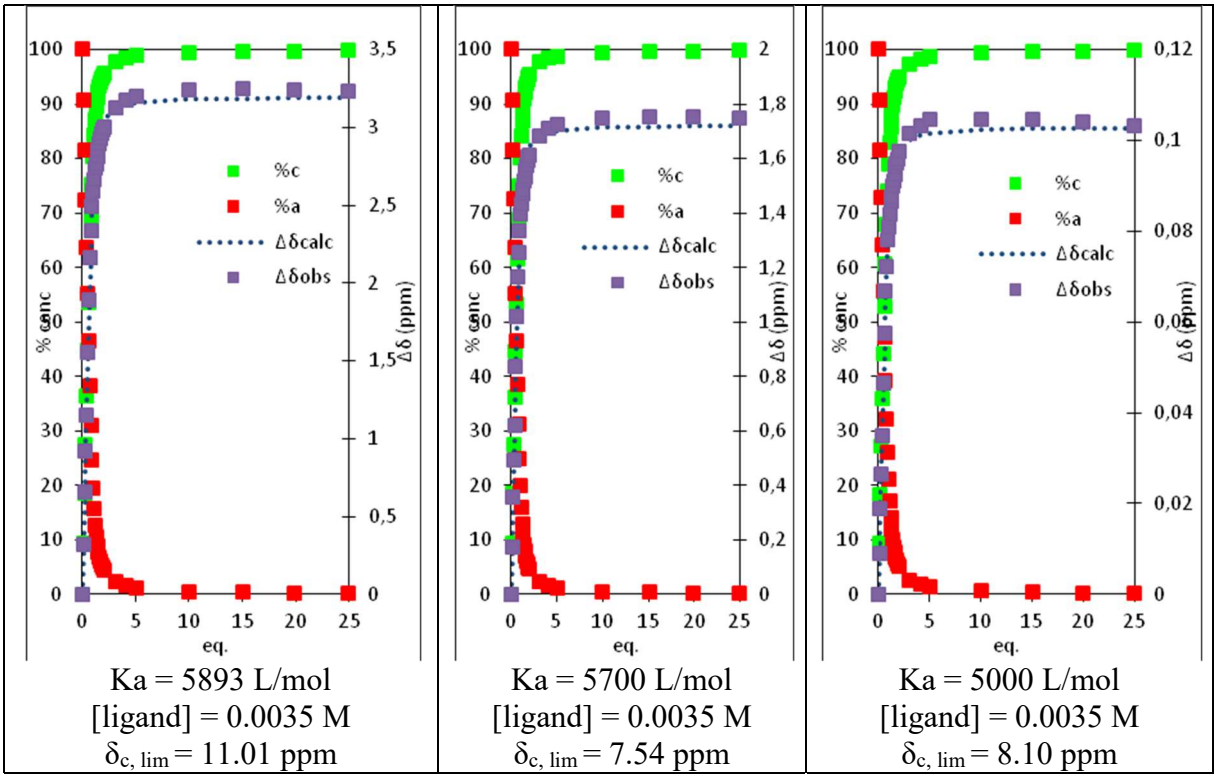

Ka = 5893 L/mol	Ka = 5700 L/mol	Ka = 5000 L/mol
[ligand] = 0.0035 M	[ligand] = 0.0035 M	[ligand] = 0.0035 M
$\delta_{c,\,lim}$ = 11.01 ppm	$\delta_{c,\,lim}$ = 7.54 ppm	$\delta_{c,\,lim}$ = 8.10 ppm

*Figure S20: ^{1}H NMR titration of **1** with tetrabutylammonium chloride (0 to 25 equivalents)*
%c = percentage of complex %a = percentage of free receptor Δδcalc = chemical shift calculated Δδobs = chemical shift observed

```
[PROGRAM]
Name = SPECFIT
Version = 3.0

[FILE]
Name = GG16+TBACL_RMN_FORMAT_SPECFIT.FAC
Path = C:\Program Files\SPECFIT\DATA\
Date = 03-déc-19
Time = 12:14:38
Ncomp = 2
Nmeas = 28
Nwave = 3

[FACTOR ANALYSIS]
Tolerance = 1,000E-09
Max.Factors = 10
Num.Factors = 3
Significant = 3
Eigen Noise = 1,333E-07
Exp't Noise = 1,333E-07
#   Eigenvalue  Square Sum  Residual    Prediction
1   6,181E+03   8,889E+00   3,273E-01   Data Vector
2   8,889E+00   1,906E-04   1,524E-03   Data Vector
3   1,906E-04   1,440E-12   1,333E-07   Data Vector

[MODEL]
Date = 03-déc-19
Time = 12:16:30
Model = 0
Index = 3
Function = 1
Species = 3
Params = 3

[SPECIES]   [COLORED]   [FIXED]   [SPECTRUM]
1 0 0       False       False
0 1 0       True        False
1 1 0       True        False

[SPECIES]   [FIXED]   [PARAMETER]              [ERROR]
1 0 0       True      0,00000E+00   +/-       0,00000E+00
0 1 0       True      0,00000E+00   +/-       0,00000E+00
1 1 0       False     3,68952E+00   +/-       4,19950E-02

[CONVERGENCE]
Iterations = 5
Convergence Limit = 1,000E-03
Convergence Found = 1,697E-05
Marquardt Parameter = 0,0
Sum(Y-y)^2 Residuals = 1,92287E-01
Std. Deviation of Fit(Y) = 4,81322E-02

[STATISTICS]
Experimental Noise = 1,333E-07
Relative Error Of Fit = 0,5574%
Durbin-Watson Factor = 0,3072
Goodness Of Fit, Chi^2 = 1,303E+11
Durbin-Watson Factor (raw data) = 0,3072
Goodness Of Fit, Chi^2 (raw data) = None

[COVARIANCE]
1,031E-02

[CORRELATION]
1,000E+00

[END FILE]
```

*Figure S21: Determination of binding constant using SPECFIT software for the ^{1}H NMR titration of **1** with tetrabutylammonium chloride*

5.3 Titration of **2** with TBACl

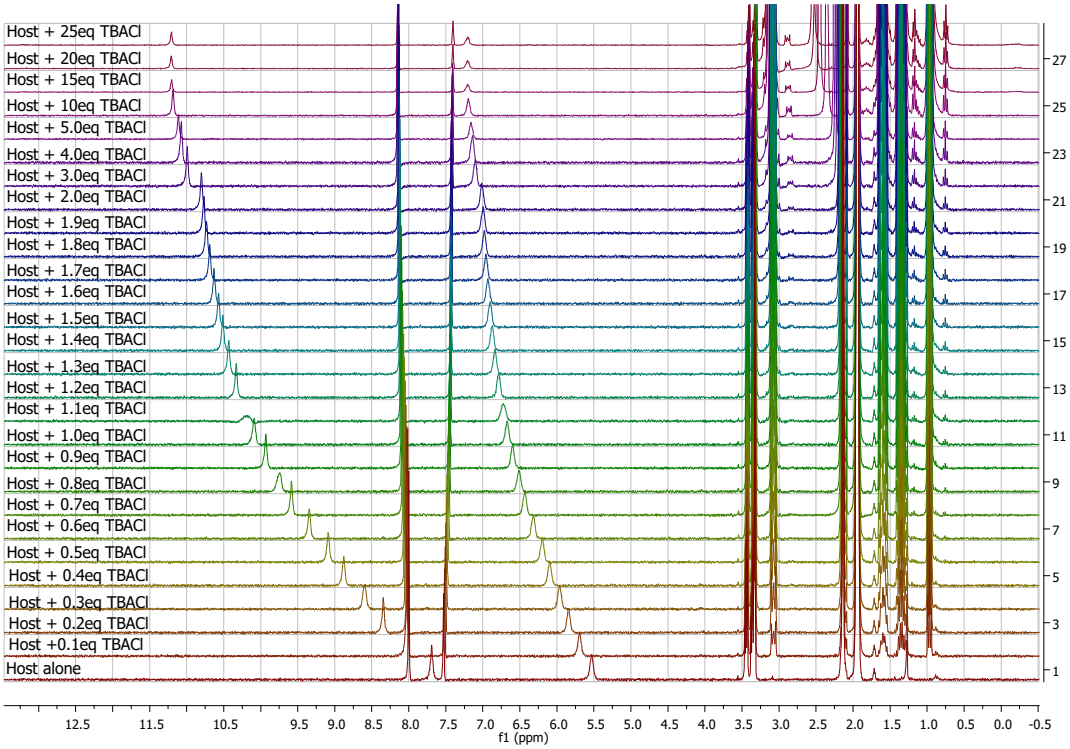

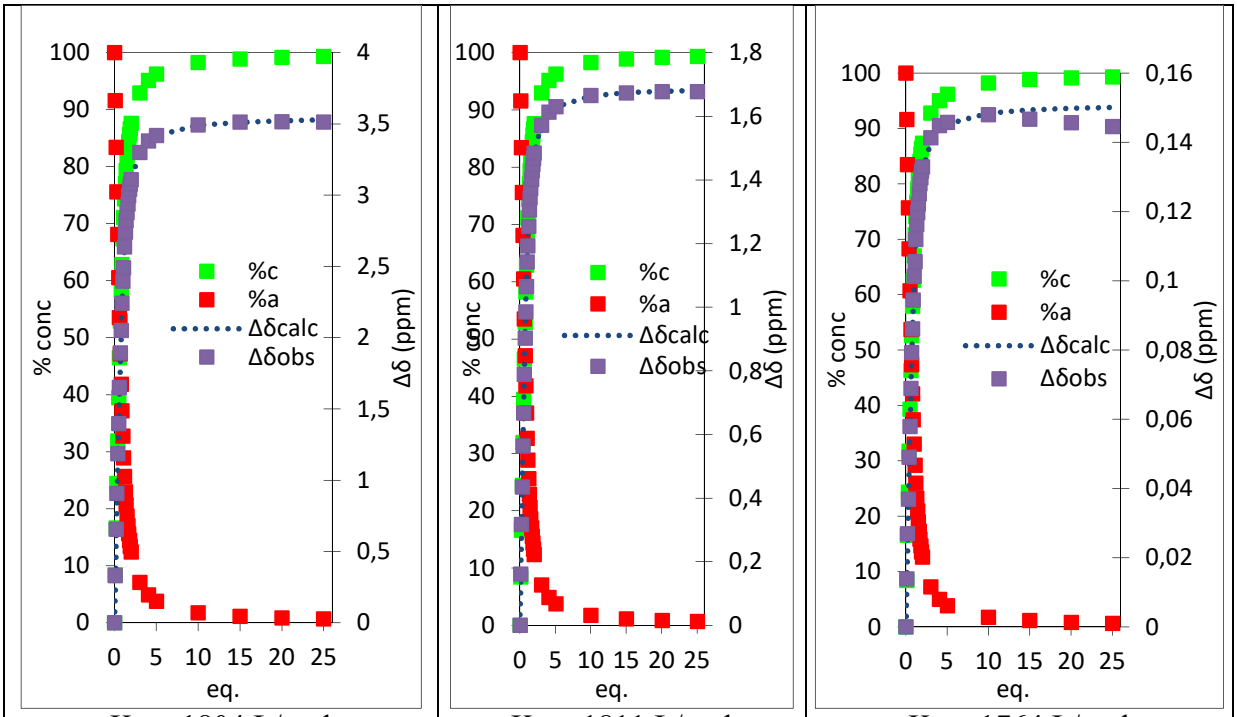

Ka = 1804 L/mol
[ligand] = 0.0035 M
$\delta_{c,\,lim}$ = 11.24 ppm

Ka = 1811 L/mol
[ligand] = 0.0035 M
$\delta_{c,\,lim}$ = 7.22 ppm

Ka = 1764 L/mol
[ligand] = 0.0035 M
$\delta_{c,\,lim}$ = 8.15 ppm

*Figure S22: ^{1}H NMR titration of **2** with tetrabutylammonium chloride (0 to 25 equivalents)*
%c = percentage of complex %a = percentage of free receptor Δδcalc = chemical shift calculated Δδobs = chemical shift observed

[PROGRAM]
Name = SPECFIT
Version = 3.0

[FILE]
Name = RP108+TBACL_RMN_FORMAT_SPECFIT.FAC
Path = C:\Program Files\SPECFIT\DATA\
Date = 04-mars-20
Time = 17:34:13
Ncomp = 2
Nmeas = 28
Nwave = 3

[FACTOR ANALYSIS]
Tolerance = 1,000E-09
Max.Factors = 10
Num.Factors = 3
Significant = 3
Eigen Noise = 9,263E-08
Exp't Noise = 9,263E-08

#	Eigenvalue	Square Sum	Residual	Prediction
1	5,972E+03	1,025E+01	3,514E-01	Data Vector
2	1,025E+01	1,272E-04	1,246E-03	Data Vector
3	1,272E-04	6,950E-13	9,263E-08	Data Vector

[MODEL]
Date = 04-mars-20
Time = 17:35:43
Model = 0
Index = 3
Function = 1
Species = 3
Params = 3

[SPECIES]	[COLORED]	[FIXED]	[SPECTRUM]
1 0 0	False	False	
0 1 0	True	False	
1 1 0	True	False	

[SPECIES]	[FIXED]	[PARAMETER]		[ERROR]
1 0 0	True	0,00000E+00	+/-	0,00000E+00
0 1 0	True	0,00000E+00	+/-	0,00000E+00
1 1 0	False	3,24475E+00	+/-	5,40102E-03

[CONVERGENCE]
Iterations = 8
Convergence Limit = 1,000E-03
Convergence Found = 3,416E-04
Marquardt Parameter = 0,0
Sum(Y-y)^2 Residuals = 7,92029E-03
Std. Deviation of Fit(Y) = 9,76858E-03

[STATISTICS]
Experimental Noise = 9,263E-08
Relative Error Of Fit = 0,1151%
Durbin-Watson Factor = 1,6449
Goodness Of Fit, Chi^2 = 1,112E+10
Durbin-Watson Factor (raw data) = None
Goodness Of Fit, Chi^2 (raw data) = None

[COVARIANCE]
1,566E-04

[CORRELATION]
1,000E+00

[END FILE]

*Figure S23: Determination of binding constant using SPECFIT software for the ^{1}H NMR titration of **2** with tetrabutylammonium chloride*

5.4 Titration of **1** with TBABr

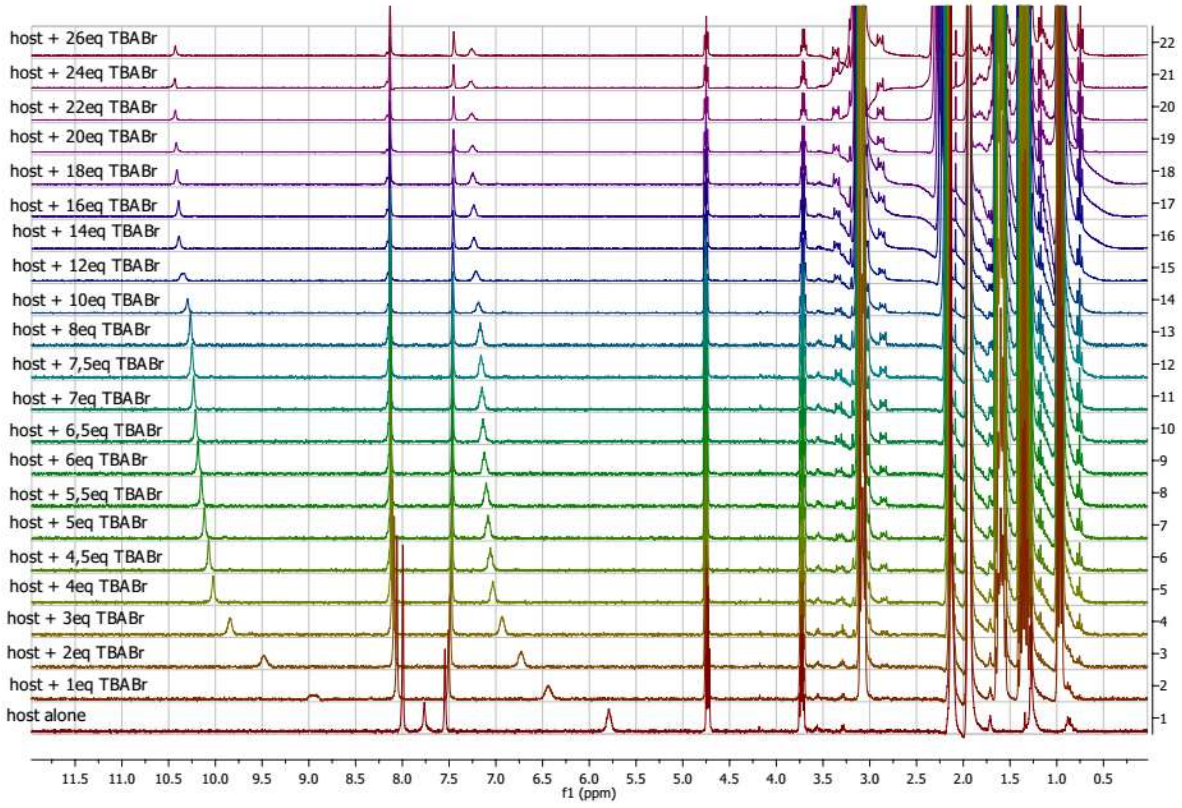

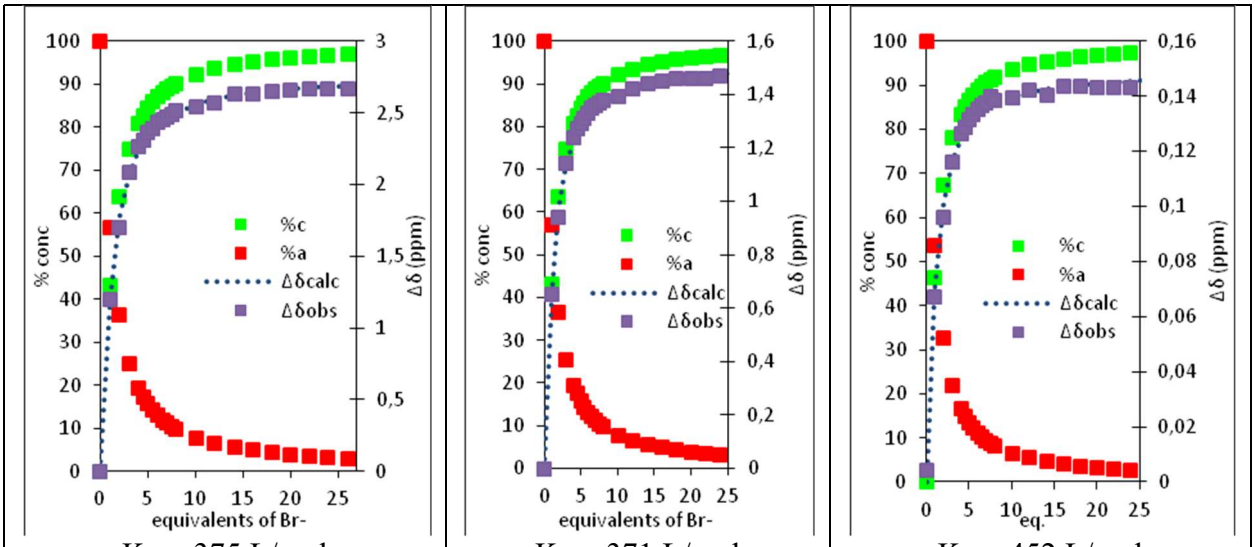

Ka = 375 L/mol	Ka = 371 L/mol	Ka = 452 L/mol
[ligand] = 0.0035 M	[ligand] = 0.0035 M	[ligand] = 0.0035 M
$\delta_{c,\,lim}$ = 10.53 ppm	$\delta_{c,\,lim}$ = 7.31 ppm	$\delta_{c,\,lim}$ = 8.14 ppm

*Figure S24: ^{1}H NMR titration of **1** with tetrabutylammonium bromide (0 to 26 equivalents)*
%c = percentage of complex %a = percentage of free receptor Δδcalc = chemical shift calculated Δδobs = chemical shift observed

[PROGRAM]
Name = SPECFIT
Version = 3.0

[FILE]
Name = RP04+TBABR_RMN_FORMAT_SPECFIT.FAC
Path = C:\Program Files\SPECFIT\DATA\
Date = 18-juil-19
Time = 11:20:39
Ncomp = 2
Nmeas = 22
Nwave = 3

[FACTOR ANALYSIS]
Tolerance = 1,000E-09
Max.Factors = 10
Num.Factors = 3
Significant = 3
Eigen Noise = 1,774E-08
Exp't Noise = 1,774E-08

#	Eigenvalue	Square Sum	Residual	Prediction
1	4,771E+03	2,856E+00	2,096E-01	Data Vector
2	2,855E+00	3,351E-04	2,288E-03	Data Vector
3	3,351E-04	1,983E-14	1,774E-08	Data Vector

[MODEL]
Date = 18-juil-19
Time = 11:21:31
Model = 0
Index = 3
Function = 1
Species = 3
Params = 3

[SPECIES]	[COLORED]	[FIXED]	[SPECTRUM]
1 0 0	False	False	
0 1 0	True	False	
1 1 0	True	False	

[SPECIES]	[FIXED]	[PARAMETER]		[ERROR]
1 0 0	True	0,00000E+00	+/-	0,00000E+00
0 1 0	True	0,00000E+00	+/-	0,00000E+00
1 1 0	False	2,57434E+00	+/-	8,36370E-03

[CONVERGENCE]
Iterations = 8
Convergence Limit = 1,000E-03
Convergence Found = 3,835E-06
Marquardt Parameter = 0,0
Sum(Y-y)^2 Residuals = 9,75058E-03
Std. Deviation of Fit(Y) = 1,22478E-02

[STATISTICS]
Experimental Noise = 1,774E-08
Relative Error Of Fit = 0,1429%
Durbin-Watson Factor = 1,4662
Goodness Of Fit, Chi^2 = 4,766E+11
Durbin-Watson Factor (raw data) = 1,4662
Goodness Of Fit, Chi^2 (raw data) = None

[COVARIANCE]
3,781E-04

[CORRELATION]
1,000E+00

[END FILE]

*Figure S25: Determination of binding constant using SPECFIT software for the ^{1}H NMR titration of **1** with tetrabutylammonium bromide*

5.5 Titration of **1** with TBAI

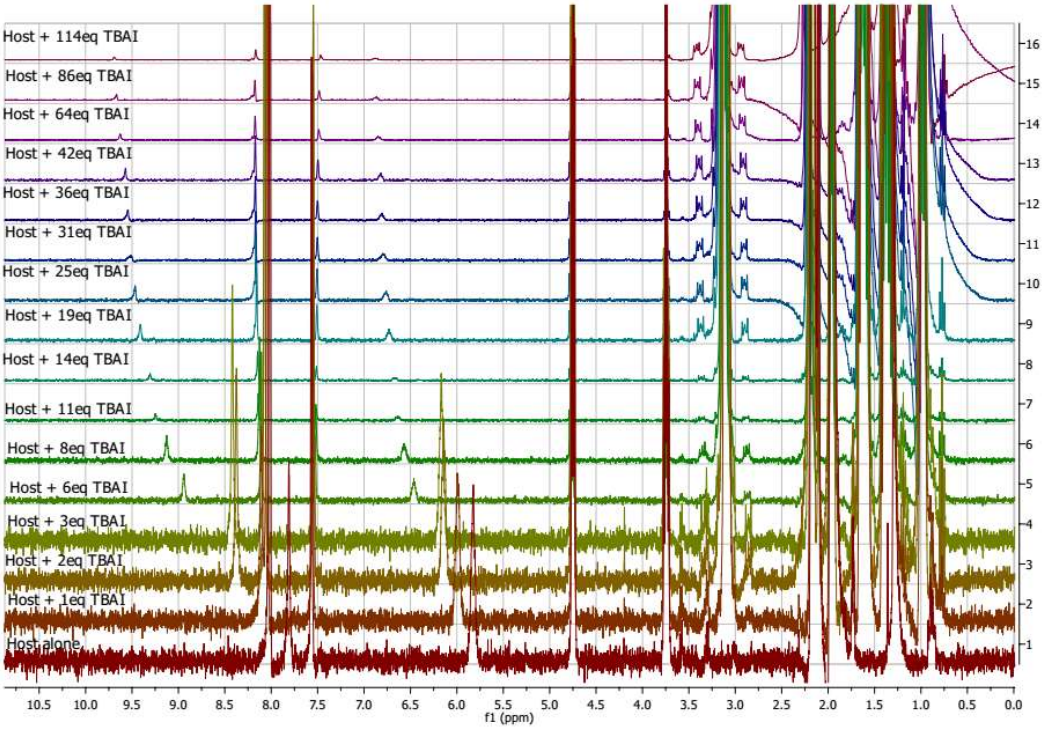

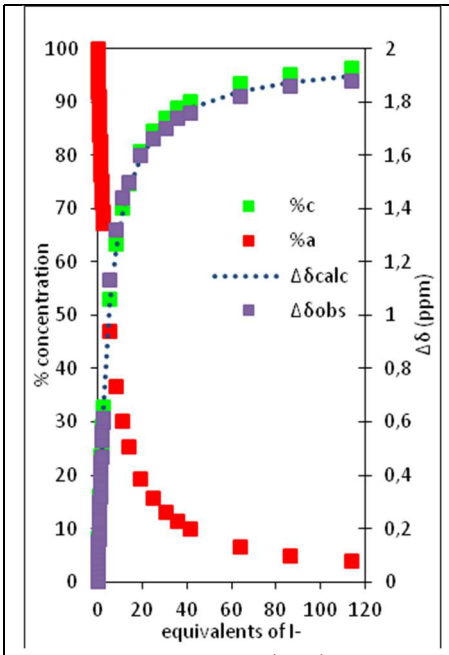

Ka = 64 L/mol
[ligand] = 0.0035 M
$\delta_{c,\,lim}$ = 9.78 ppm

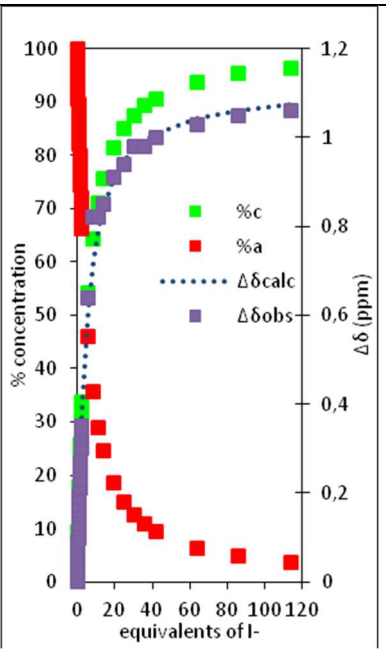

Ka = 67 L/mol
[ligand] = 0.0035 M
$\delta_{c,\,lim}$ = 6.93 ppm

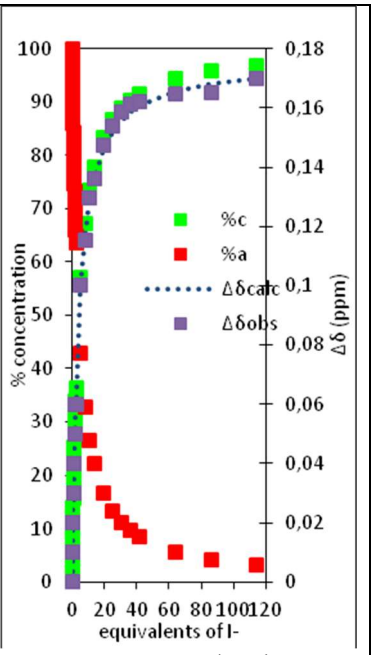

Ka = 77 L/mol
[ligand] = 0.0035 M
$\delta_{c,\,lim}$ = 8.19 ppm

*Figure S26: ^{1}H NMR titration of **1** with tetrabutylammonium iodide (0 to 114 equivalents)*
%c = percentage of complex %a = percentage of free receptor Δδcalc = chemical shift calculated Δδobs = chemical shift observed

```
[PROGRAM]
Name = SPECFIT
Version = 3.0

[FILE]
Name = RP04+TBAI_RMN_FORMAT_SPECFIT.FAC
Path = C:\Program Files\SPECFIT\DATA\
Date = 18-juil-19
Time = 18:25:49
Ncomp = 2
Nmeas = 38
Nwave = 3

[FACTOR ANALYSIS]
Tolerance = 1,000E-09
Max.Factors = 10
Num.Factors = 3
Significant = 3
Eigen Noise = 6,121E-08
Exp't Noise = 6,121E-08
#  Eigenvalue  Square Sum  Residual    Prediction
1  6,725E+03  6,499E+00  2,398E-01  Data Vector
2  6,494E+00  4,300E-03  6,196E-03  Data Vector
3  4,300E-03  4,159E-13  6,121E-08  Data Vector

[MODEL]
Date = 18-juil-19
Time = 18:26:03
Model = 0
Index = 3
Function = 1
Species = 3
Params = 3

[SPECIES]    [COLORED]    [FIXED]      [SPECTRUM]
1 0 0        False        False
0 1 0        True         False
1 1 0        True         False

[SPECIES]    [FIXED]      [PARAMETER]          [ERROR]
1 0 0        True         0,00000E+00  +/-     0,00000E+00
0 1 0        True         0,00000E+00  +/-     0,00000E+00
1 1 0        False        1,84534E+00  +/-     1,07339E-02

[CONVERGENCE]
Iterations = 8
Convergence Limit = 1,000E-03
Convergence Found = 2,135E-05
Marquardt Parameter = 0,0
Sum(Y-y)^2 Residuals = 3,60982E-02
Std. Deviation of Fit(Y) = 1,78732E-02

[STATISTICS]
Experimental Noise = 6,121E-08
Relative Error Of Fit = 0,2316%
Durbin-Watson Factor = 0,8860
Goodness Of Fit, Chi^2 = 8,527E+10
Durbin-Watson Factor (raw data) = None
Goodness Of Fit, Chi^2 (raw data) = None

[COVARIANCE]
6,262E-04

[CORRELATION]
1,000E+00

[END FILE]
```

*Figure S27: Determination of binding constant using SPECFIT software for the ^{1}H NMR titration of **1** with tetrabutylammonium iodide*

5.6 Titration of **1** with TBASCN

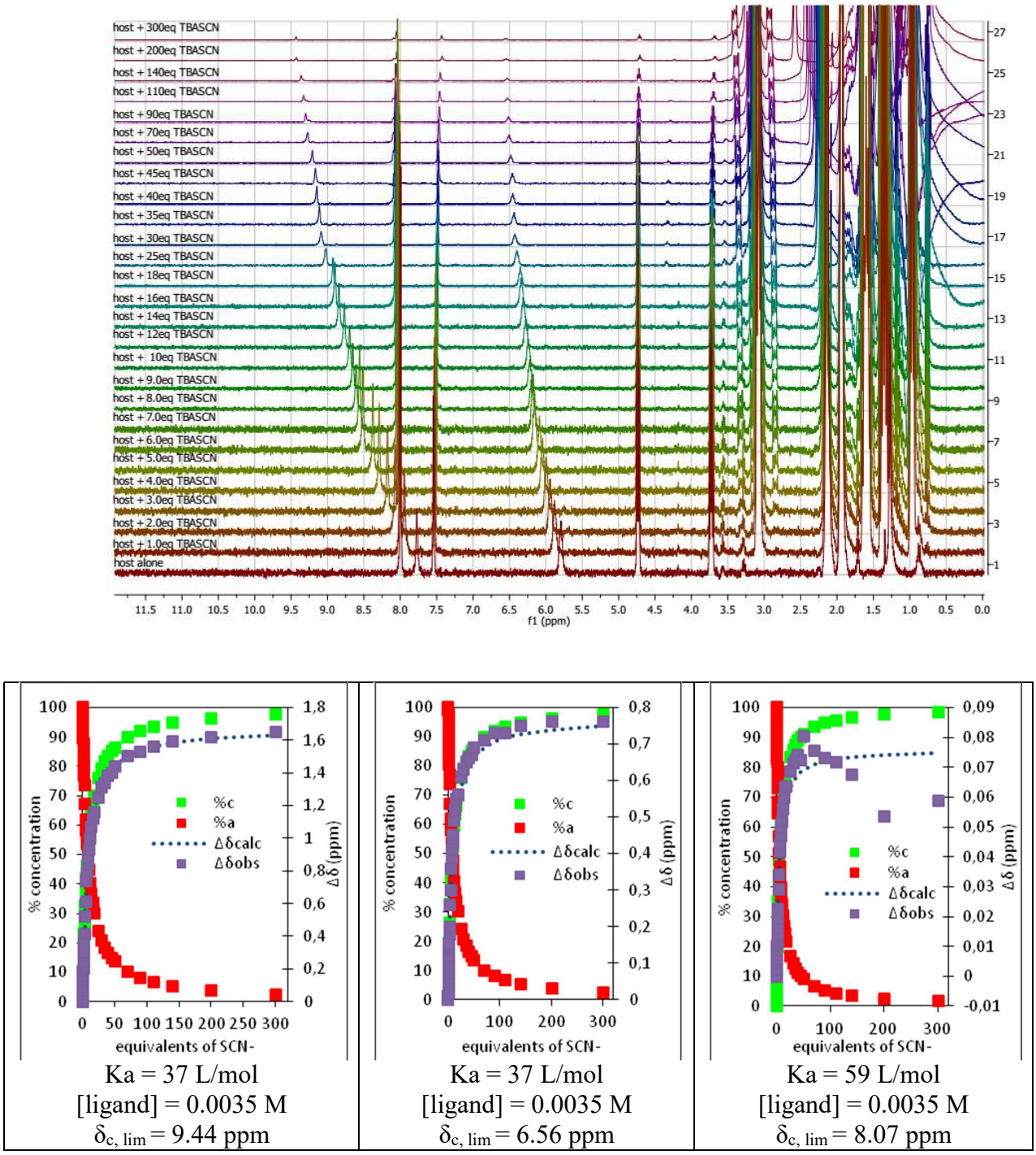

*Figure S28: ^{1}H NMR titration of **1** with tetrabutylammonium thioisocyanate (0 to 320 equivalents)*
%c = percentage of complex %a = percentage of free receptor Δδcalc = chemical shift calculated Δδobs = chemical shift observed

```
[PROGRAM]
Name = SPECFIT
Version = 3.0

[FILE]
Name = RP04+TBASCN_RMN_FORMAT_SPECFIT.FAC
Path = C:\Program Files\SPECFIT\DATA\
Date = 18-juil-19
Time = 18:31:39
Ncomp = 2
Nmeas = 41
Nwave = 3

[FACTOR ANALYSIS]
Tolerance = 1,000E-09
Max.Factors = 10
Num.Factors = 3
Significant = 3
Eigen Noise = 1,157E-07
Exp't Noise = 1,157E-07
#   Eigenvalue  Square Sum  Residual    Prediction
1   7,165E+03   5,728E+00   2,167E-01   Data Vector
2   5,660E+00   6,804E-02   2,371E-02   Data Vector
3   6,804E-02   1,607E-12   1,157E-07   Data Vector

[MODEL]
Date = 18-juil-19
Time = 18:32:02
Model = 0
Index = 3
Function = 1
Species = 3
Params = 3

[SPECIES]       [COLORED]       [FIXED]         [SPECTRUM]
1 0 0           False           False
0 1 0           True            False
1 1 0           True            False

[SPECIES]       [FIXED]         [PARAMETER]             [ERROR]
1 0 0           True            0,00000E+00   +/-       0,00000E+00
0 1 0           True            0,00000E+00   +/-       0,00000E+00
1 1 0           False           1,56247E+00   +/-       1,67367E-02

[CONVERGENCE]
Iterations = 8
Convergence Limit = 1,000E-03
Convergence Found = 6,467E-04
Marquardt Parameter = 0,0
Sum(Y-y)^2 Residuals = 9,59235E-02
Std. Deviation of Fit(Y) = 2,80403E-02

[STATISTICS]
Experimental Noise = 1,157E-07
Relative Error Of Fit = 0,3658%
Durbin-Watson Factor = 1,9633
Goodness Of Fit, Chi^2 = 5,870E+10
Durbin-Watson Factor (raw data) = None
Goodness Of Fit, Chi^2 (raw data) = None

[COVARIANCE]
1,544E-03

[CORRELATION]
1,000E+00

[END FILE]
```

*Figure S29 : Determination of binding constant using SPECFIT software for the ^{1}H NMR titration of **1** with tetrabutylammonium thioisocyanate*

5.7 Superposition of experimental curves

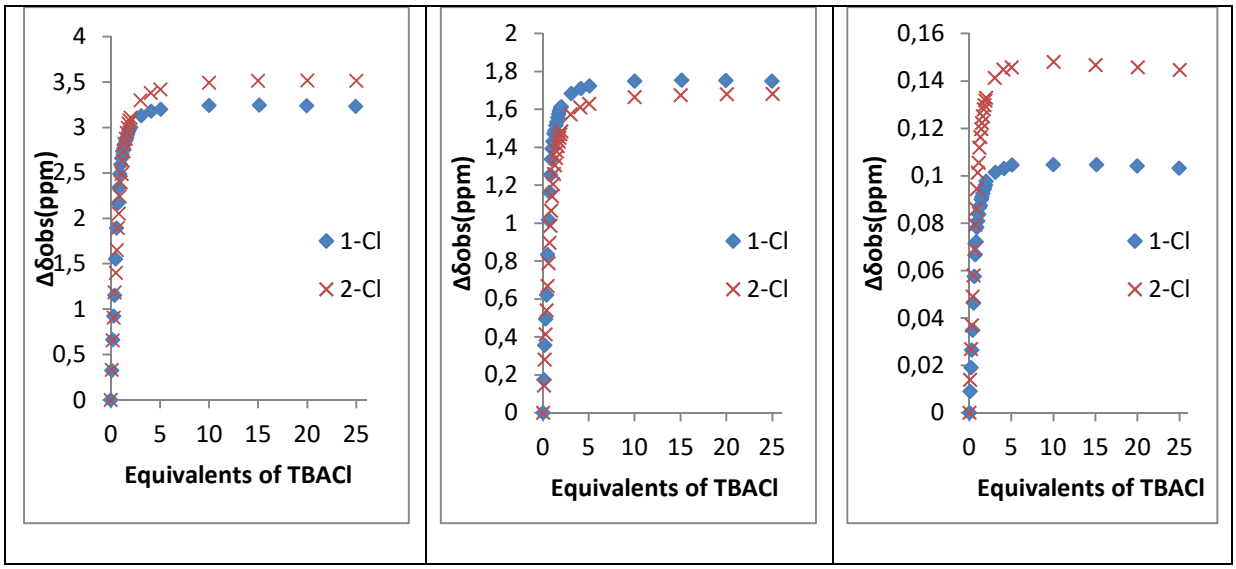

*Figure S30 – Differences in chemical shifts observed as a function of the number of equivalents of salts added protons a, b and c for **1** and **2** with tetrabutylammonium chloride*

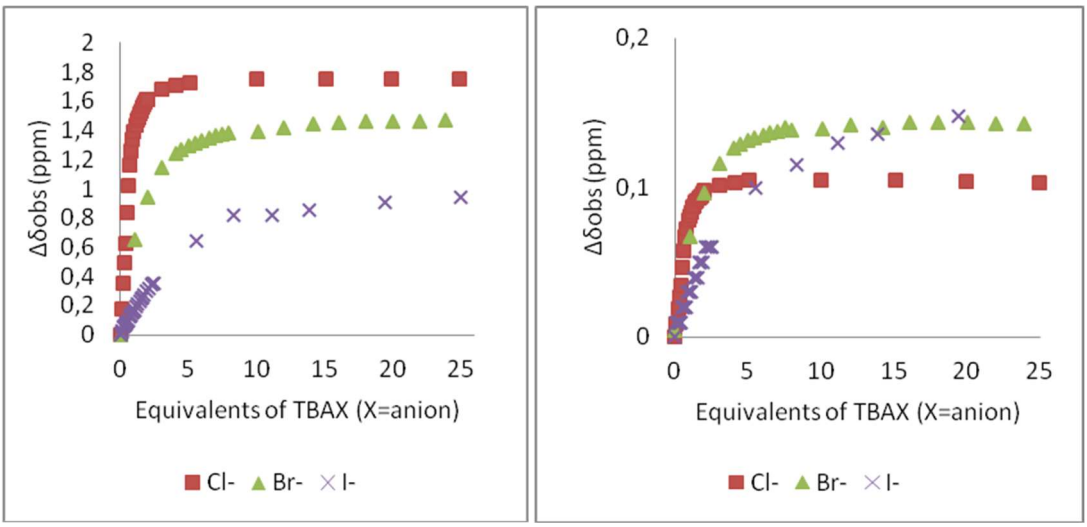

Figure S31 – Differences in chemical shifts observed as a function of the number of equivalents of salts added protons b and c

6. Photophysical analysis and procedures

6.1 General practical analysis procedure

Previously to each analysis, anion salts were solubilized into acetone and precipitated by addition of diethylether to remove water. Salts were then dried to remove residual solvents and stored in the dessicator until use.

10mL of a stock solution of the anion receptor were prepared (10^{-3}mol/L) in acetonitrile. 2mL of this solution was taken and diluted at 2.10^{-5}mol/L. 2mL of this solution at 2.10^{-5}mol/L were introduced into a quartz cuvette. 2mL of the stock solution was taken, desired amount of salt was added (150mg for TBACl, 330mg for TBABr, 600mg for TBAI and 600mg for TBASCN) and diluted at 2.10^{-5}mol/L.

2.5mL of solution were added to a 1cm quartz glass cuvette. Aliquots of the solution containing the anion and the receptor are subsequently added to the sample cuvette for each measurement.

After blank subtraction, absorbance spectra were measured from 200 to 700nm. From the absorbance spectra were determined the absorbance maximum (510nm), that corresponds to the excitation wavelength for the emission spectra.

Emission spectra were measured from 520 nm ($\lambda_{abs,max}$+10) to 700nm using the wavelength determined before as excitation wavelength. Slites were calibrated at 2.1nm. All experiments were proceeded in temperature-controlled room at 300K.

Fluorescence decay data were analyzed using the Globals software package developed at the Laboratory for Fluorescence Dynamics at the University of Illinois at Urbana-Champaign, which includes reconvolution analysis and global non-linear least-squares minimization method.

Experimental measurements were plotted using Excel software. Determination of binding constants was done using a method developed by Valeur *et al.* [8] using non-linear least-squares minimization method.

$$Y = Y_0 + \frac{Y_{lim} - Y_0}{2}\left\{1 + \frac{c_M}{c_L} + \frac{1}{K_s c_L} - \left[\left(1 + \frac{c_M}{c_L} + \frac{1}{K_s c_L}\right)^2 - 4\frac{c_M}{c_L}\right]^{1/2}\right\}$$

Where :

Y : Measured intensity at fluorescence maximum

Y_0 : Measured intensity when no salt was added

Y_{lim} : Calculated intensity when an infinity of equivalents of salts are added

c_M : Anion concentration

c_L : Receptor concentration

K_s : Association constant of receptor/anion complex

Binding constants were also determined using SPECFIT/32 ™ Global Analysis System software [9,10]. This software allows global analysis of equilibrium and kinetic systems with Expanded SVD and nonlinear regression modeling by the Levenberg-Marquardt method.

6.2 Determination of quantum yield of **1**

Emission spectra of reference and compound **1** were recorded using the maximum absorption wavelength of the reference, Rhodamine-6G, as excitation wavelength. The fluorescence quantum yield Φ_F was determined using Rhodamine-6G as reference (Φ_F= 0.91 in ethanol). [11]

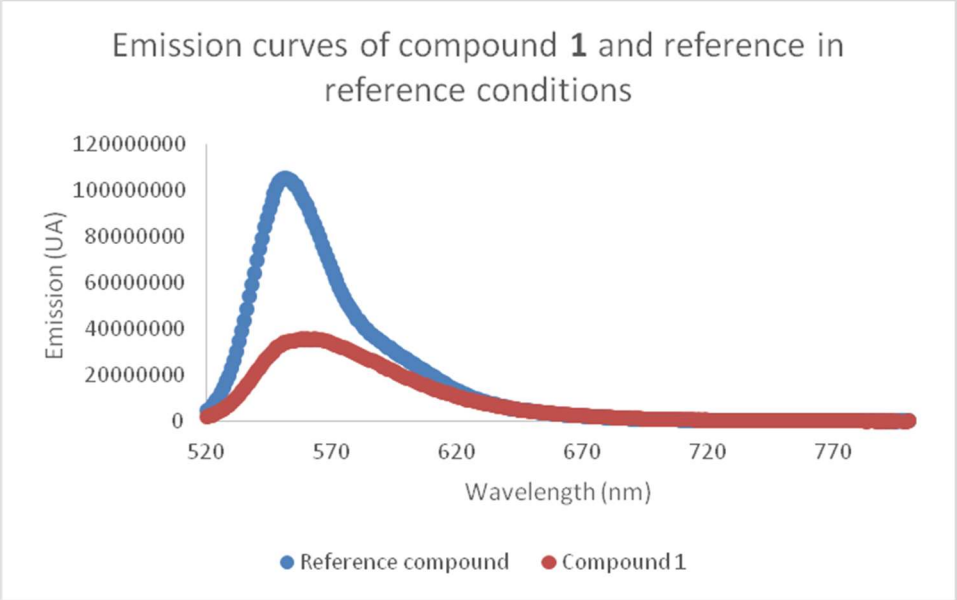

*Figure S32 – Emission curves of compound **1** and reference in reference conditions*

From these spectra was determined the quantum yield using the definition described by Brouwer *et al.* [12] :

$$\Phi_f^i = \frac{F^i f_s n_i^2}{F^s f_i n_s^2} \Phi_f^s$$

Where :

Φ_f^i and Φ_f^s are fluorescence quantum yields of sample and standard reference

F^i and F^s are integrated areas of sample and standard fluorescence curves

f_i and f_s are absorption factors of sample and standard reference, calculated from the formula $f_x = 1 - 10^{-A_x}$, where A_x is the absorbance of species x

n_i and n_s correspond to refraction indexes of sample and standard reference

6.3 Time dependant DFT analysis of **1**

In order to attribute bands on the different fragments of **1**, theoretical UV spectra were calculated on three compounds **1**, **S1** and **S2**.

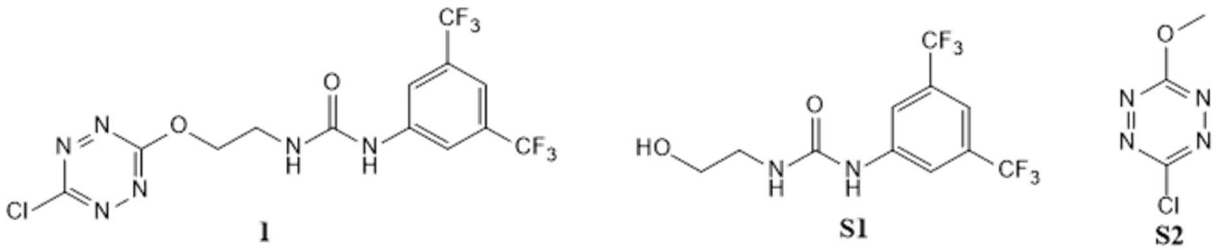

Figure S33 – Compounds studied by time dependent DFT analysis

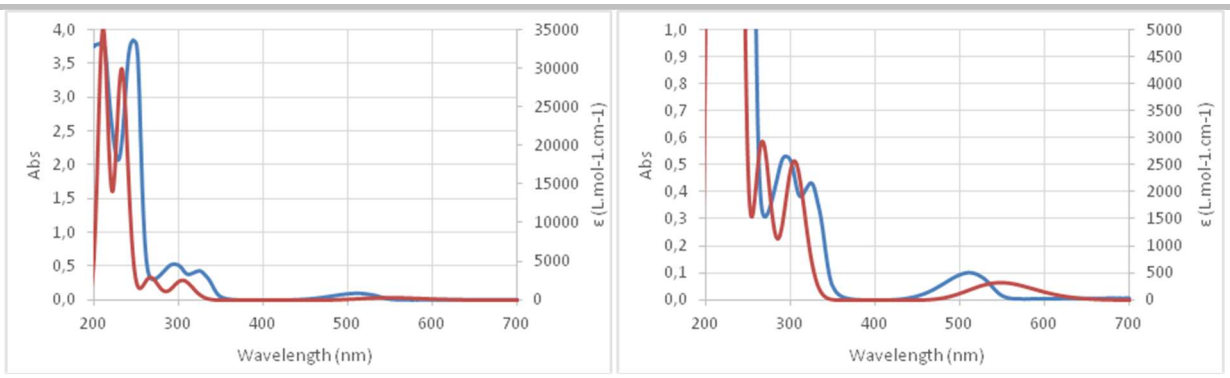

Figure S34 – Experimental (blue) and calculated (orange) absorption spectra

No.	*Wavelength (nm)* [a]	*Osc. Strength*	*Major contributions*	*Transition*
1	***548 (511)***	***0.0045***	***H-1->LUMO (100%)***	***n-π* Tetrazine***
2	*357*	*0*	*HOMO->LUMO (100%)*	
3	***305 (324)***	***0.0348***	***H-2->LUMO (84%), H-3->LUMO (14%)***	***π-π* Tetrazine***
4	*302*	*0*	*H-1->L+2 (99%)*	
5	*288*	*0.0023*	*H-3->LUMO (75%), H-2->LUMO (13%), H-4->LUMO (10%)*	
6	***266 (295)***	***0.04***	***HOMO->L+1 (88%)***	***π-π* Phenylurea***
7	*266*	*0.0002*	*H-4->LUMO (84%)*	
8	*265*	*0.0001*	*H-5->LUMO (90%)*	
9	*255*	*0*	*H-8->LUMO (45%), H-6->LUMO (46%)*	
10	*252*	*0*	*H-8->LUMO (43%), H-6->LUMO (46%)*	
11	*238*	*0.0001*	*HOMO->L+2 (99%)*	
12	***232 (246)***	***0.4106***	***HOMO->L+3 (89%)***	***π-π* Phenylurea***

[a] *values in parenthesis are the corresponding experimental maxima*

Figure S35 - Calculated transitions (major transitions in bold)

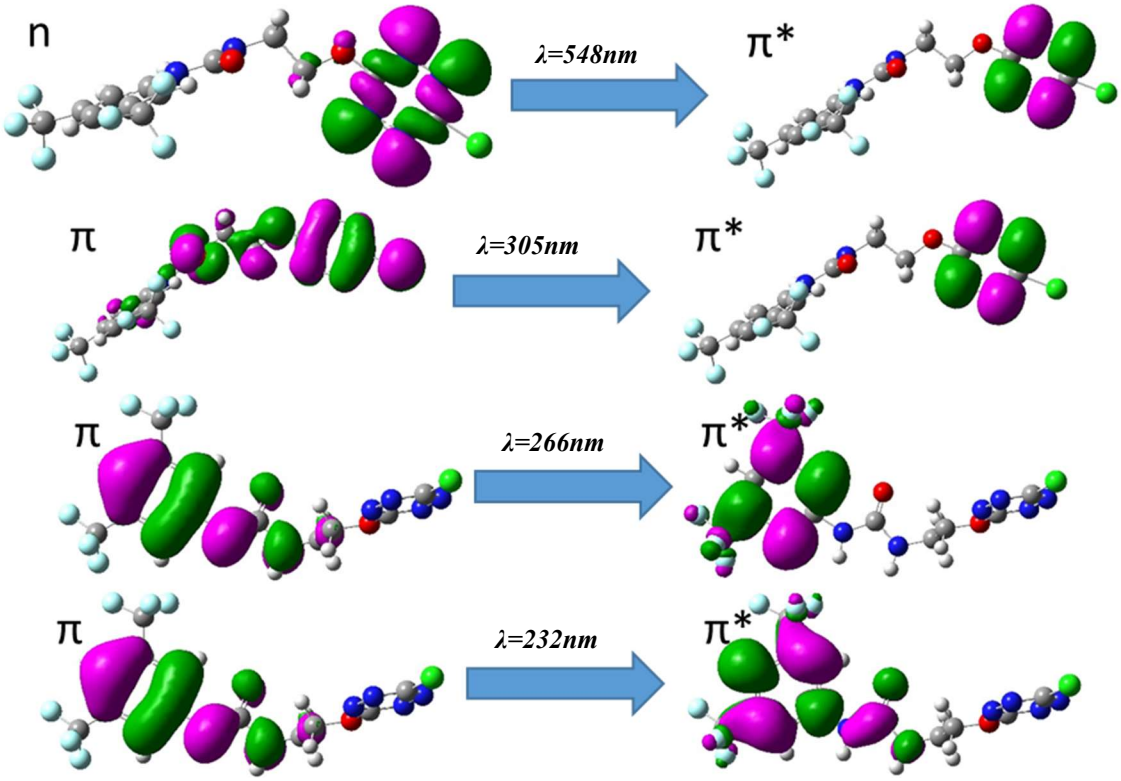

Figure S36 – Molecular orbitals involved in the main transitions

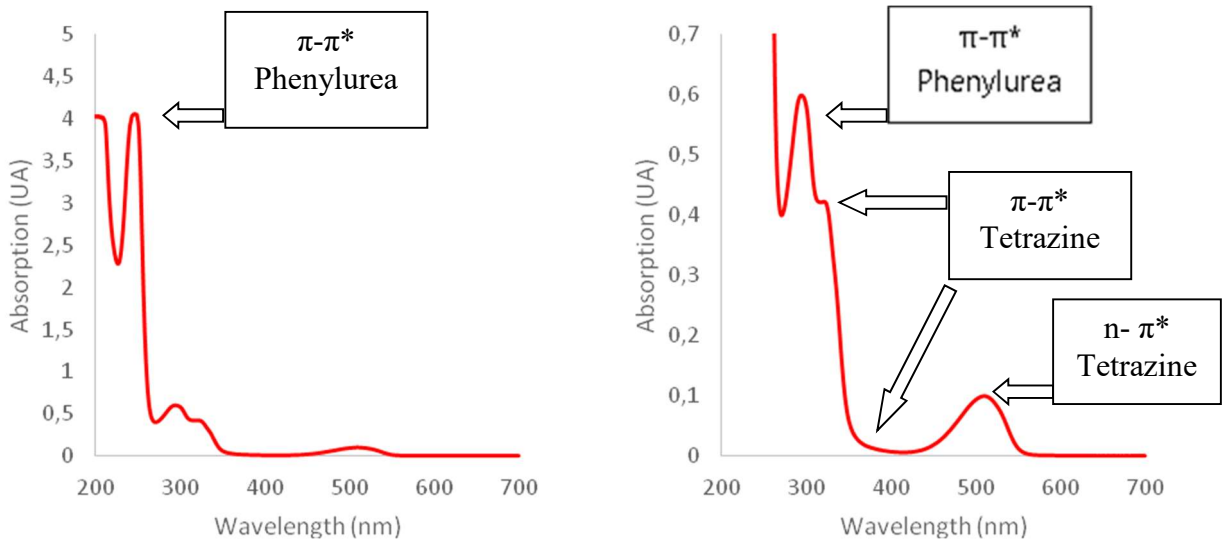

*Figure S37 – Experimental UV-Visible spectrum of **1** and attribution of different bands observed*

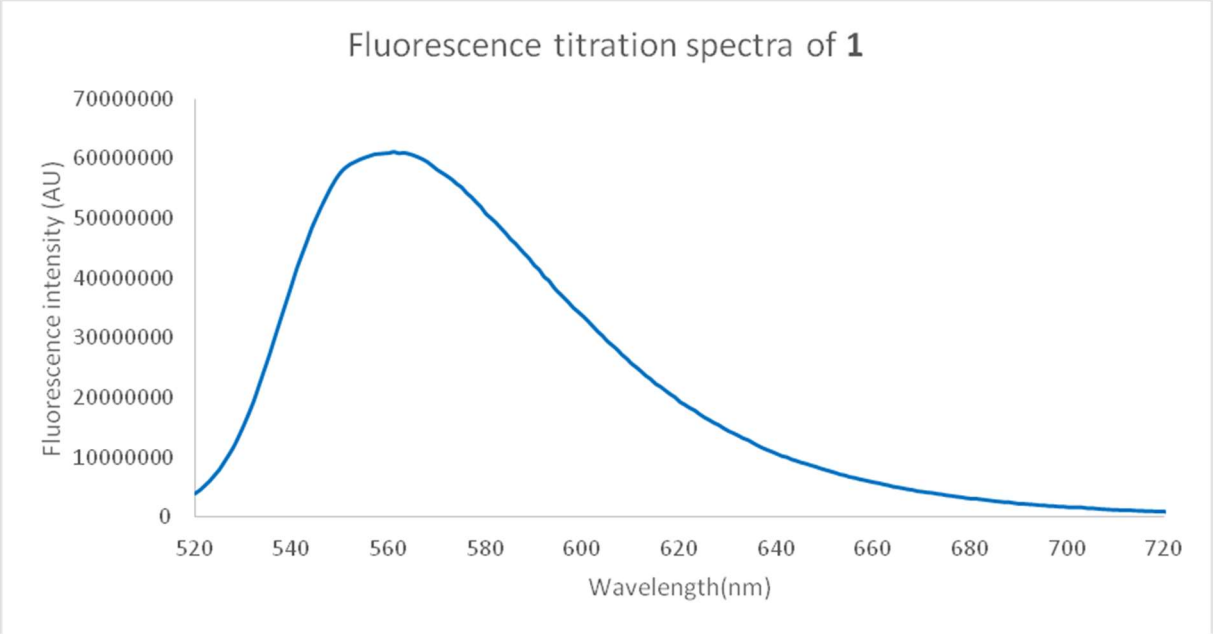

*Figure S38 – Experimental Fluorescence spectrum of **1***

6.4 Titration of **1** with TBACl

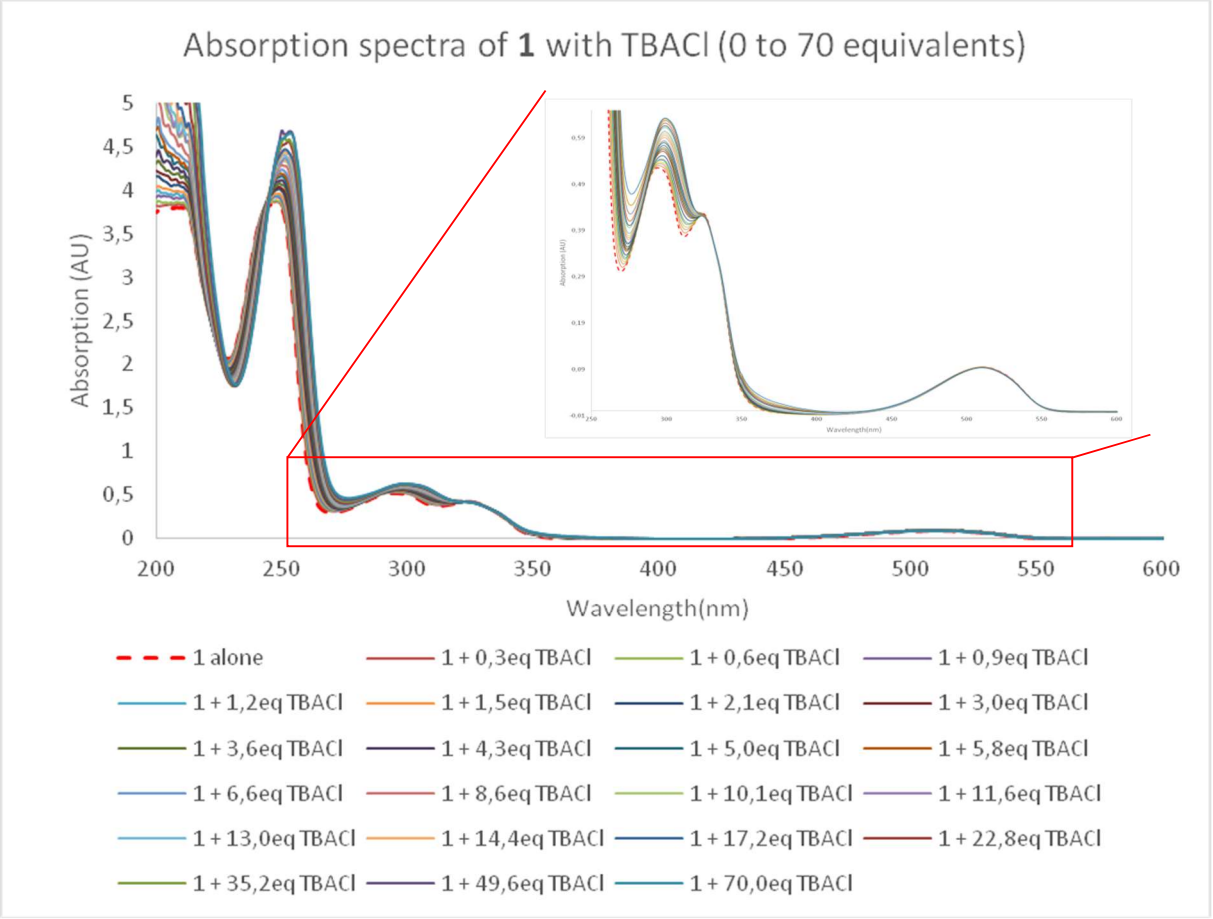

*Figure S39 – Experimental UV-Visible spectra measured during the titration of **1** with TBACl (0 to 70 equivalents)*

```
[PROGRAM]
Name = SPECFIT
Version = 3.0

[FILE]
Name = RP04+TBACL_ABS_FORMAT_SPECFIT.FAC
Path = C:\Program Files\SPECFIT\DATA\
Date = 18-juil-19
Time = 10:51:52
Ncomp = 2
Nmeas = 23
Nwave = 501

[FACTOR ANALYSIS]
Tolerance = 1,000E-09
Max.Factors = 10
Num.Factors = 5
Significant = 2
Eigen Noise = 1,436E-01
Exp't Noise = 1,436E-01
#  Eigenvalue  Square Sum  Residual   Prediction
1  2,119E+04   7,586E+02  2,566E-01  Data Vector
2  5,209E+02   2,377E+02  1,436E-01  Data Vector
3  1,187E+02   1,189E+02  1,016E-01  Possibly Data
4  6,034E+01   5,859E+01  7,132E-02  Probably Noise
5  1,988E+01   3,871E+01  5,797E-02  Probably Noise

[MODEL]
Date = 18-juil-19
Time = 10:58:50
Model = 0
Index = 3
Function = 1
Species = 3
Params = 3

[SPECIES]   [COLORED]   [FIXED]    [SPECTRUM]
1 0 0       False       False
0 1 0       True        False
1 1 0       True        False

[SPECIES]   [FIXED]   [PARAMETER]            [ERROR]
1 0 0       True      0,00000E+00  +/-       0,00000E+00
0 1 0       True      0,00000E+00  +/-       0,00000E+00
1 1 0       False     2,03451E+00  +/-       1,36125E-01

[CONVERGENCE]
Iterations = 3
Convergence Limit = 1,000E-03
Convergence Found = 7,249E-11
Marquardt Parameter = 0,0
Sum(Y-y)^2 Residuals = 2,31966E+02
Std. Deviation of Fit(Y) = 1,41889E-01

[STATISTICS]
Experimental Noise = 1,436E-01
Relative Error Of Fit = 10,3448%
Durbin-Watson Factor = 0,7676
Goodness Of Fit, Chi^2 = 9,759E-01
Durbin-Watson Factor (raw data) = None
Goodness Of Fit, Chi^2 (raw data) = None

[COVARIANCE]
1,355E-01

[CORRELATION]
1,000E+00

[END FILE]
```

*Figure S40 : Determination of binding constant using SPECFIT software for the UV-Visible titration of **1** with tetrabutylammonium chloride*

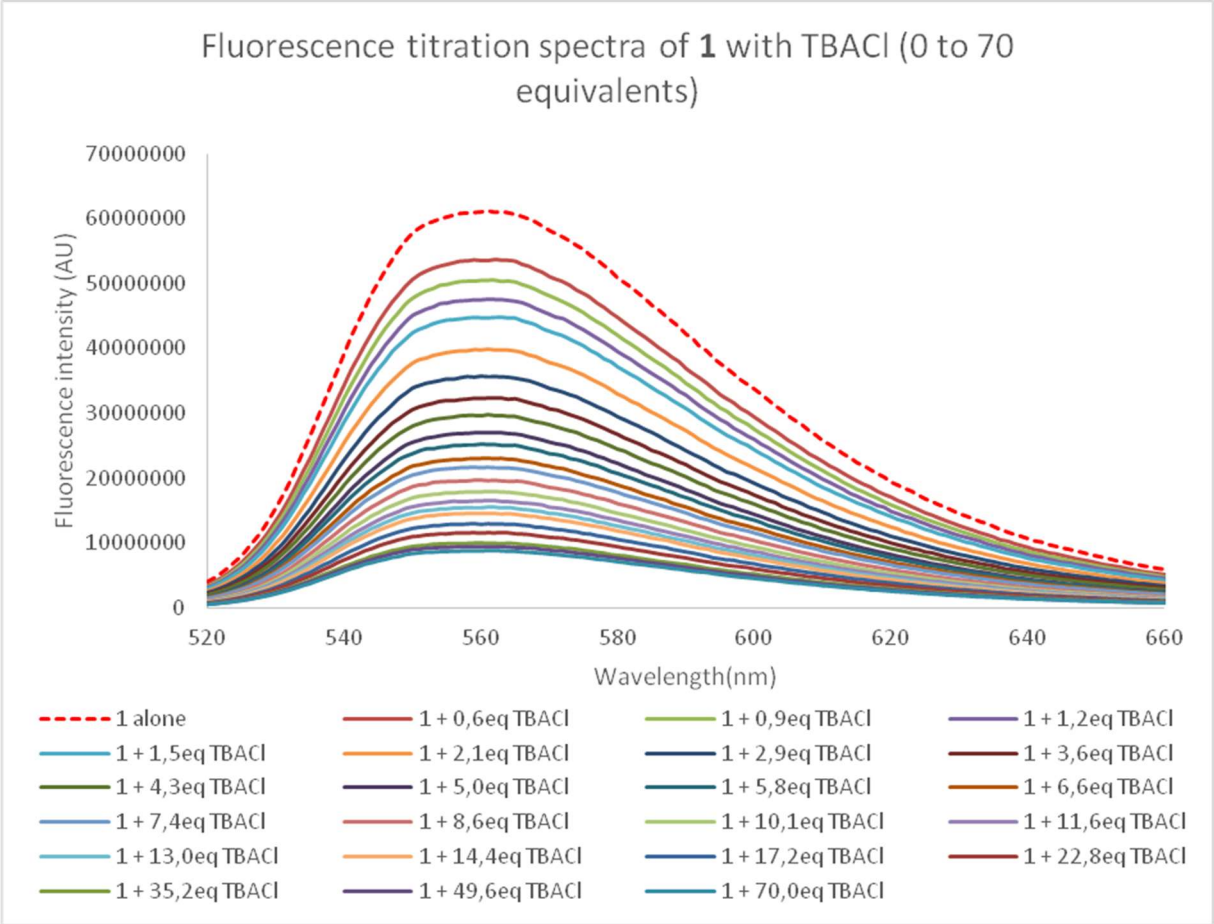

*Figure S41 – Experimental fluorescence spectra during the titration of **1** with TBACl (0 to 70 equivalents)*

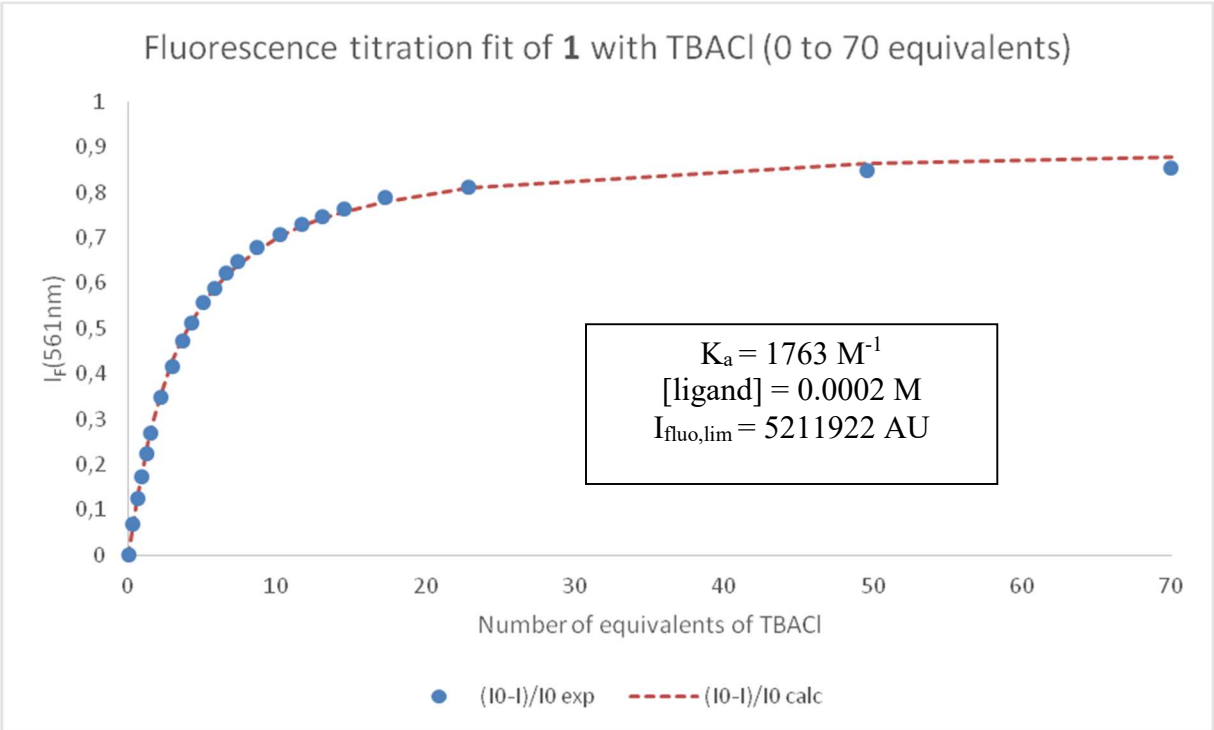

*Figure S42 – Mathematical fit during the fluorescence titration of **1** with TBACl (0 to 70 equivalents) and determination of the association constant*

```
[PROGRAM]
Name = SPECFIT
Version = 3.0

[FILE]
Name = RP04+TBACL_FLUO_FORMAT_SPECFIT.FAC
Path = C:\Program Files\SPECFIT\DATA\
Date = 18-juil-19
Time = 11:54:55
Ncomp = 2
Nmeas = 23
Nwave = 281

[FACTOR ANALYSIS]
Tolerance = 1,000E-09
Max.Factors = 10
Num.Factors = 4
Significant = 2
Eigen Noise = 2,844E+04
Exp't Noise = 2,844E+04
#   Eigenvalue  Square Sum  Residual    Prediction
1   1,153E+18   4,713E+13   8,540E+04   Data Vector
2   4,191E+13   5,224E+12   2,844E+04   Data Vector
3   1,256E+12   3,968E+12   2,478E+04   Probably Noise
4   4,815E+11   3,487E+12   2,323E+04   Probably Noise

[MODEL]
Date = 18-juil-19
Time = 11:55:55
Model = 0
Index = 3
Function = 1
Species = 3
Params = 3

[SPECIES]   [COLORED]   [FIXED]   [SPECTRUM]
1 0 0       False       False
0 1 0       True        False
1 1 0       True        False

[SPECIES]   [FIXED]   [PARAMETER]          [ERROR]
1 0 0       True      0,00000E+00  +/-     0,00000E+00
0 1 0       True      0,00000E+00  +/-     0,00000E+00
1 1 0       False     3,27294E+00  +/-     7,97601E-03

[CONVERGENCE]
Iterations = 8
Convergence Limit = 1,000E-03
Convergence Found = 5,151E-04
Marquardt Parameter = 0,0
Sum(Y-y)^2 Residuals = 2,43797E+14
Std. Deviation of Fit(Y) = 1,94236E+05

[STATISTICS]
Experimental Noise = 2,844E+04
Relative Error Of Fit = 1,4541%
Durbin-Watson Factor = 0,3806
Goodness Of Fit, Chi^2 = 4,666E+01
Durbin-Watson Factor (raw data) = None
Goodness Of Fit, Chi^2 (raw data) = None

[COVARIANCE]
3,436E-04

[CORRELATION]
1,000E+00

[END FILE]
```

*Figure S43: Determination of binding constant using SPECFIT software for the fluorescence titration of **1** with tetrabutylammonium chloride*

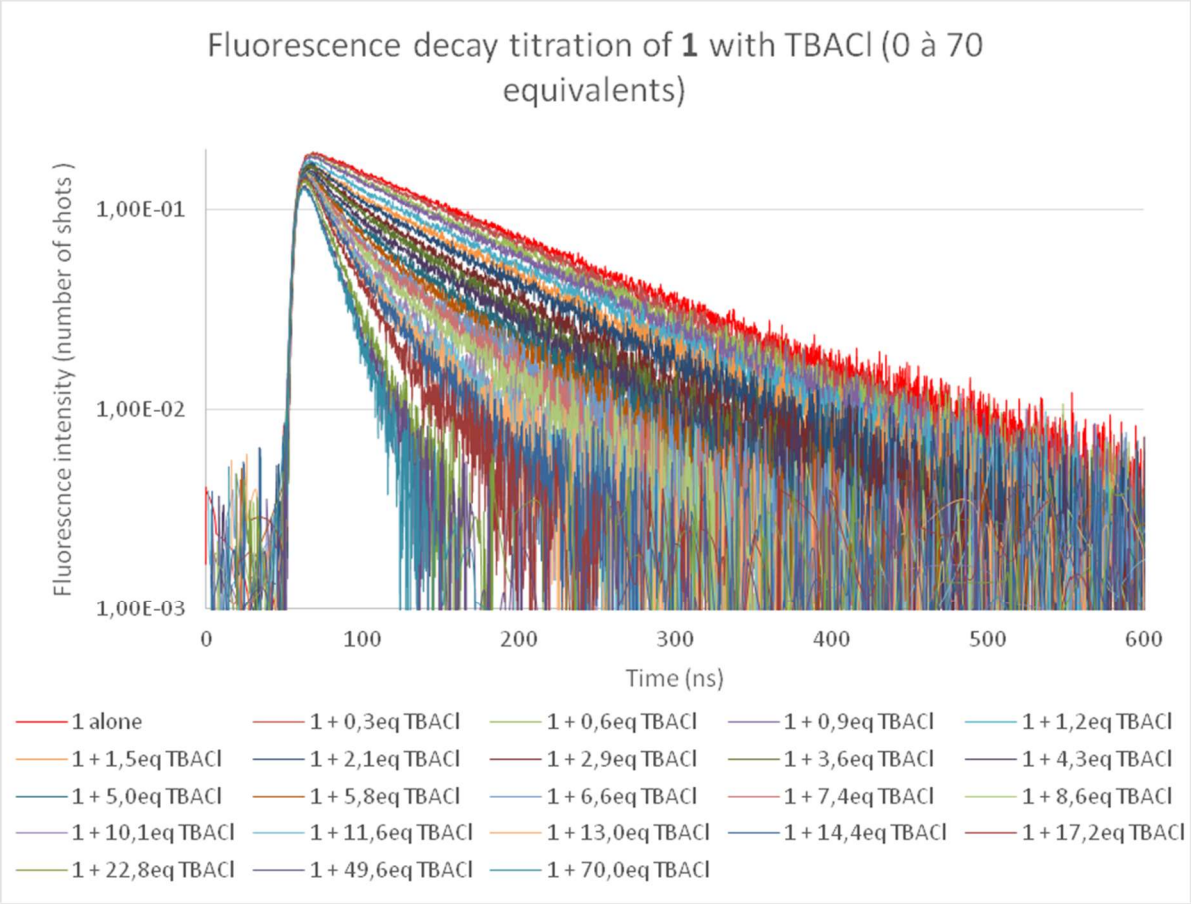

*Figure S44 –Fluorescence decay titration of **1** with TBACl (0 to 70 equivalents) Logarithmic scale*

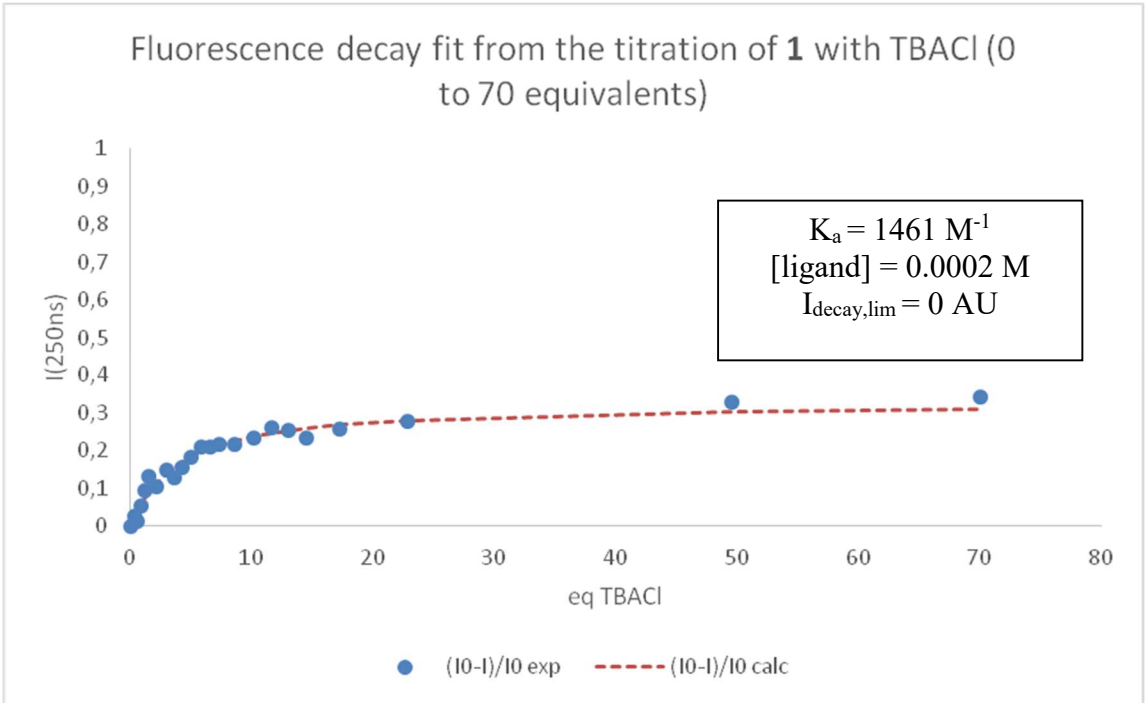

*Figure S45 –Mathematical fit during the fluorescence decay titration of **1** with TBACl (0 to 70 equivalents) and determination of the association constant*

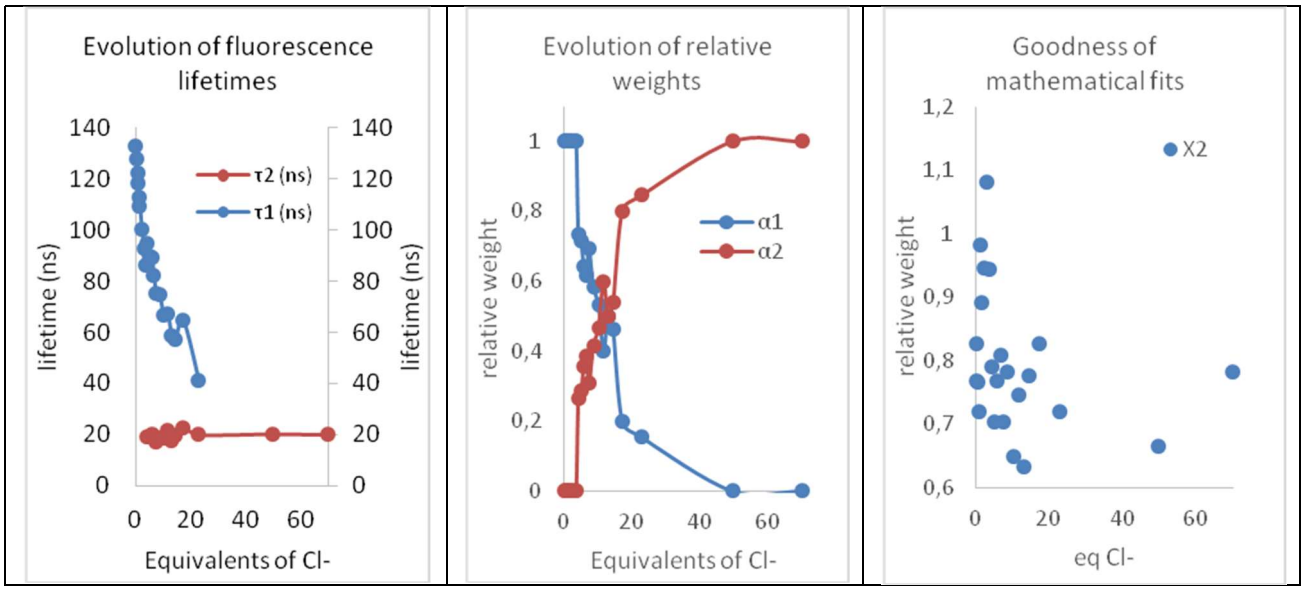

*Figure S46 –Analysis of fluorescence decay titration of **1** with TBACl*

6.5 Titration of **1** with TBABr

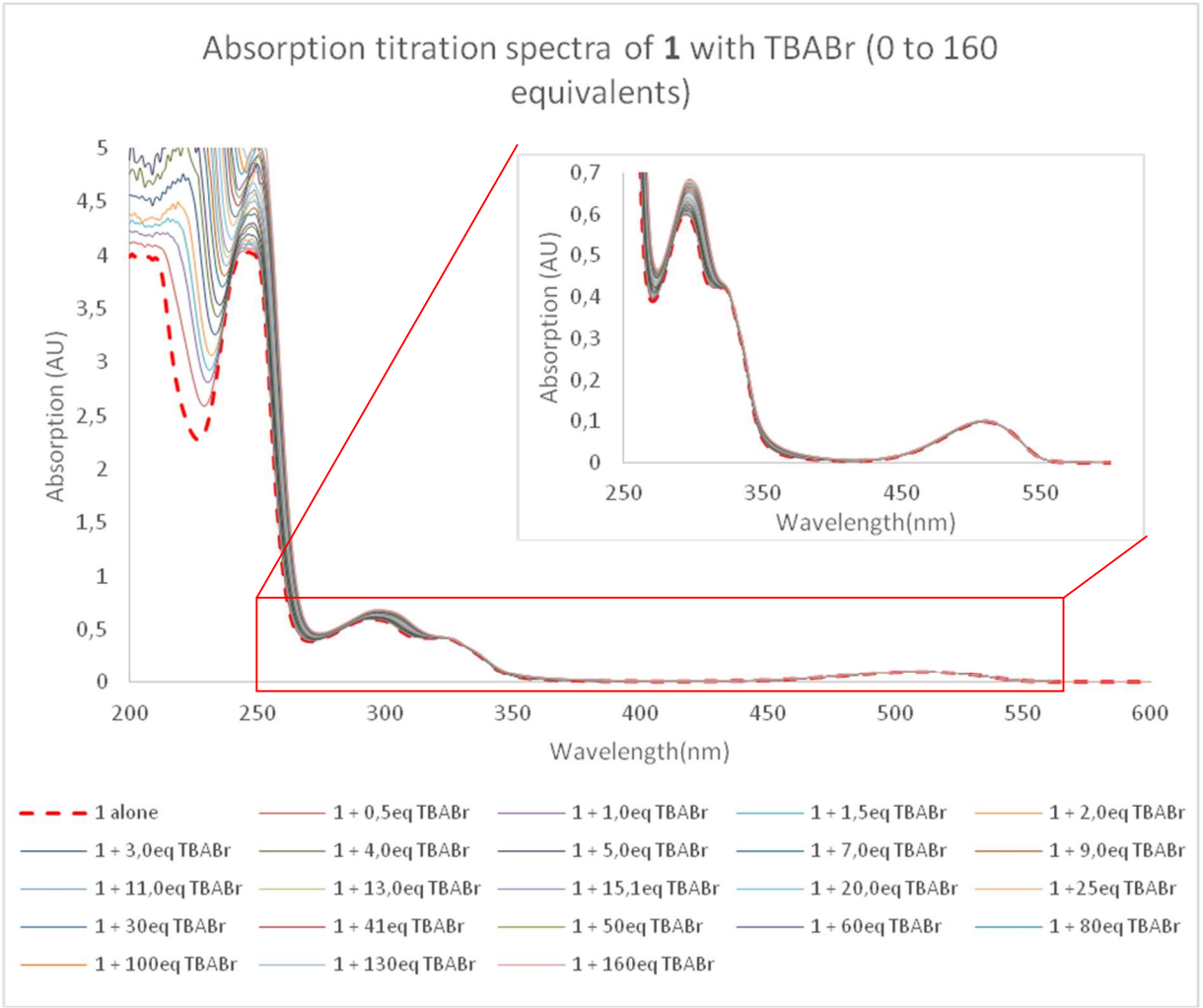

*Figure S47 – Experimental UV-Visible spectra measured during the titration of **1** with TBABr (0 to 160 equivalents)*

```
[PROGRAM]
Name = SPECFIT
Version = 3.0

[FILE]
Name = RP04+TBABR_ABS_FORMAT_SPECFIT.FAC
Path = C:\Program Files\SPECFIT\DATA\
Date = 18-juil-19
Time = 11:11:02
Ncomp = 2
Nmeas = 23
Nwave = 501

[FACTOR ANALYSIS]
Tolerance = 1,000E-09
Max.Factors = 10
Num.Factors = 2
Significant = 1
Eigen Noise = 3,667E-01
Exp't Noise = 3,667E-01
#   Eigenvalue  Square Sum  Residual    Prediction
1   6,481E+04   1,549E+03   3,667E-01   Data Vector
2   6,063E+02   9,428E+02   2,861E-01   Probably Noise

[MODEL]
Date = 18-juil-19
Time = 11:12:52
Model = 0
Index = 3
Function = 1
Species = 3
Params = 3

[SPECIES]   [COLORED]   [FIXED]   [SPECTRUM]
1 0 0       False       False
0 1 0       True        False
1 1 0       True        False

[SPECIES]   [FIXED]   [PARAMETER]              [ERROR]
1 0 0       True      0,00000E+00   +/-       0,00000E+00
0 1 0       True      0,00000E+00   +/-       0,00000E+00
1 1 0       False     2,90868E+00   +/-       9,01560E-02

[CONVERGENCE]
Iterations = 7
Convergence Limit = 1,000E-03
Convergence Found = 4,597E-05
Marquardt Parameter = 0,0
Sum(Y-y)^2 Residuals = 8,12114E+02
Std. Deviation of Fit(Y) = 2,65488E-01

[STATISTICS]
Experimental Noise = 3,667E-01
Relative Error Of Fit = 11,2116%
Durbin-Watson Factor = 0,2173
Goodness Of Fit, Chi^2 = 5,243E-01
Durbin-Watson Factor (raw data) = None
Goodness Of Fit, Chi^2 (raw data) = None

[COVARIANCE]
5,323E-02

[CORRELATION]
1,000E+00

[END FILE]
```

*Figure S48 – Determination of binding constant using SPECFIT software for the UV-Visible titration of **1** with tetrabutylammonium bromide*

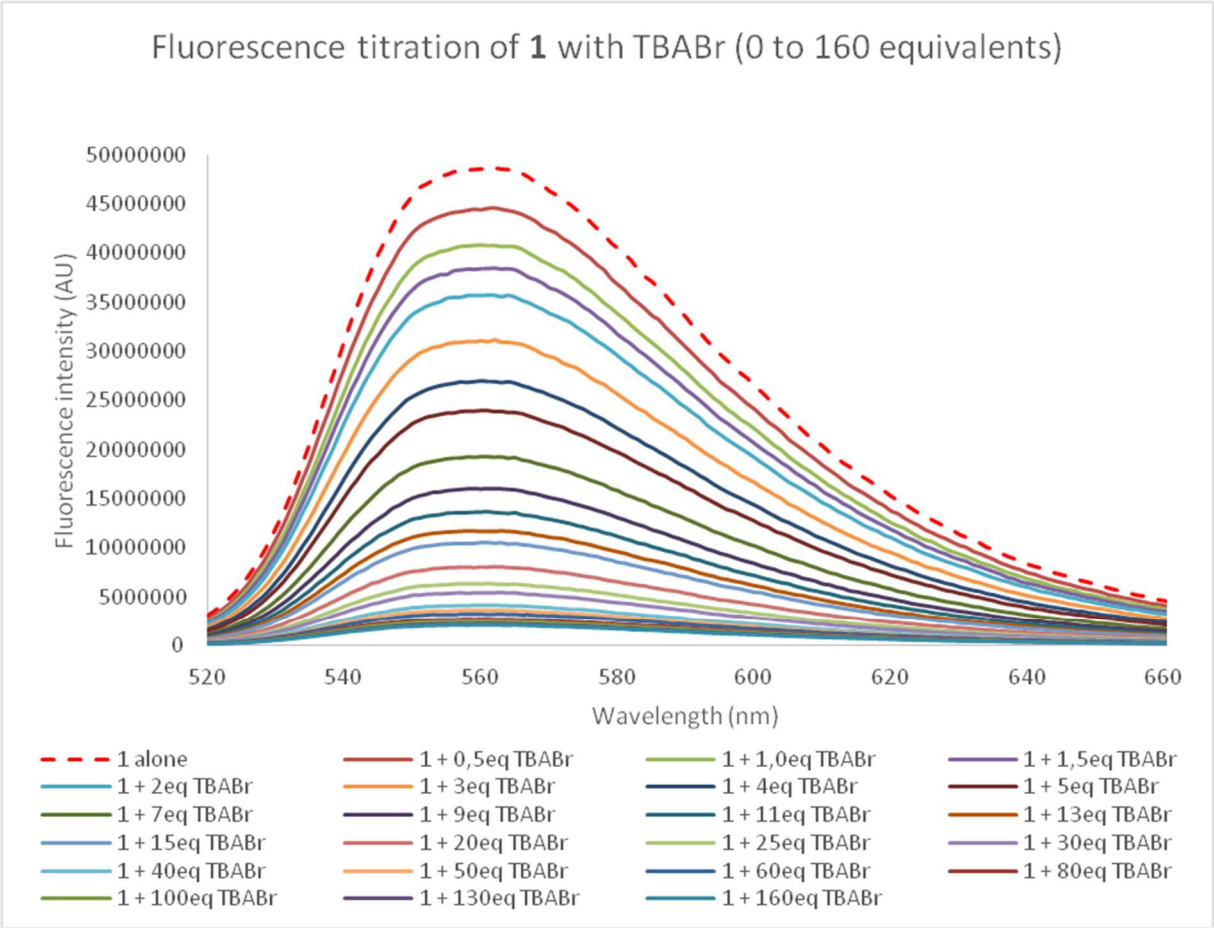

*Figure S49 – Experimental fluorescence spectra during the titration of **1** with TBABr (0 to 160 equivalents)*

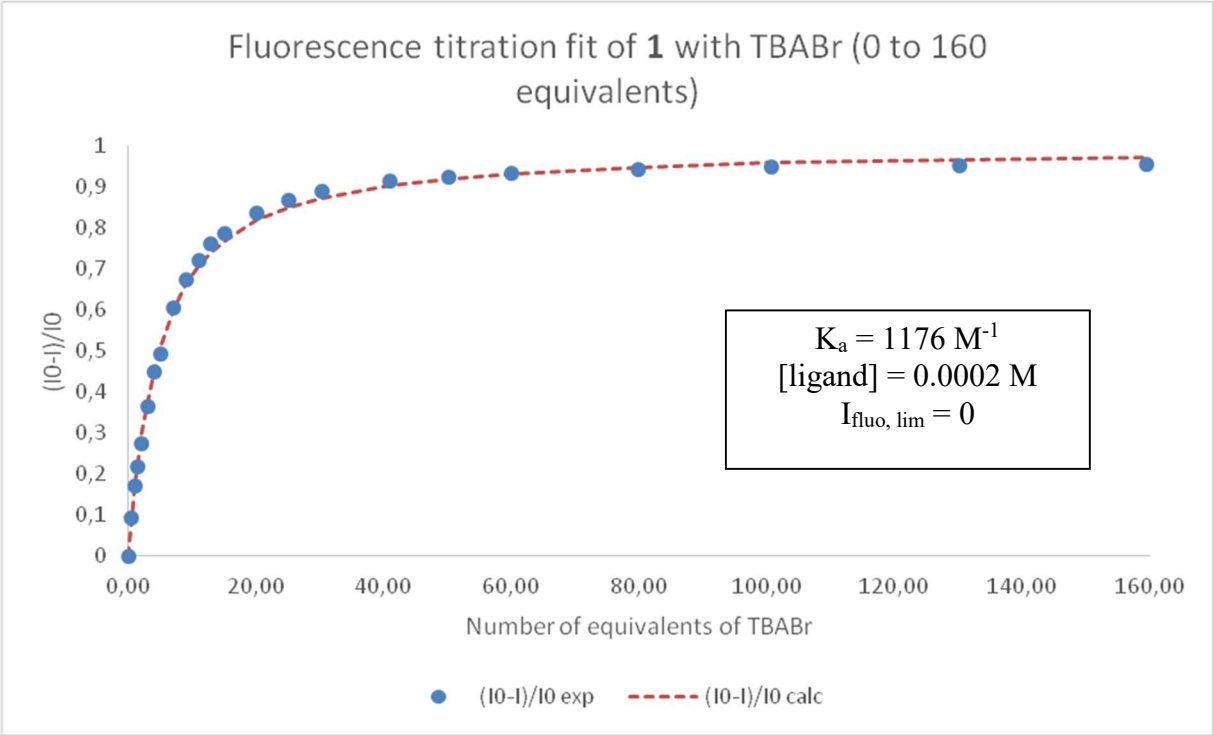

*Figure S50 – Mathematical fit during the fluorescence titration of **1** with TBABr (0 to 160 equivalents) and determination of the association constant*

```
[PROGRAM]
Name = SPECFIT
Version = 3.0

[FILE]
Name = RP04+TBABR_FLUO_FORMAT_SPECFIT.FAC
Path = C:\Program Files\SPECFIT\DATA\
Date = 18-juil-19
Time = 11:15:51
Ncomp = 2
Nmeas = 23
Nwave = 281

[FACTOR ANALYSIS]
Tolerance = 1,000E-09
Max.Factors = 10
Num.Factors = 4
Significant = 2
Eigen Noise = 2,039E+04
Exp't Noise = 2,039E+04
#  Eigenvalue  Square Sum  Residual   Prediction
1  6,247E+17  1,426E+13  4,698E+04  Data Vector
2  1,158E+13  2,686E+12  2,039E+04  Data Vector
3  3,943E+11  2,292E+12  1,884E+04  Probably Noise
4  3,216E+11  1,971E+12  1,747E+04  Probably Noise

[MODEL]
Date = 18-juil-19
Time = 11:16:20
Model = 0
Index = 3
Function = 1
Species = 3
Params = 3

[SPECIES]   [COLORED]   [FIXED]    [SPECTRUM]
1 0 0       False       False
0 1 0       True        False
1 1 0       True        False

[SPECIES]   [FIXED]   [PARAMETER]              [ERROR]
1 0 0       True      0,00000E+00  +/-        0,00000E+00
0 1 0       True      0,00000E+00  +/-        0,00000E+00
1 1 0       False     3,08538E+00  +/-        1,09406E-02

[CONVERGENCE]
Iterations = 7
Convergence Limit = 1,000E-03
Convergence Found = 1,902E-04
Marquardt Parameter = 0,0
Sum(Y-y)^2 Residuals = 4,37575E+14
Std. Deviation of Fit(Y) = 2,60221E+05

[STATISTICS]
Experimental Noise = 2,039E+04
Relative Error Of Fit = 2,6475%
Durbin-Watson Factor = 0,2592
Goodness Of Fit, Chi^2 = 1,629E+02
Durbin-Watson Factor (raw data) = None
Goodness Of Fit, Chi^2 (raw data) = None

[COVARIANCE]
6,508E-04

[CORRELATION]
1,000E+00

[END FILE]
```

*Figure S51: Determination of binding constant using SPECFIT software for the fluorescence titration of **1** with tetrabutylammonium bromide*

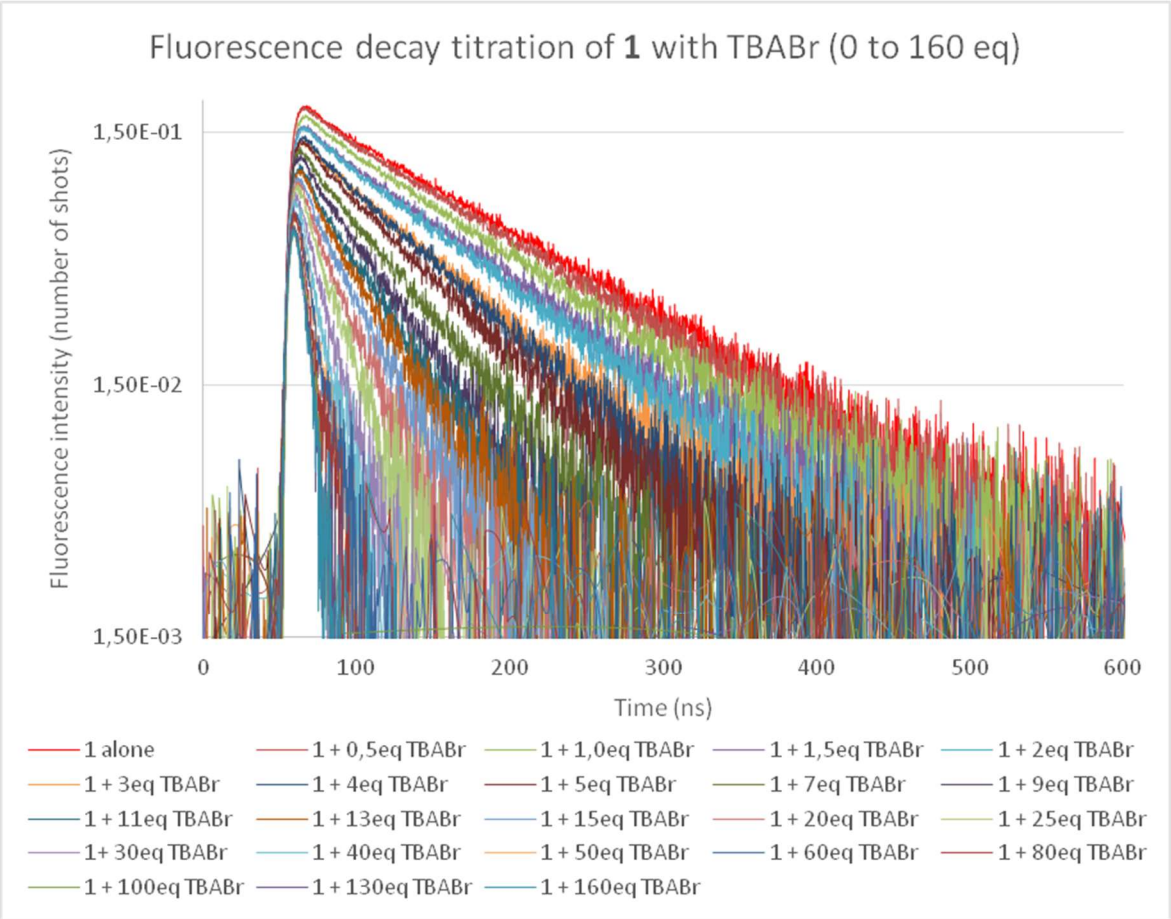

*Figure S52 –Fluorescence decay titration of **1** with tetrabutylammonium bromide (0 to 160 equivalents) Logarithmic scale*

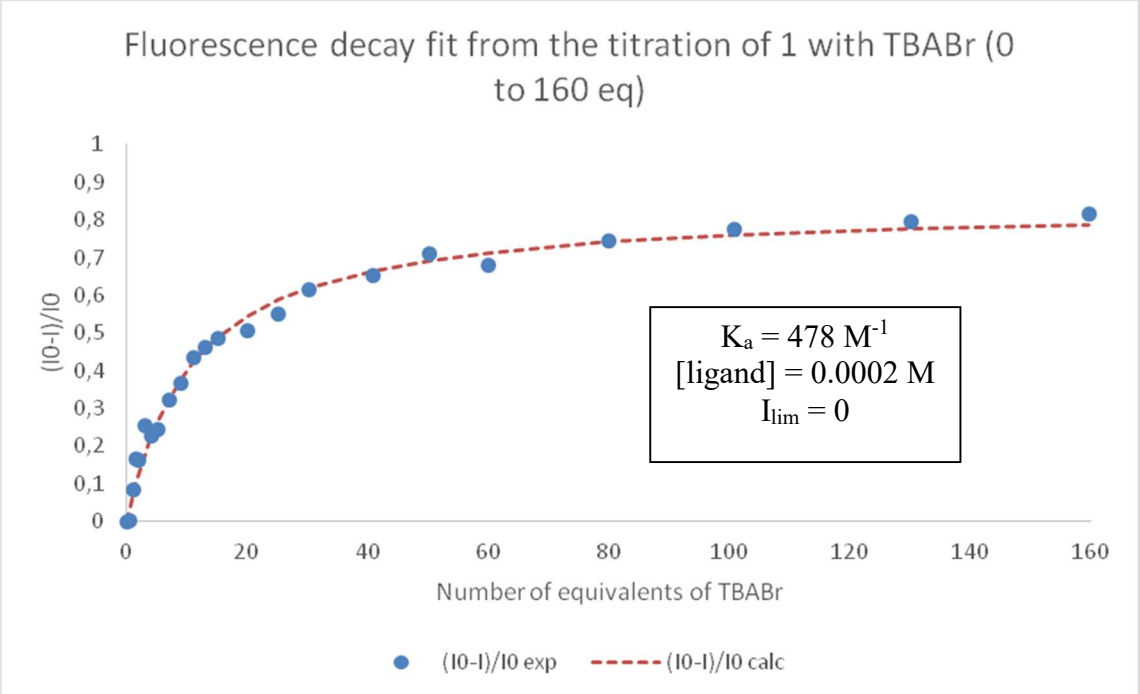

*Figure S53 –Mathematical fit during the fluorescence decay titration of **1** with TBABr (0 to 160 equivalents) and determination of the association constant*

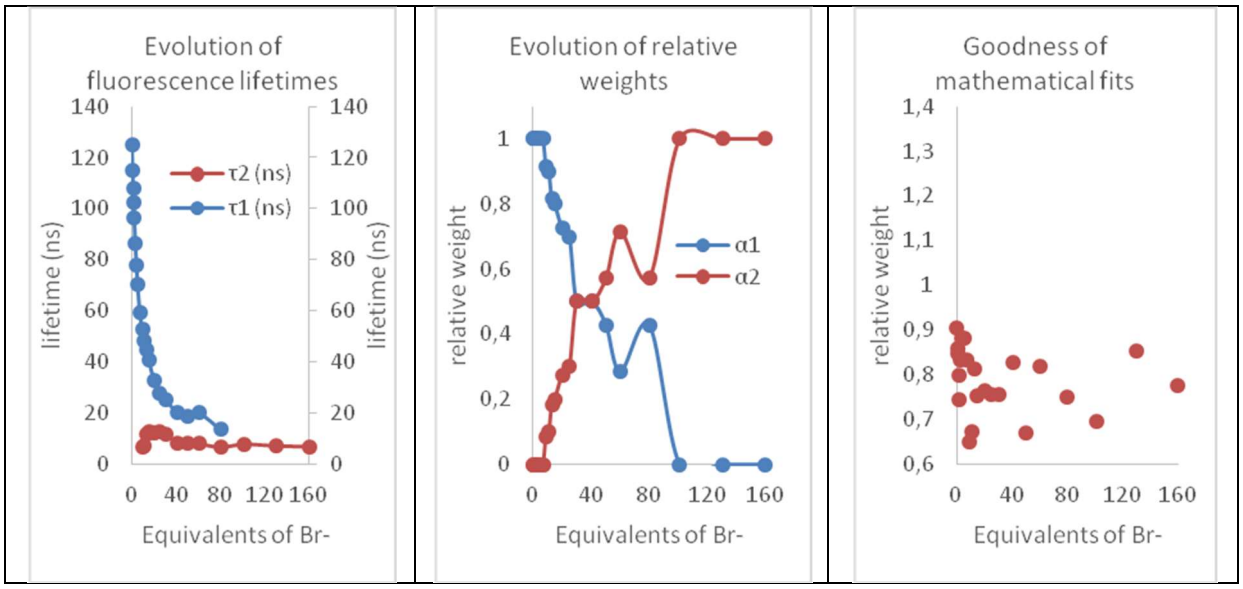

*Figure S54 –Analysis of fluorescence decay titration of **1** with tetrabutylammonium bromide*

6.6 Titration of **1** with TBAI

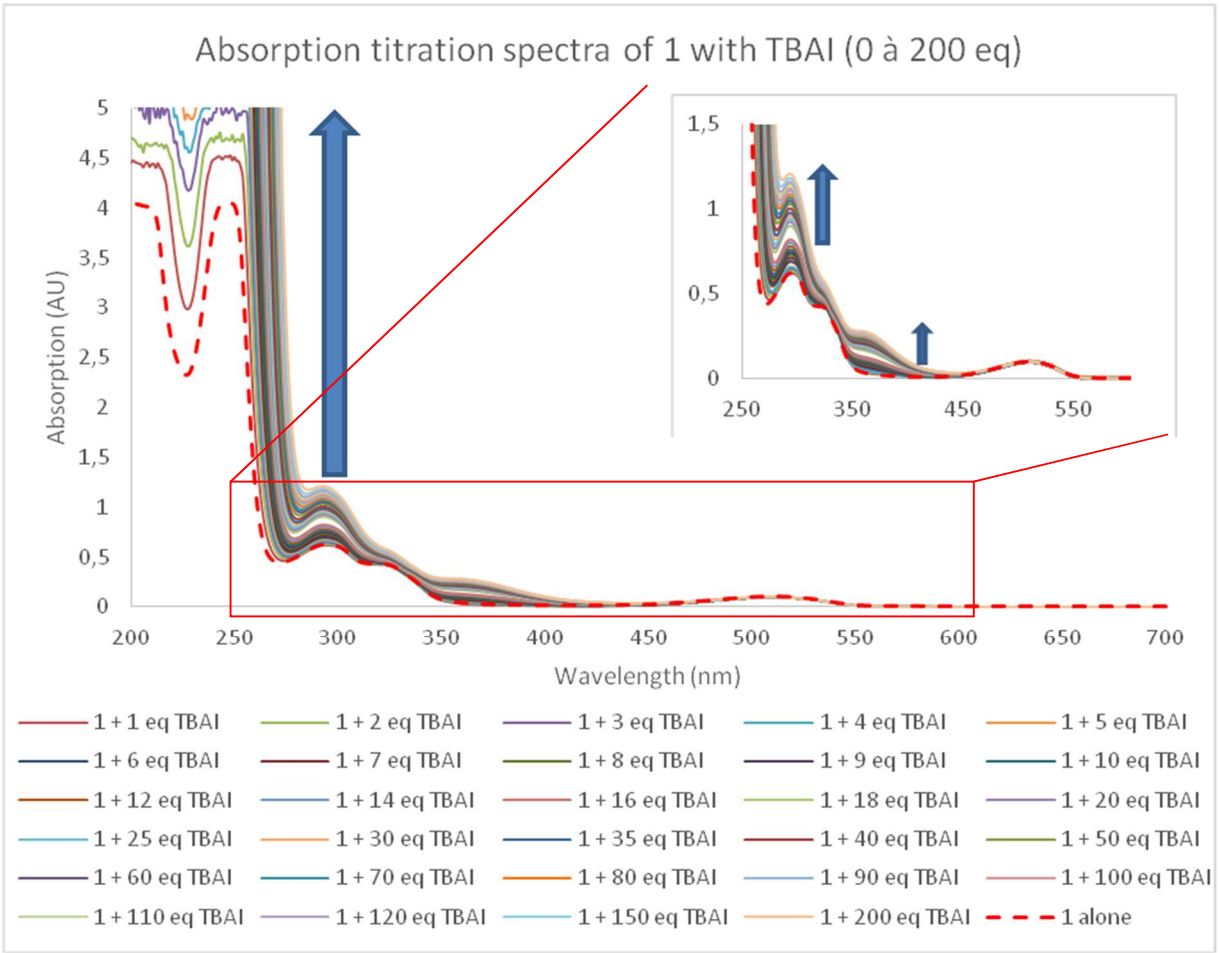

*Figure S55 – Experimental UV-Visible spectra measured during the titration of **1** with TBAI (0 to 200 equivalents)*

```
[PROGRAM]
Name = SPECFIT
Version = 3.0

[FILE]
Name = RP04+TBAI_ABS_FORMAT_SPECFIT.FAC
Path = C:\Program Files\SPECFIT\DATA\
Date = 18-juil-19
Time = 18:13:27
Ncomp = 2
Nmeas = 30
Nwave = 501

[FACTOR ANALYSIS]
Tolerance = 1,000E-09
Max.Factors = 10
Num.Factors = 6
Significant = 2
Eigen Noise = 2,914E-01
Exp't Noise = 2,914E-01
#  Eigenvalue  Square Sum  Residual    Prediction
1  1,593E+05   3,584E+03   4,883E-01   Data Vector
2  2,308E+03   1,276E+03   2,914E-01   Data Vector
3  4,839E+02   7,925E+02   2,297E-01   Possibly Data
4  1,942E+02   5,984E+02   1,996E-01   Probably Noise
5  1,367E+02   4,617E+02   1,753E-01   Probably Noise
6  9,464E+01   3,670E+02   1,563E-01   Probably Noise

[MODEL]
Date = 18-juil-19
Time = 18:14:09
Model = 0
Index = 3
Function = 1
Species = 3
Params = 3

[SPECIES]   [COLORED]   [FIXED]   [SPECTRUM]
1 0 0       False       False
0 1 0       True        False
1 1 0       True        False

[SPECIES]   [FIXED]   [PARAMETER]              [ERROR]
1 0 0       True      0,00000E+00   +/-        0,00000E+00
0 1 0       True      0,00000E+00   +/-        0,00000E+00
1 1 0       False     2,99164E+00   +/-        9,59849E-02

[CONVERGENCE]
Iterations = 8
Convergence Limit = 1,000E-03
Convergence Found = 6,572E-04
Marquardt Parameter = 0,0
Sum(Y-y)^2 Residuals = 3,12100E+03
Std. Deviation of Fit(Y) = 4,55703E-01

[STATISTICS]
Experimental Noise = 2,914E-01
Relative Error Of Fit = 13,9932%
Durbin-Watson Factor = 0,3771
Goodness Of Fit, Chi^2 = 2,445E+00
Durbin-Watson Factor (raw data) = None
Goodness Of Fit, Chi^2 (raw data) = None

[COVARIANCE]
6,118E-02

[CORRELATION]
1,000E+00

[END FILE]
```

*Figure S56 – Determination of binding constant using SPECFIT software for the UV-Visible titration of **1** with tetrabutylammonium iodide*

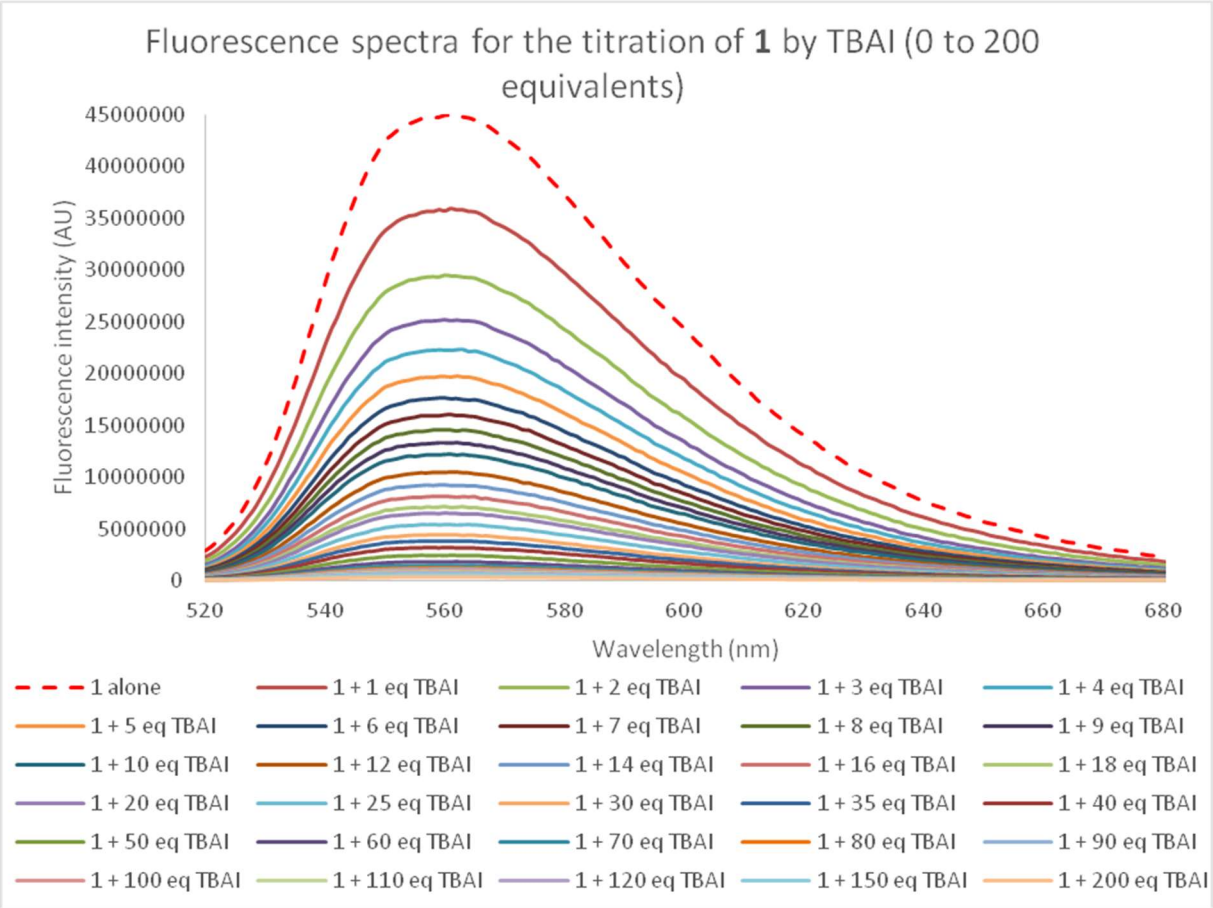

*Figure S57 – Experimental fluorescence spectra during the titration of **1** with TBAI (0 to 200 equivalents)*

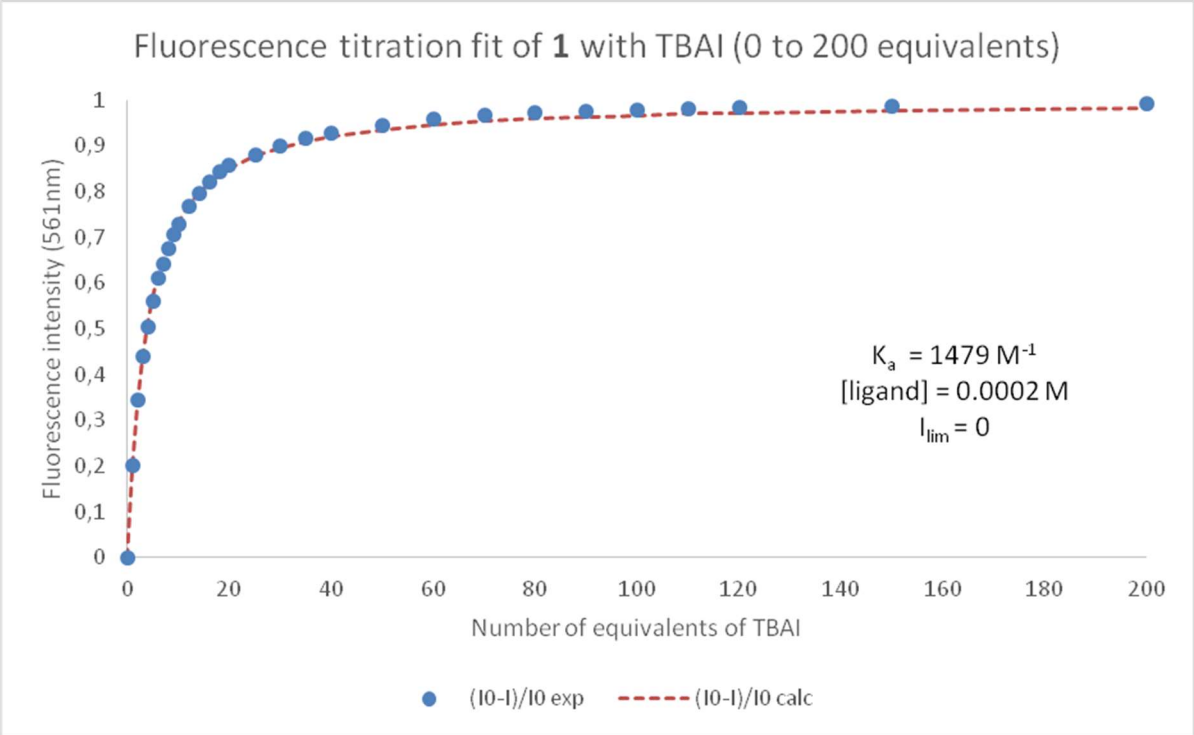

*Figure S58 – Mathematical fit during the fluorescence titration of **1** with TBAI (0 to 200 equivalents) and determination of the association constant*

```
[PROGRAM]
Name = SPECFIT
Version = 3.0

[FILE]
Name = RP04+TBAI_FLUO_FORMAT_SPECFIT.FAC
Path = C:\Program Files\SPECFIT\DATA\
Date = 18-juil-19
Time = 18:19:25
Ncomp = 2
Nmeas = 30
Nwave = 281

[FACTOR ANALYSIS]
Tolerance = 1,000E-09
Max.Factors = 10
Num.Factors = 6
Significant = 2
Eigen Noise = 1,781E+04
Exp't Noise = 1,781E+04
#   Eigenvalue  Square Sum  Residual    Prediction
1   3,657E+17   1,117E+13   3,640E+04   Data Vector
2   8,491E+12   2,675E+12   1,781E+04   Data Vector
3   7,145E+11   1,960E+12   1,525E+04   Probably Noise
4   2,803E+11   1,680E+12   1,412E+04   Probably Noise
5   2,118E+11   1,468E+12   1,320E+04   Probably Noise
6   1,625E+11   1,305E+12   1,245E+04   Probably Noise

[MODEL]
Date = 18-juil-19
Time = 18:20:09
Model = 0
Index = 3
Function = 1
Species = 3
Params = 3

[SPECIES]   [COLORED]   [FIXED]   [SPECTRUM]
1 0 0       False       False
0 1 0       True        False
1 1 0       True        False

[SPECIES]   [FIXED]   [PARAMETER]              [ERROR]
1 0 0       True      0,00000E+00   +/-       0,00000E+00
0 1 0       True      0,00000E+00   +/-       0,00000E+00
1 1 0       False     3,14306E+00   +/-       3,98912E-03

[CONVERGENCE]
Iterations = 3
Convergence Limit = 1,000E-03
Convergence Found = 1,311E-06
Marquardt Parameter = 0,0
Sum(Y-y)^2 Residuals = 7,45462E+13
Std. Deviation of Fit(Y) = 9,40426E+04

[STATISTICS]
Experimental Noise = 1,781E+04
Relative Error Of Fit = 1,4279%
Durbin-Watson Factor = 0,8954
Goodness Of Fit, Chi^2 = 2,787E+01
Durbin-Watson Factor (raw data) = None
Goodness Of Fit, Chi^2 (raw data) = None

[COVARIANCE]
8,515E-05

[CORRELATION]
1,000E+00

[END FILE]
```

*Figure S59: Determination of binding constant using SPECFIT software for the fluorescence titration of **1** with tetrabutylammonium iodide*

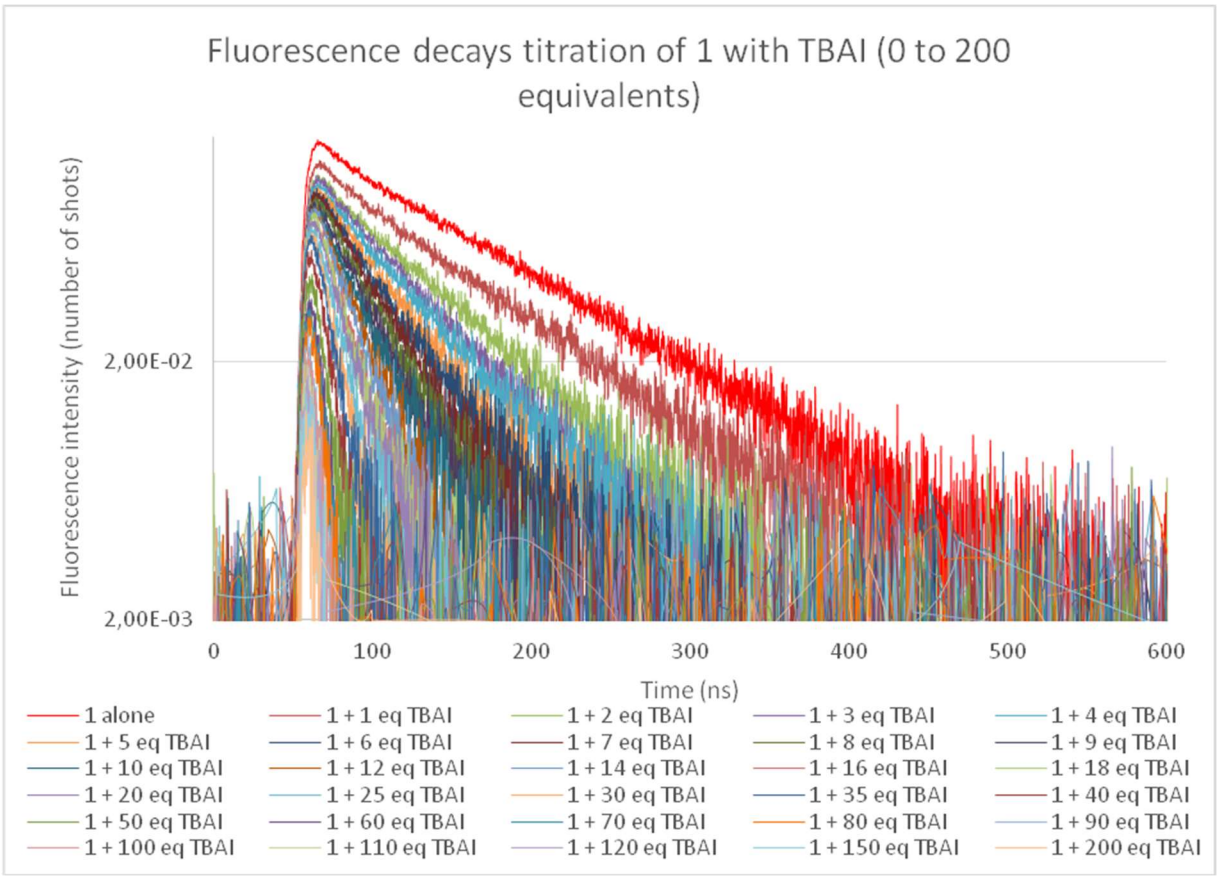

*Figure S60 – Fluorescence decay titration of **1** with tetrabutylammonium iodide (0 to 200 equivalents) Logarithmic scale*

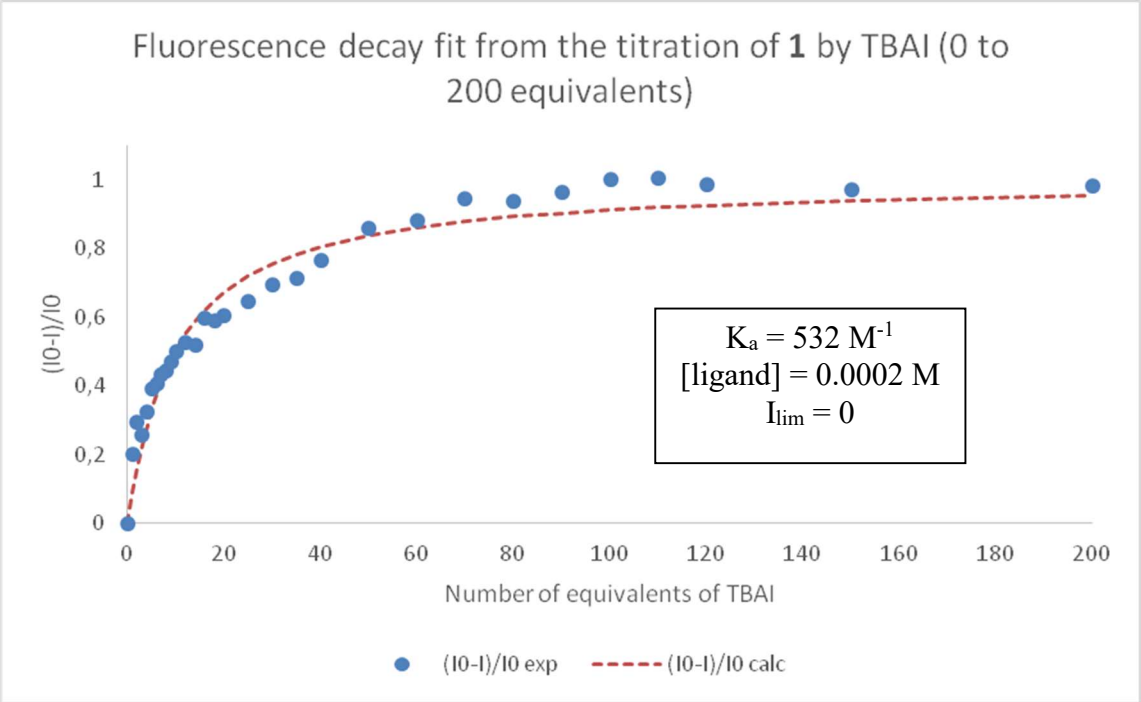

*Figure S61 –Mathematical fit during the fluorescence decay titration of **1** with TBAI (0 to 200 equivalents) and determination of the association constant*

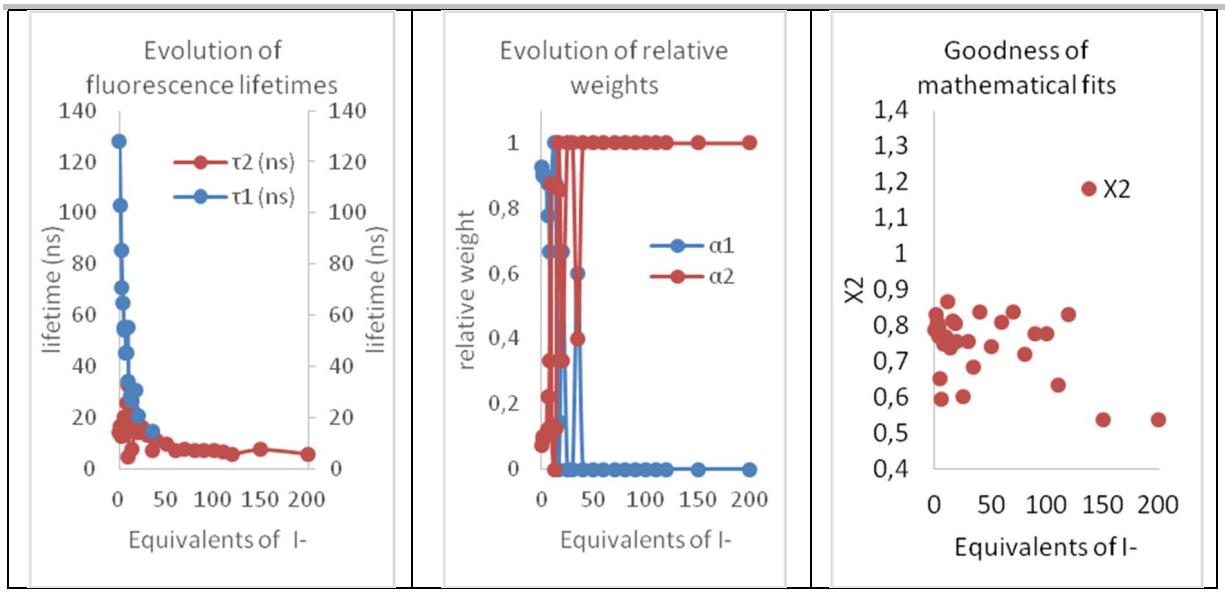

*Figure S62 –Analysis of fluorescence decay titration of **1** with tetrabutylammonium iodide*

6.7 Titration of **1** with TBASCN

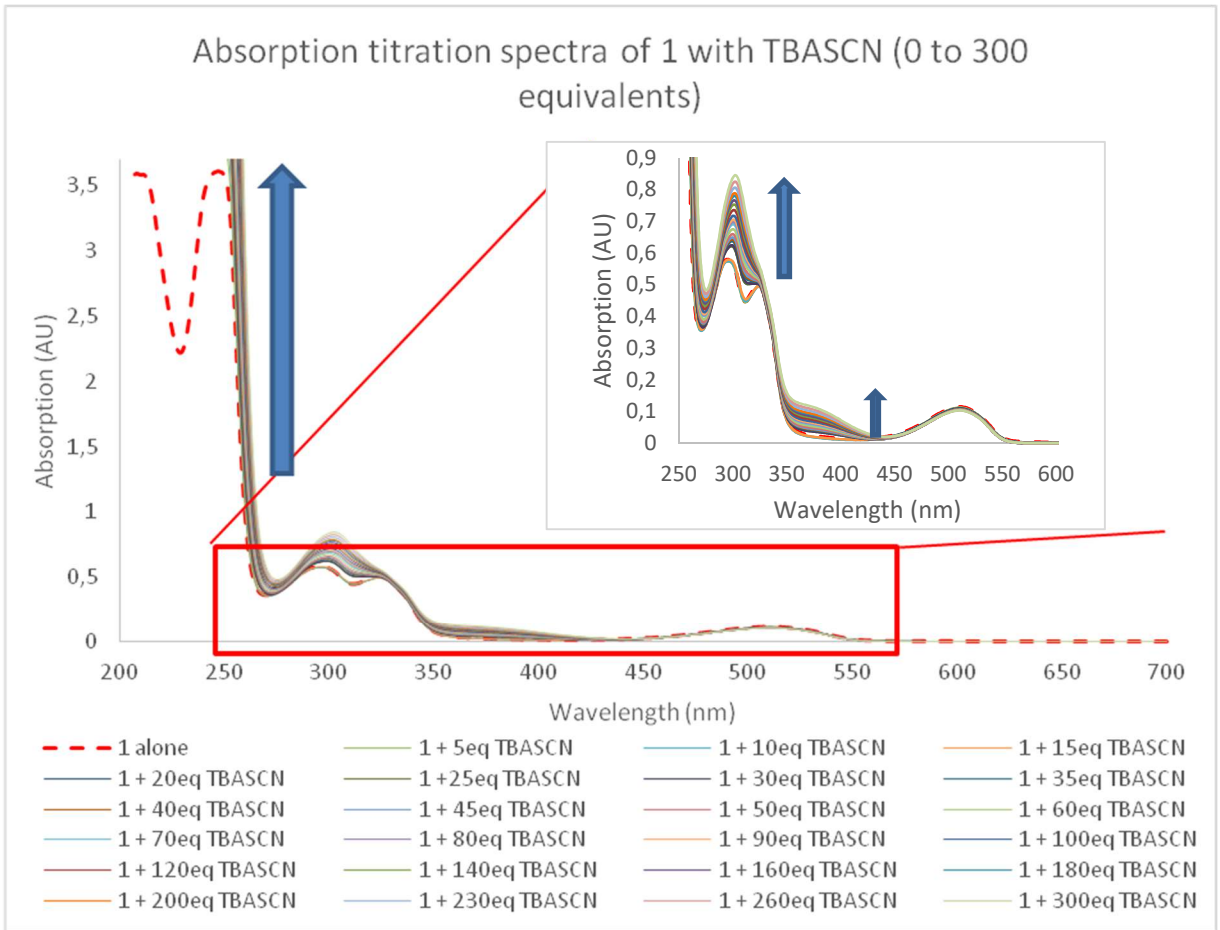

*Figure S63 – Experimental UV-Visible spectra measured during the titration of **1** with TBASCN (0 to 300 equivalents)*

```
[PROGRAM]
Name = SPECFIT
Version = 3.0

[FILE]
Name = RP04+TBASCN_ABS_FORMAT_SPECFIT.FAC
Path = C:\Program Files\SPECFIT\DATA\
Date = 26-juil-19
Time = 10:24:36
Ncomp = 2
Nmeas = 24
Nwave = 430

[FACTOR ANALYSIS]
Tolerance = 1,000E-09
Max.Factors = 10
Num.Factors = 10
Significant = 6
Eigen Noise = 7,805E-05
Exp't Noise = 7,805E-05
#  Eigenvalue  Square Sum  Residual    Prediction
1  5,226E+02   1,510E+00   1,210E-02   Data Vector
2  1,479E+00   3,078E-02   1,727E-03   Data Vector
3  2,874E-02   2,036E-03   4,442E-04   Data Vector
4  1,574E-03   4,625E-04   2,117E-04   Data Vector
5  2,649E-04   1,976E-04   1,384E-04   Data Vector
6  1,348E-04   6,282E-05   7,805E-05   Data Vector
7  1,887E-05   4,395E-05   6,528E-05   Possibly Data
8  1,092E-05   3,303E-05   5,660E-05   Probably Noise
9  4,922E-06   2,811E-05   5,221E-05   Probably Noise
10  3,178E-06  2,493E-05   4,918E-05   Probably Noise

[MODEL]
Date = 26-juil-19
Time = 10:24:55
Model = 0
Index = 3
Function = 1
Species = 3
Params = 3

[SPECIES]   [COLORED]   [FIXED]   [SPECTRUM]
1 0 0       False       False
0 1 0       True        False
1 1 0       True        False

[SPECIES]   [FIXED]   [PARAMETER]            [ERROR]
1 0 0       True      0,00000E+00  +/-       0,00000E+00
0 1 0       True      0,00000E+00  +/-       0,00000E+00
1 1 0       False     1,40981E+00  +/-       4,85821E-02

[CONVERGENCE]
Iterations = 29
Convergence Limit = 1,000E-03
Convergence Found = 1,857E-05
Marquardt Parameter = 0,0
Sum(Y-y)^2 Residuals = 9,87474E-02
Std. Deviation of Fit(Y) = 3,09346E-03

[STATISTICS]
Experimental Noise = 7,805E-05
Relative Error Of Fit = 1,3727%
Durbin-Watson Factor = 1,0642
Goodness Of Fit, Chi^2 = 1,571E+03
Durbin-Watson Factor (raw data) = None
Goodness Of Fit, Chi^2 (raw data) = None

[COVARIANCE]
1,401E-02

[CORRELATION]
1,000E+00

[END FILE]
```

*Figure S64 – Determination of binding constant using SPECFIT software for the UV-Visible titration of **1** with tetrabutylammonium thiocyanate*

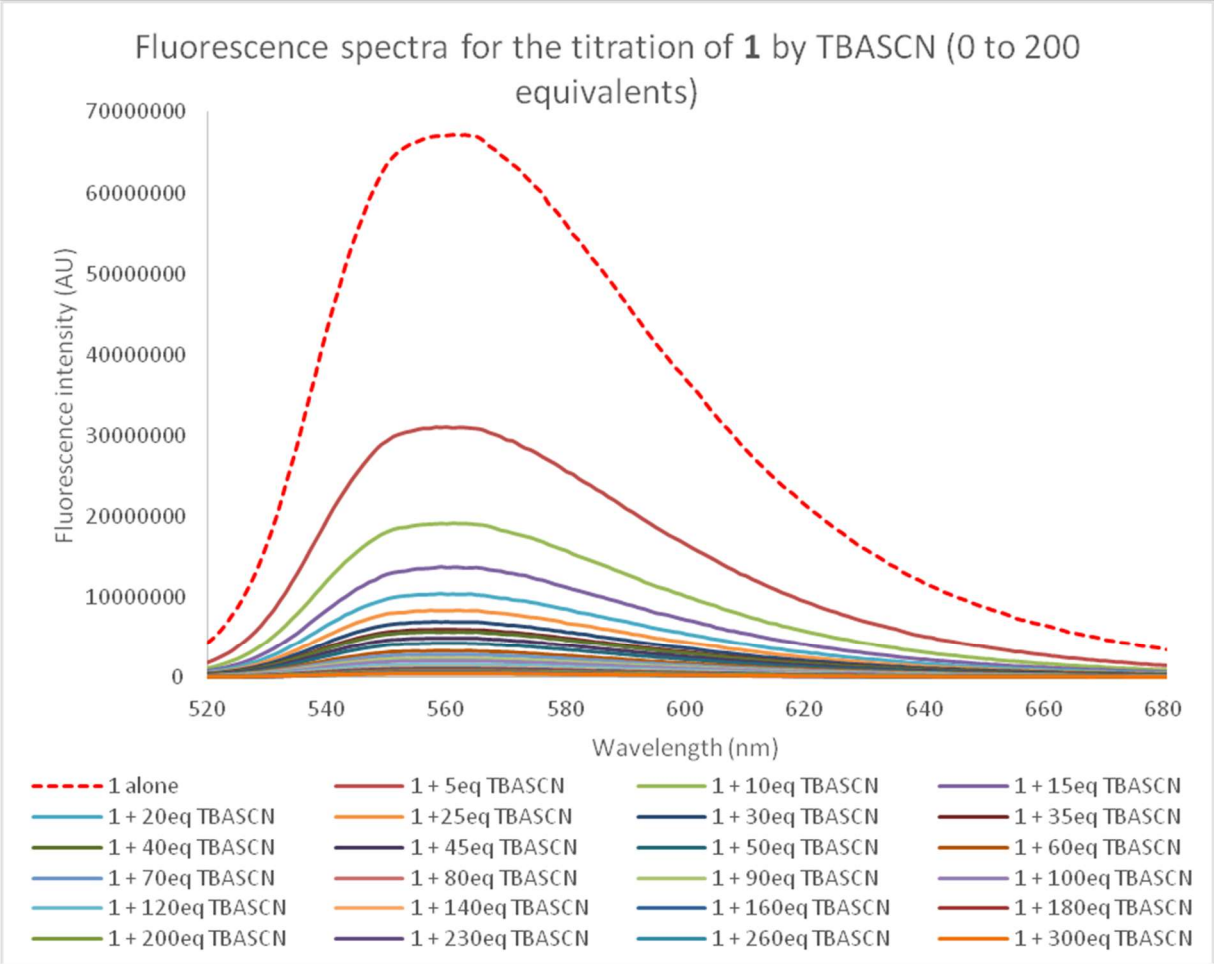

*Figure S65 – Experimental fluorescence spectra during the titration of **1** with TBASCN (0 to 300 equivalents)*

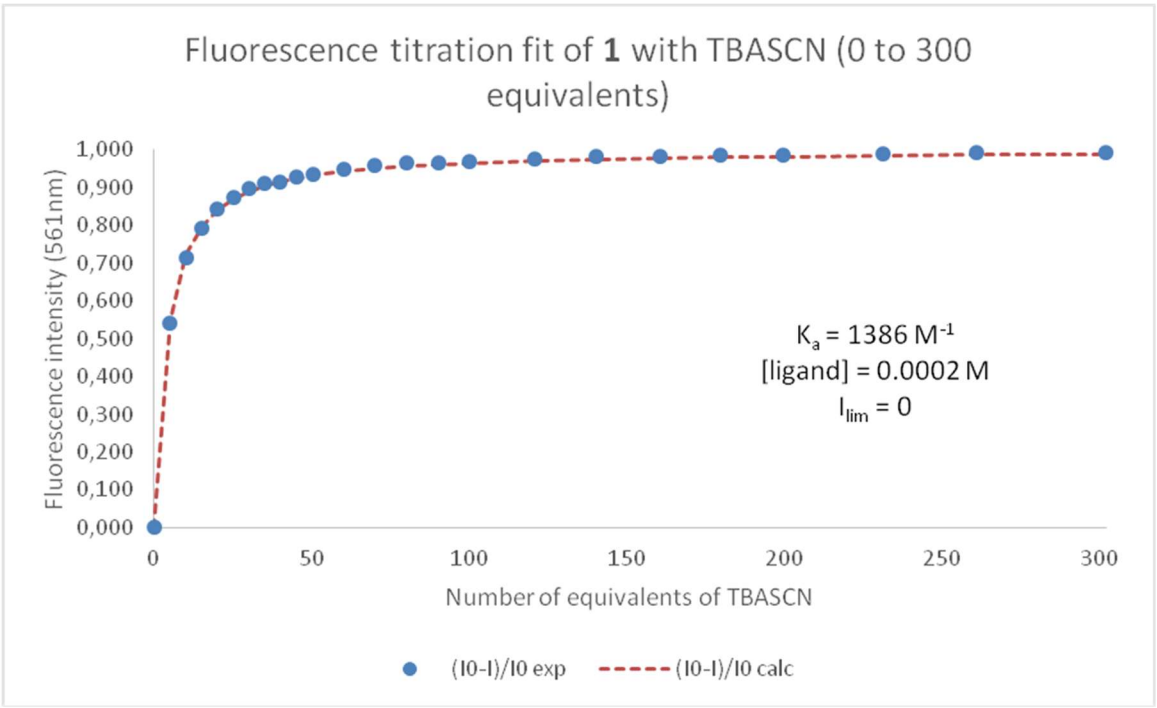

*Figure S66 – Mathematical fit during the fluorescence titration of **1** with TBASCN (0 to 300 equivalents) and determination of the association constant*

```
[PROGRAM]
Name = SPECFIT
Version = 3.0

[FILE]
Name = RP04+TBASCN_FLUO_FORMAT_SPECFIT.FAC
Path = C:\Program Files\SPECFIT\DATA\
Date = 26-juil-19
Time = 10:31:22
Ncomp = 2
Nmeas = 24
Nwave = 281

[FACTOR ANALYSIS]
Tolerance = 1,000E-09
Max.Factors = 10
Num.Factors = 5
Significant = 2
Eigen Noise = 1,545E+04
Exp't Noise = 1,545E+04
#   Eigenvalue  Square Sum  Residual    Prediction
1   3,288E+17   1,800E+13   5,166E+04   Data Vector
2   1,639E+13   1,609E+12   1,545E+04   Data Vector
3   6,204E+11   9,884E+11   1,211E+04   Possibly Data
4   2,472E+11   7,412E+11   1,049E+04   Probably Noise
5   1,148E+11   6,264E+11   9,641E+03   Probably Noise

[MODEL]
Date = 26-juil-19
Time = 10:31:39
Model = 0
Index = 3
Function = 1
Species = 3
Params = 3

[SPECIES]   [COLORED]   [FIXED]   [SPECTRUM]
1 0 0       False       False
0 1 0       True        False
1 1 0       True        False

[SPECIES]   [FIXED]   [PARAMETER]              [ERROR]
1 0 0       True      0,00000E+00   +/-       0,00000E+00
0 1 0       True      0,00000E+00   +/-       0,00000E+00
1 1 0       False     3,12736E+00   +/-       2,88376E-03

[CONVERGENCE]
Iterations = 13
Convergence Limit = 1,000E-03
Convergence Found = 7,936E-08
Marquardt Parameter = 0,0
Sum(Y-y)^2 Residuals = 4,03185E+13
Std. Deviation of Fit(Y) = 7,73260E+04

[STATISTICS]
Experimental Noise = 1,545E+04
Relative Error Of Fit = 1,1074%
Durbin-Watson Factor = 1,0856
Goodness Of Fit, Chi^2 = 2,506E+01
Durbin-Watson Factor (raw data) = None
Goodness Of Fit, Chi^2 (raw data) = None

[COVARIANCE]
4,438E-05

[CORRELATION]
1,000E+00

[END FILE]
```

*Figure S67: Determination of binding constant using SPECFIT software for the fluorescence titration of **1** with tetrabutylammonium thiocyanate*

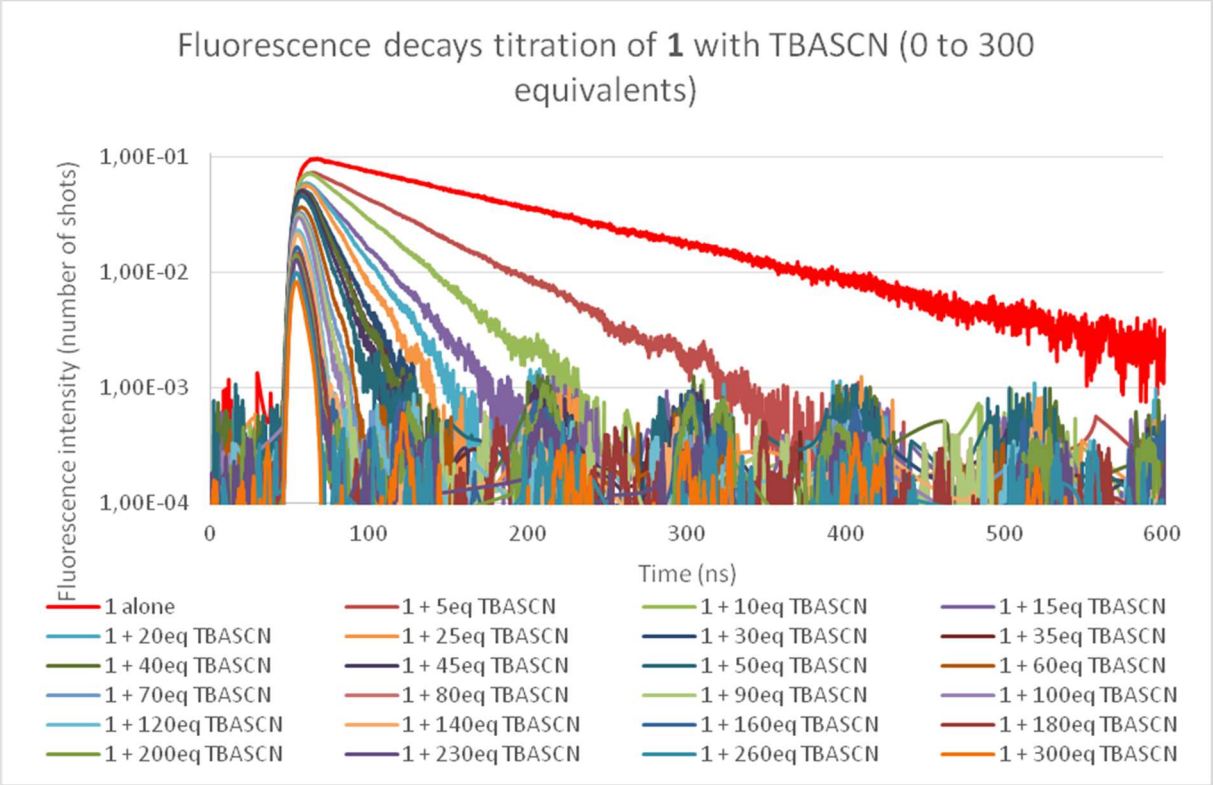

*Figure S68 –Fluorescence decay titration of **1** with tetrabutylammonium thiocyanate (0 to 300 equivalents) Logarithmic scale*

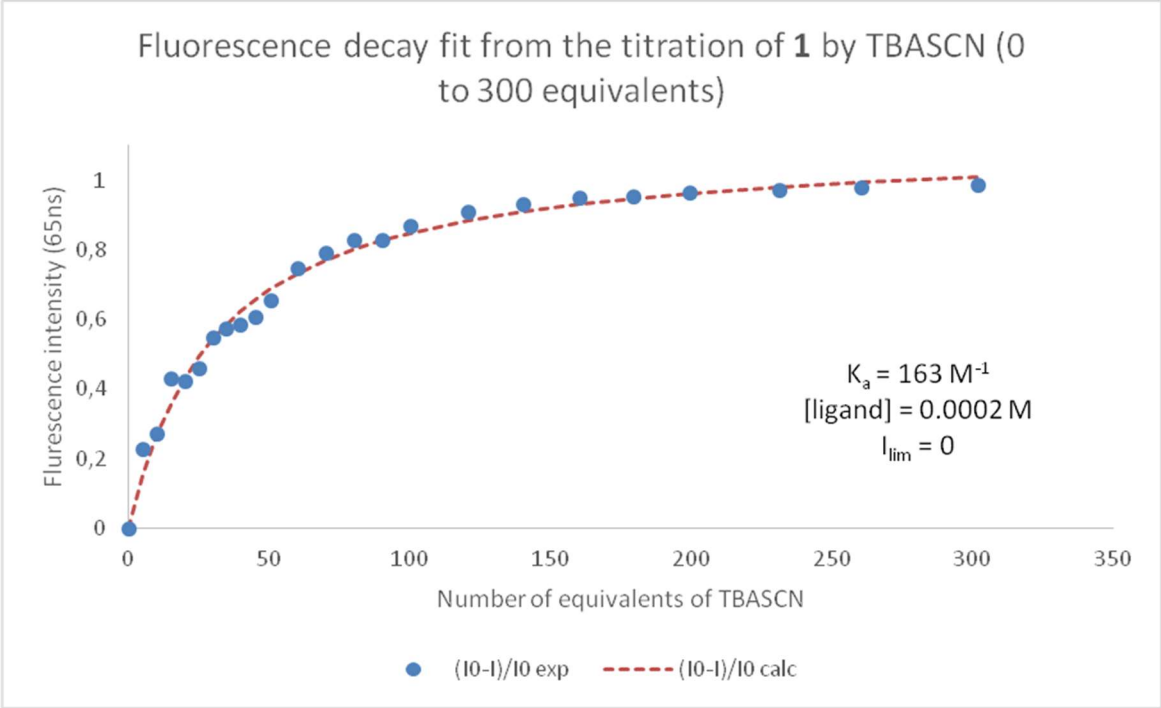

*Figure S69 –Mathematical fit during the fluorescence decay titration of **1** with TBASCN (0 to 300 equivalents) and determination of the association constant*

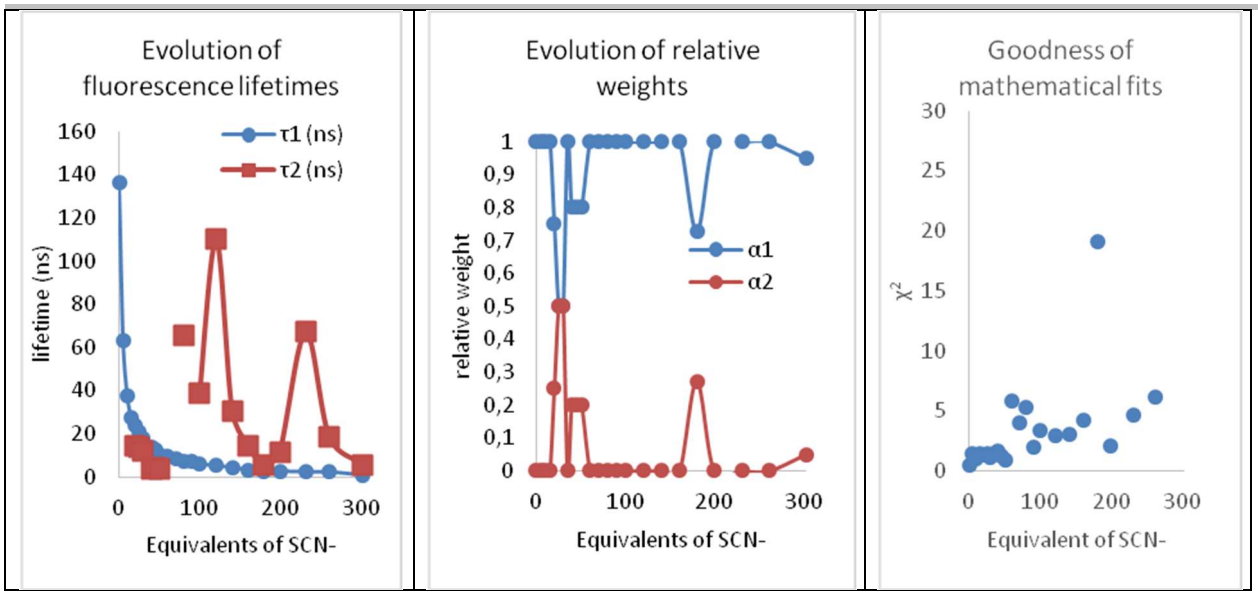

*Figure S70 –Analysis of fluorescence decay titration of **1** with tetrabutylammonium thiocyanate*

7. References

[1] H. E. Gottlieb, V. Kotlyar, A. Nudelman, *J. Org. Chem.* **1997**, *62*, 7512–7515.
[2] W. R. Dolbier, *Guide to Fluorine NMR for Organic Chemists*, John Wiley & Sons, Inc., Hoboken, NJ, USA, **2016**.
[3] J. Contreras-García, E. R. Johnson, S. Keinan, R. Chaudret, J. P. Piquemal, D. N. Beratan, W. Yang, *J. Chem. Theory Comput.* **2011**, *7*, 625–632.
[4] Henry S. Rzepa, "Script for creating an NCI surface as a JVXL compressed file from a (Gaussian) cube of total electron density," can be found under https://www.ch.ic.ac.uk/rzepa/cub2nci/, **2013**.
[5] R. D. J. Gless, S. K. Anandan, *Soluble Epoxide Hydrolase Inhibitors*, **2008**, WO 2008/116145 A2.
[6] Y. H. Gong, P. Audebert, G. Clavier, F. Miomandre, J. Tang, S. Badré, R. Méallet-Renault, E. Naidus, *New J. Chem.* **2008**, *32*, 1235–1242.
[7] G. González-Gaitano, G. Tardajos, *J. Chem. Educ.* **2004**, *81*, 270–274.
[8] B. Valeur, M. N. Berberan-Santos, *Molecular Fluorescence: Principles and Applications, Second Edition*, Wiley-VCH, **2012**.
[9] H. Gampp, M. Maeder, C. J. Meyer, A. D. Zuberbühler, *Talanta* **1985**, *32*, 95–101.
[10] H. Gampp, M. Maeder, C. J. Meyer, A. D. Zuberbühler, *Talanta* **1985**, *32*, 257–264.
[11] C. Würth, M. Grabolle, J. Pauli, M. Spieles, U. Resch-Genger, *Nat. Protoc.* **2013**, *8*, 1535–1550.
[12] A. M. Brouwer, *Pure Appl. Chem.* **2011**, *83*, 2213–2228.

8. Author Contributions

All authors contributed equally. D.P. brought lead contribution.